

SPECTRAL METHODS FOR OUTLIER DETECTION IN MACHINE LEARNING

by

Göker Erdoğan

B.S., Computer Engineering, Istanbul Technical University, 2008

Submitted to the Institute for Graduate Studies in
Science and Engineering in partial fulfillment of
the requirements for the degree of
Master of Science

Graduate Program in Computer Engineering
Boğaziçi University

2012

ACKNOWLEDGEMENTS

First and foremost, I would like to express my deepest gratitude to my supervisor Prof. Ethem Alpaydm for motivating me to carry out research in this field with his inspiring lectures. He always showed me the right way, reviewed countless revisions carefully and more importantly taught me how to perform research. This thesis would not have been possible without his invaluable guidance. I would also like to thank the members of my thesis committee, Assist. Prof. Arzucan Özgür and Assoc. Prof. Olcay T. Yıldız, for their precious reviews.

I sincerely thank The Scientific and Technological Research Council of Turkey (TÜBİTAK) for the scholarship that made it possible to channel my whole energy to my studies.

I would also like to express my heartfelt appreciation to my closest friend Akin Unan for all he provided throughout our 12 years of friendship. He beared with me even when I got bored of myself and motivated me with his sarcastic attitude in times I lost my faith.

No words are enough to describe my love and gratitude to İlayda Gümüş. She gave me the strength to quit my job and follow my dreams and the reason to better myself everyday. She will always have a very special place in my heart.

Above all, I consider myself lucky to have such a wonderful family. My whole family stood by me at all times and supported all my decisions in every possible way. I'm deeply grateful to my mother, father and brother for trusting me fully and believing in my success. It is not possible to express my love for them adequately.

ABSTRACT

SPECTRAL METHODS FOR OUTLIER DETECTION IN MACHINE LEARNING

Outliers are those instances in a sample that deviate significantly from the others. Their identification bears much importance since they carry valuable and actionable information in many real life scenarios. Spectral methods are unsupervised learning techniques that reveal low dimensional structure in high dimensional data. We analyze spectral methods, such as, Principal Components Analysis (PCA), Laplacian Eigenmaps (LEM), Kernel PCA (KPCA), Multidimensional Scaling (MDS) and present a unified view. We argue that the ability of such methods to reduce dimensionality is valuable for outlier detection. Hence, we propose spectral outlier detection algorithms where spectral decomposition precedes outlier detection. The four outlier detection methods we use are Active-Outlier, Local Outlier Factor, One-Class Support Vector Machine and Parzen Windows. We combine these methods with the spectral methods of LEM and MDS to form our algorithm. We evaluate the performance of our approach on various data sets and compare it with the performance of outlier detection without spectral transformation and with PCA. We observe that combining outlier detection methods with LEM increases the outlier detection accuracy. We discuss how the unique characteristics of LEM make it a valuable spectral method for outlier detection. We also confirm the merits of our approach on a face detection problem. Additionally, we provide an outlier detection toolbox in MATLAB that will be useful for researchers in this field containing the implementations of the outlier detection algorithms and the spectral methods discussed in this thesis.

ÖZET

YAPAY ÖĞRENMEDE AYKIRILIK SEZİMİ İÇİN İZGESEL YÖNTEMLER

Aykırılıklar verinin genelinden önemli farklılık gösteren örneklerdir. Gerçek yaşamda karşımıza çıkan pek çok uygulamada aykırı örneklerin bulunması hem kavramsal hem de eylemsel açıdan değerli bilgi taşıdıkları için önemlidir. İzgesel yöntemler yüksek boyutlu verilerdeki düşük boyutlu yapıları ortaya çıkarabilen gözetimsiz öğrenme yaklaşımlarıdır. Bu yöntemlerden Temel Bileşenler Çözümlemesi (TBC), Laplasyen Özharitalar (LÖH) ve Çok Boyutlu Ölçekleme incelenerek ortak bir çatı altında sunulmaktadır. Bu çalışmada, izgesel yöntemlerin boyut düşürme özelliklerinin aykırılık bulmakta değerli olduğu öne sürülmekte ve aykırılık bulma öncesinde izgesel yaklaşımla veriyi dönüştüren izgesel aykırılık bulma yöntemi önerilmektedir. Etkin-Aykırı, Yerel Aykırılık Etkeni, Tek Sınıflı Karar Vektör Makineleri ve Parzen Pencereyi aykırılık bulma yöntemleri olarak kullanılmakta ve bu yöntemler Temel Bileşenler Çözümlemesi (TBC), Laplasyen Özharitalar (LÖH) ve Çok Boyutlu Ölçekleme'yle birleştirilerek farklı veri kümeleri üzerinde aykırılık bulma başarımı sınanmaktadır. Deney sonuçları özellikle LÖH izgesel yönteminin başarımı artırdığını göstermektedir. Sonrasında, LÖH yöntemini aykırılık bulma için değerli kılan özgün özellikleri tartışılmaktadır. Önerdiğimiz yaklaşım yüz tanıma problemine de uygulanarak, öne sürülen yöntemin geçerliliği doğrulanmaktadır. Ayrıca, bu alandaki araştırmalarda kullanılmak için, aykırılık bulma ve izgesel yöntemlerin gerçekleştirilmesini içeren bir MATLAB kütüphanesi de bu tez ile paylaşılmaktadır.

TABLE OF CONTENTS

ACKNOWLEDGEMENTS	iii
ABSTRACT	iv
ÖZET	v
LIST OF FIGURES	viii
LIST OF TABLES	xii
LIST OF SYMBOLS	xv
LIST OF ACRONYMS/ABBREVIATIONS	xvii
1. INTRODUCTION	1
1.1. Outlier Detection Problem Definition	3
1.2. Outlier Detection Methods	4
1.3. Outline of Thesis	6
2. OUTLIER DETECTION METHODS	7
2.1. Outlier Detection by Active Learning	7
2.2. LOF: Identifying Density-Based Local Outliers	10
2.2.1. Feature Bagging for Outlier Detection	13
2.3. One-Class Support Vector Machine	16
2.4. Parzen Windows	18
3. SPECTRAL METHODS	21
3.1. Principal Components Analysis	22
3.2. Kernel Principal Components Analysis	23
3.3. Multidimensional Scaling	25
3.4. Laplacian Eigenmaps	25
3.5. Discussion	26
3.5.1. Approximating Dot Products or Euclidean Distances	28
3.5.2. Mean Centered KPCA is Equivalent to Classical MDS	29
3.5.3. How LEM Differs from MDS and KPCA	29
4. SPECTRAL OUTLIER DETECTION	30
4.1. The Idea	30
4.2. Related Work	32

5. EXPERIMENTS	34
5.1. Evaluated Methods and Implementation Notes	34
5.2. Synthetic Data	35
5.3. Real Data	43
5.3.1. Data Sets	44
5.4. Face Detection	78
6. CONCLUSIONS AND FUTURE WORK	81
APPENDIX A: OUTLIER DETECTION TOOLBOX IN MATLAB	84
REFERENCES	88

LIST OF FIGURES

Figure 2.1.	Active-Outlier method.	10
Figure 2.2.	Example data set.	11
Figure 2.3.	LOF method.	13
Figure 2.4.	Feature bagging method.	14
Figure 2.5.	Feature bagging breadth-first combination.	15
Figure 2.6.	Feature bagging cumulative-sum combination.	16
Figure 2.7.	Parzen Windows algorithm.	20
Figure 3.1.	LEM, KPCA, KPCA-Mean centered and MDS transformations of a synthetic sample with Gaussian kernel with $\sigma = .1$ and neighbor count $k = 2$	28
Figure 4.1.	Boundary learned by Active-Outlier on a synthetic circular data set.	31
Figure 4.2.	Boundary learned by Active-Outlier on a synthetic circular data set after KPCA with Gaussian kernel ($k = 2, \sigma = .4$).	32
Figure 4.3.	Spectral outlier detection algorithm.	33
Figure 5.1.	Synthetic data set 1.	37
Figure 5.2.	Synthetic data set 2.	37

Figure 5.3.	Outlier scores and discriminants for outlier count 2, 10, 50 with the Active-Outlier method.	38
Figure 5.4.	Outlier scores and discriminants for outlier count 2, 10, 50 with the LOF method.	40
Figure 5.5.	Outlier scores and discriminants for outlier count 2, 10, 50 with the Parzen Windows method.	41
Figure 5.6.	Outlier scores and discriminants for outlier count 2, 10, 50 with the One-Class Support Vector Machine.	42
Figure 5.7.	AUC vs. kernel type on <i>Optdigits</i> data set.	48
Figure 5.8.	AUC vs. kernel type on <i>Shuttle</i> data set.	49
Figure 5.9.	AUC vs. neighbor count on <i>Optdigits</i> data set with constant kernel.	50
Figure 5.10.	AUC vs. neighbor count on <i>Shuttle</i> data set with constant kernel.	50
Figure 5.11.	AUC vs. neighbor count on <i>Optdigits</i> data set with Gaussian kernel.	51
Figure 5.12.	AUC vs. neighbor count on <i>Shuttle</i> data set with Gaussian kernel.	51
Figure 5.13.	AUC vs. neighbor count on <i>Optdigits</i> data set with quadratic kernel.	52
Figure 5.14.	AUC vs. neighbor count on <i>Shuttle</i> data set with quadratic kernel.	52
Figure 5.15.	AUC vs. input dimensionality on <i>Optdigits</i> data set.	53
Figure 5.16.	AUC vs. input dimensionality on <i>Shuttle</i> data set.	54

Figure 5.17. Plots of AUCs for the semi-supervised case.	56
Figure 5.18. Plots of AUCs for the unsupervised case.	57
Figure 5.19. Plots of AUCs for spectral outlier detection with PCA for the semi-supervised case.	60
Figure 5.20. Plots of AUCs for spectral outlier detection with PCA for the unsupervised case.	60
Figure 5.21. Plots of AUCs for spectral outlier detection with LEM for the semi-supervised case.	64
Figure 5.22. Plots of AUCs for spectral outlier detection with LEM for the unsupervised case.	64
Figure 5.23. Plots of AUCs for spectral outlier detection with MDS for the semi-supervised case.	65
Figure 5.24. Plots of AUCs for spectral outlier detection with MDS for the unsupervised case.	68
Figure 5.25. Plots of AUCs for AO with different spectral methods for the semi-supervised case.	70
Figure 5.26. Plots of AUCs for AO with different spectral methods for the unsupervised case.	70
Figure 5.27. Plots of AUCs for LOF with different spectral methods for the semi-supervised case.	72

Figure 5.28. Plots of AUCs for LOF with different spectral methods for the unsupervised case.	72
Figure 5.29. Plots of AUCs for SVM with different spectral methods for the semi-supervised case.	73
Figure 5.30. Plots of AUCs for SVM with different spectral methods for the unsupervised case.	73
Figure 5.31. Plots of AUCs for PW with different spectral methods for the semi-supervised case.	74
Figure 5.32. Plots of AUCs for PW with different spectral methods for the unsupervised case.	74
Figure 5.33. CBCL Face data set reduced to two dimensions with PCA.	79
Figure 5.34. CBCL Face data set reduced to two dimensions with LEM (Gaussian kernel, $k = 3$ and $\sigma = 101.70$).	80
Figure A.1. Spectral methods demonstration <code>demo</code> script's first screen where points and kernel parameters are selected.	85
Figure A.2. Spectral methods demonstration <code>demo</code> script's second screen where spectral transformations are plotted.	85
Figure A.3. Outlier detection toolbox demonstration <code>od</code> script's GUI.	86

LIST OF TABLES

Table 1.1.	Summary of outlier detection methods.	6
Table 3.1.	Comparison of cost functions optimized by dimensionality reduction methods.	27
Table 5.1.	Data sets used in the experiments.	47
Table 5.2.	Average values and standard deviations of AUCs for the semi-supervised case.	55
Table 5.3.	Average values and standard deviations of AUCs for the unsupervised case.	56
Table 5.4.	Wins/ties/losses of each algorithm with 5×2 cv F test.	57
Table 5.5.	Average values and standard deviations of AUCs for spectral outlier detection with PCA, semi-supervised case.	58
Table 5.6.	Average values and standard deviations of AUCs for spectral outlier detection with PCA, unsupervised case.	59
Table 5.7.	Wins/ties/losses of outlier detection methods combined with PCA with 5×2 cv F test.	59
Table 5.8.	Average values and standard deviations of AUCs for spectral outlier detection with LEM, semi-supervised case.	62

Table 5.9.	Average values and standard deviations of AUCs for spectral outlier detection with LEM, unsupervised case.	63
Table 5.10.	Wins/ties/losses of outlier detection methods combined with LEM with 5×2 cv F test.	65
Table 5.11.	Average values and standard deviations of AUCs for spectral outlier detection with MDS, semi-supervised case.	66
Table 5.12.	Average values and standard deviations of AUCs for spectral outlier detection with MDS, unsupervised case.	67
Table 5.13.	Wins/ties/losses of outlier detection methods combined with MDS.	68
Table 5.14.	Average ranks of outlier detection methods.	69
Table 5.15.	Significant differences between outlier detection methods for each spectral method for the semi-supervised case.	69
Table 5.16.	Significant differences between outlier detection methods for each spectral method for the unsupervised case.	69
Table 5.17.	Average ranks of spectral methods with respect to outlier detection methods.	71
Table 5.18.	Significant differences between spectral methods for each outlier detection method for the semi-supervised case.	75
Table 5.19.	Significant differences between spectral methods for each outlier detection method for the unsupervised case.	75

Table 5.20.	Wins/ties/losses of outlier detection methods combined with spectral methods for the semi-supervised case.	76
Table 5.21.	Wins/ties/losses of outlier detection methods combined with spectral method for the unsupervised case.	77

LIST OF SYMBOLS

B	Background distribution
\mathbf{B}	Dot product matrix
C_i	Class i
C	Cost function
d	Number of input dimensions
D	Distribution
\mathbf{D}	Diagonal matrix of row/column sums
$e(x)$	Error function
\mathbf{E}	Distance matrix
$g(x)$	Model/Classifier
$\mathcal{G}(x)$	Set of classifiers
H	Subset of input space
\mathcal{H}	Set of subsets of input space
k	Neighbor count
k_{min}	Minimum neighbor count
k_{max}	Maximum neighbor count
K	Kernel function
\mathcal{L}	Lagrangian function
\mathbf{K}	Kernel matrix
m	Number of output dimensions
M	Number of combined/trained methods
$M(\mathcal{G} \mathbf{x})$	Margin for the instance \mathbf{x} with classifiers in set \mathcal{G}
N	Number of instances
$p(x)$	Probability function
$\hat{p}(x)$	Estimated probability
\mathbf{r}	Output vector
s	Variance
\mathbf{S}	Similarity matrix

tr	Trace operator
U	Data distribution
w	Bin size
\boldsymbol{w}	Eigenvector
\mathbf{W}	Transformation matrix
\boldsymbol{x}	Input vector
\mathbf{X}	Input data matrix
\mathcal{X}	Input data set
\boldsymbol{y}	Outlier scores
\mathbf{Z}	Transformed data matrix
λ	Eigenvalue
μ	Mean
ϕ	Partition of space
σ	Variance
θ	Model parameters
Θ	Decision threshold
ϕ	Mapping function

LIST OF ACRONYMS/ABBREVIATIONS

AO	Active-Outlier
ANOVA	Analysis of Variances
AUC	Area Under the Curve
CV	Cross Validation
GUI	Graphical User Interface
KPCA	Kernel Principal Components Analysis
LEM	Laplacian Eigenmaps
LOF	Local Outlier Factor
MDS	Multidimensional Scaling
ML	Machine Learning
PCA	Principal Components Analysis
PR	Precision-Recall
PW	Parzen Windows
ROC	Receiver Operating Characteristic
SS	Semi-Supervised
SVM	One-Class Support Vector Machine
US	Unsupervised

1. INTRODUCTION

Machine learning (ML) is the engineering of methods that enable machines, i.e., computers to adapt their behavior based on empirical data. ML analyzes example data or past experience and uses the theory of statistics to build mathematical models to predict events in the future and/or describe the observed behavior [1]. ML methods are generally categorized according to the nature of the learning problem or the statistical assumptions they make. According to the nature of the learning problem, ML methods can be classified as *supervised* or *unsupervised*. The following paragraphs are largely adopted from [1].

In supervised learning, the data set contains the actual output value for each input instance. For example, for the task of determining if a person is a high-risk customer for giving loans, we have past customer attributes together with the label for each customer indicating if they are a high-risk customer or not. Here our training set consists of input pairs

$$\mathcal{X} = \{(\mathbf{x}^{(t)}, \mathbf{r}^{(t)})\}_{t=1}^N \quad (1.1)$$

where $\mathbf{x}^{(t)} \in \mathbb{R}^d$ is the vector denoting instance t in our sample of size N and $\mathbf{r}^{(t)}$ specifies the output for the instance. If $\mathbf{r}^{(t)}$ takes only discrete values, such as 1 for high-risk and otherwise 0, this problem is called a *classification* problem. In classification problems, we aim to predict the class that a future instance belongs to by making inference from the past data \mathcal{X} . For a classification problem with m classes denoted as $C_i, i = 1, \dots, m$, $\mathbf{r}^{(t)}$ is m -dimensional and

$$r_i^{(t)} = \begin{cases} 1 & \text{if } \mathbf{x}^{(t)} \in C_i \\ 0 & \text{if } \mathbf{x}^{(t)} \in C_j, j \neq i \end{cases} \quad (1.2)$$

If there are only two classes, which is called a binary classification problem, one class is chosen as positive with $r^{(t)} = 1$ and the other as negative class with $r^{(t)} = 0$. If the output values are continuous, it is a *regression* problem. For instance, estimating the life expectancy of a person from his/her personal data is a regression problem. In supervised learning, our aim is to learn a model $g(\mathbf{x}|\theta)$ where θ are the model parameters that we need to estimate from the sample \mathcal{X} . We look for θ^* that minimize a loss function measuring the difference between actual $\mathbf{r}^{(t)}$ values and our model's predictions $g(\mathbf{x}^{(t)}|\theta)$. For classification problems, $g(\mathbf{x}|\theta)$ divides the input space into regions for each class and the boundaries that separate classes are called *discriminants*.

In *unsupervised* learning, we only have the input data $\mathbf{x}^{(t)}$ and no $\mathbf{r}^{(t)}$. The aim is to find patterns, regularities or groupings in data. This type of learning is known as *density estimation* in statistics. An important problem in unsupervised learning is *clustering*, that is, extracting a mapping function from training set that assigns each instance to a group. For example, discovering customer profiles from customer data can be achieved by clustering. The middle road between supervised and unsupervised learning is where only labels or output values for a subset of the training set are available.

Every ML method makes some statistical assumptions in order to solve an otherwise intractable problem. *Parametric* methods assume that the sample \mathcal{X} is drawn from a distribution and estimate the values of the parameters of this distribution. In the case of classification, every class conditional density $p(\mathbf{x}|C_i)$ is assumed to be of some form and $p(\mathbf{x}|C_i)$, $p(C_i)$ densities are estimated to calculate the posterior probability $p(C_i|\mathbf{x})$ using Bayes' rule to make our predictions. Parametric methods are advantageous since learning is reduced to estimating the values of a small number of parameters. However, these assumptions may not always hold and we need to turn to *non-parametric* methods. In non-parametric methods, we only assume that similar instances have similar outputs and our algorithm finds similar instances from \mathcal{X} and uses them to predict the right output. However, this lack of assumptions comes with a price on time and space complexity. Non-parametric methods need to store the past

data and carry out extra computation to find the similar instances whereas parametric methods only store the values of a few parameters and are less time and memory consuming.

1.1. Outlier Detection Problem Definition

In this thesis, we deal with the problem of *outlier detection*. Outlier (or anomaly) is just another one of those concepts where we all know one when we see one. However, our every attempt at delineating a formal definition falls short, perhaps because of the unconscious processes of our brain in identifying outliers. One widely referenced definition by Grubbs [2] is as follows.

“An outlying observation, or outlier, is one that appears to deviate markedly from other members of the sample in which it occurs.”

Although it is quite hard to frame *outlierness* without resorting to ambiguous concepts such as “deviation”, the detection of outliers bears high importance since such outliers convey valuable and actionable information in many real life scenarios. An outlier may be an attack in a network, a potential fault in a machine or denote a cancerous tumor [3]. Apart from the practical applications, outliers also have theoretical value from the perspective of learning theory. In his inspiring book *Society of Mind* [4], Minsky elaborates on various types of learning and also mentions the importance of outliers. *Uniframing*, as called by Minsky, refers to our abilities of combining several distinct descriptions into one and inferring a general model that largely explains our observations. However, uniframing does not always work, since some of our experiences may lack a common ground to be included in our established models. In that case, another type of learning, *accumulation*, plays a role where incompatible observations are collected and stored as exceptions to our models. This dual strategy of learning enables us to efficiently create descriptions of things without getting lost in details of the individual objects and prevents our models from losing their generalization capabilities by wrongly incorporating examples that deviate from the description into the model. In such a learning method, detecting outliers bears importance since it determines the

learning type to employ for the observation in question.

From a more formal perspective, outlier detection can be considered as a classification problem. We want to calculate a function $g(\mathbf{x})$ that predicts if an instance is an outlier. This function may provide hard decisions, e.g., 0 for typicals and 1 for outliers, or return a real number corresponding to the degree of being an outlier. However, the availability of labels as typical vs. outlier is not always possible. We may have only a sample from the class of typical examples or a mixed sample without any labels. Hence, outlier detection is sometimes a supervised learning problem and in some cases, an unsupervised or a semi-supervised learning problem.

Outlier detection differs from classification in a few aspects. Class distributions in outlier detection problems are highly unbalanced, since the outlier instances are much fewer compared to the typical ones. Additionally, classification costs are not symmetric. Generally, the misclassification of an outlier as typical, e.g., missing a cancerous tumor, is more costly than assigning a typical instance as outlier. Another consideration for outlier detection problems is that the noisy instances are usually similar to the outliers and they may be hard to remove or to disregard. Lastly, it is usually the case that we do not have labeled outlier instances. These characteristics of outlier detection limit the applicability of classification methods and call for specially designed algorithms.

1.2. Outlier Detection Methods

In this section, we present a taxonomy of outlier detection methods; see [3] for a more extended review.

Discriminant based methods learn a discriminative model over the input space, separating outliers and the typical instances. The most distinctive property of these methods is the requirement that data be labeled as typical or outlier and this requirement limits their applicability. However, once labeled data are available, the well-established theory of classification and the vast number of diverse methods can be

used. These methods can be further categorized into two. Two-class methods require data labeled as typical vs. outlier, while one-class methods use only the sample of typicals to learn a boundary that discriminates typical and outlier instances. There are outlier detection methods that use multi-layered perceptrons trained with the sample of typicals and identify an instance as outlier if the network rejects it [5,6]. Autoassociative networks, adaptive resonance theory and radial basis function based techniques are also proposed [7–9]. Rule based methods extract rules that describe typical behavior and detect outliers based on these rules [10]. Support Vector Machines have been applied to outlier detection as one-class methods [11,12]. Kernel Fisher discriminants have also been used as a one-class method for outlier detection [13].

Density based methods assume that the outliers occur far from the typical instances, that is, in low density regions of the input space. Estimating the density can be carried out using parametric methods that assume an underlying model, semi-parametric ones such as clustering methods, or non-parametric methods like Parzen Windows [14]. In parametric methods, sample of typical instances is assumed to obey a known distribution and statistical tests are used for identifying outliers [15,16]. There are also regression based methods where the residuals for test instances are used as outlier scores [17]. Semi-parametric methods assume a mixture of parametric distributions for the typical and/or outlier sample and use statistical tests to find outliers [18,19]. Non-parametric methods use histogram based or kernel based techniques to estimate densities to calculate outlier scores [20,21]. Then, these estimated densities are transformed into a measure of being an outlier. Semi-parametric clustering based methods make different assumptions to decide on the outliers. In [22], an instance that does not belong to any cluster is deemed outlier while in [23], an instance that is far from any cluster center and/or in a small sized cluster is considered an outlier. Non-parametric nearest neighbor based methods use different measures to determine the outliers, such as distance to the k th neighbor [24], the sum of distances to the k nearest neighbors [25] or the number of neighbors in the neighborhood of a certain size [26]. There are also techniques that take into account the relative densities around an instance to calculate an outlier score such as the Local Outlier Factor (LOF) method [27].

Table 1.1. Summary of outlier detection methods.

Discriminant Based Methods	Neural Networks Based: [5], [6], [7], [8], [9] Rule Based: [10] One-Class: [11], [12], [13]
Density Based Methods	Parametric: [24], [25], [26], [27] Semi-parametric: [22], [23] Non-parametric: [15], [16], [17], [18], [19], [20], [21]

Density based methods can be used in a supervised manner estimating distinct typical sample and outlier sample densities or in a semi-supervised manner by using only the typical sample. It is also possible to operate in an unsupervised setting, since the relative size of the outlier sample is generally quite small compared to the sample size. The primary disadvantages of these methods are their high computational complexity and their low performance on high-dimensional input spaces, due to the curse of dimensionality. Summary of the mentioned methods can be found in Table 1.1.

1.3. Outline of Thesis

In Chapter 2, we review four outlier detection methods. We discuss spectral methods used for reducing dimensionality to reveal low dimensional structure in high-dimensional data in Chapter 3. In Chapter 4, we argue how and when spectral methods are useful for outlier detection and propose our method of spectral outlier detection. Afterwards, in Chapter 5, we carry out experiments to analyze the behavior of outlier detection algorithms, compare their performances individually and with three spectral methods on various data sets. We conclude and discuss future work in Chapter 6.

2. OUTLIER DETECTION METHODS

2.1. Outlier Detection by Active Learning

Supervised, classification based Active-Outlier (AO) method [28] is an ensemble of classifiers that are trained on selectively sampled subsets of training data in order to learn a tight boundary around typical instances. When compared to outlier detection methods based on probabilistic or nearest-neighbor approaches, the Active-Outlier method requires much less computation since it does not need the training data in the testing phase and also provides a much more rational and semantic explanation for being an outlier.

Assuming that our data is drawn from a distribution U , our purpose is to find the partition π with the minimum size that covers all the instances from U and none of the other instances; these latter are assumed to originate from a background distribution B . The error for this unsupervised learning problem can be defined as follows:

$$e_{U,B}(\pi) = \frac{1}{2}(p_{x \sim U}(\mathbf{x} \notin \pi) + p_{x \sim B}(\mathbf{x} \in \pi)) \quad (2.1)$$

We may convert the above unsupervised learning problem to a classification problem by drawing instances evenly from U and B and by considering data and background distribution to be labelled as different classes. Let us assume that instances $\mathcal{X} = \{(\mathbf{x}^{(t)}, \mathbf{r}^{(t)})\}_{t=1}^N$, where $r^{(t)} \in \{0, 1\}$, are drawn from a distribution D , our purpose is find a classifier $g : \mathbf{x} \rightarrow r$ that minimizes the classification error:

$$e_D(g) = p_{x,r \sim D}(g(\mathbf{x}) \neq r) \quad (2.2)$$

Let us say D is composed of instances from U and B in equal sizes and that we label instances from U with class label 1 and instances from B with class label 0. Then, minimizing the classification error is equivalent to minimizing the error for the

unsupervised learning problem:

$$e_D(g) = p_{x,r \sim D}(g(\mathbf{x}) \neq 0 | r = 0) p_{x,r \sim D}(r = 0) \quad (2.3)$$

$$+ p_{x,r \sim D}(g(\mathbf{x}) \neq 1 | r = 1) p_{x,r \sim D}(r = 1) \quad (2.4)$$

$$= 0.5 p_{x \sim B}(\mathbf{x} \in \pi) + 0.5 p_{x \sim U}(\mathbf{x} \notin \pi) \quad (2.5)$$

With the above reduction, the outlier detection problem can be interpreted as a classification problem where we look for an accurate classifier that discriminates between the labeled training instances which are considered typical and the artificially generated instances that we insert into training data as potential outliers. In this manner, the classifier learns a tight boundary around the sample of typical instances and any instance outside is deemed an outlier. However, the accuracy of this approach relies heavily on the quality of background distribution. In order to decrease the dependence of the method on the background distribution, authors employ the *active learning* approach where the training instances given to the classifier are chosen dynamically. For the specific case of Active-Outlier, the next instance is drawn from regions close to the classification boundaries in order to have the boundary as tight as possible. Moreover, instead of training a single classifier on the generated data set, an ensemble of classifiers is formed by training multiple classifiers consecutively on selectively sampled subsets of data. This combination of *active learning* and sampling based on margin is called *ensemble-based minimum margin active learning* [28].

The pseudo-code of the algorithm is given in Figure 2.1. Given a data set containing typical instances, in the first step, synthetically generated data are added as potential outliers to the data set. In the selective sampling step, margins, indicating the confidence of classifier in its decision, are calculated for each instance. A new data set is formed by drawing a sample from our original data set in a manner that gives higher probability to instances with low margin. Then, the next classifier is trained on this new data set and these selective sampling and training steps are repeated as many times as necessary to form an ensemble of classifiers. In testing, we apply majority voting on the classifier outputs.

For an instance, the margin gives a measure of confidence in the decision and can be defined as follows:

$$M(\mathcal{G}, \mathbf{x}) = \left| \sum_{g \in \mathcal{G}} g(1|\mathbf{x}) - \sum_{g \in \mathcal{G}} g(0|\mathbf{x}) \right| \quad (2.6)$$

where $g(1|\mathbf{x})$ is the score for \mathbf{x} to be a typical instance, $g(0|\mathbf{x})$ is the score for \mathbf{x} to be a outlier instance and \mathcal{G} is the set of classifiers. Selective sampling strategy gives more importance to instances with low margin where the ensemble of classifiers is not very confident in the final decision. For each instance, the probability of it being picked in the next data set is given as:

$$\text{Sampling Probability}(\mathbf{x}) = \text{Gauss} \left(i/2, \sqrt{i}/2, \frac{i + M(\mathbf{x})}{2} \right) \quad (2.7)$$

$$\text{Gauss}(\mu, \sigma, a) = \int_a^{\infty} \frac{1}{\sigma\sqrt{2\pi}} \exp -\frac{(x - \mu)^2}{2\sigma^2} dx \quad (2.8)$$

where i is the current classifier index and $M(\mathbf{x})$ is the margin of instance \mathbf{x} . Equation 2.7 is based on the intuition that for n classifiers each with accuracy 1/2, the probability of obtaining k more votes for one class is the discrete probability of $(n + k)/2$ successes in n Bernoulli trials which can be approximated by a Gaussian distribution. Given that k more votes are observed for a certain instance, the likelihood of predicting the two class labels with equal probability is proportional to above probability.

There may be various candidates for the background distribution that the artificially generated potential outliers are drawn from. Although, this distribution may depend on the specific problem at hand, the authors propose the uniform distribution and the product distribution of marginals as a possible background distributions. In order to sample from the uniform distribution, the boundaries for each dimension are set as 10% below the minimum and above the maximum value observed in the sample.

For the product distribution of marginals, the marginal distributions are estimated as Gaussian distributions. It should be noted that proper care must also be taken when drawing samples with categorical features.

In the algorithm, each classifier is weighted according to its error by employing AdaBoost's weighting strategy [29]. A problem that may arise during the implementation of Active-Outlier is that as more classifiers are trained, sampled data sets tend to get smaller. In that case, the sampling probabilities may be normalized to ensure that sizes are reasonable.

Active-Outlier(Learner g , Sample of Typical Instances $\mathcal{X}_{typical}$, Classifier Count M , Decision Threshold Θ , Background Distribution B)

Generate a synthetic sample, $\mathcal{X}_{syn} \sim B$ of size $|\mathcal{X}_{typical}|$

Let $\mathcal{X} = \{(\mathbf{x}, 0), \mathbf{x} \in \mathcal{X}_{typical}\} \cup \{(\mathbf{x}, 1), \mathbf{x} \in \mathcal{X}_{syn}\}$

for $i = 1$ to M **do**

Calculate margin: $M(\{g_0, \dots, g_{i-1}\}, \mathcal{X})$

Sample from \mathcal{X} with sampling probability from Equation 2.7 and form \mathcal{X}'

Train learner g on \mathcal{X}' to obtain classifier g_i

Calculate ϵ_i : error rate of g_i on \mathcal{X}'

Set weight of g_i ; $\alpha_i = \log(\frac{1-\epsilon_i}{\epsilon_i})$

end for

return $g(\mathbf{x}) = \text{sign}(\sum_{i=1}^M \alpha_i g_i(\mathbf{x}) - \Theta(\sum_{i=1}^M \alpha_i))$

Figure 2.1. Active-Outlier method algorithm.

2.2. LOF: Identifying Density-Based Local Outliers

The nearest-neighbor based methods in outlier detection attract much attention and enjoy much popularity due to the intuitive connection between neighborhoods and outlierness. Breunig *et al.* presented one such method called the Local Outlier Factor (LOF) that is widely used [27]. Their method calculates the degree of being an outlier

for each instance based on the local density around it. Generally, the nearest-neighbor based outlier detection methods measure outlierness in terms of distance to other instances in data set. That is why, this approach risks missing outliers in data sets where local density varies greatly. Two clusters C_1 and C_2 can be seen in Figure 2.2 where it is expected that \mathbf{o}_1 and \mathbf{o}_2 will be deemed outliers by the outlier detection method. However, most nearest-neighbor based methods that rely on distances will label instances from cluster C_1 as outliers if they are tuned to detect \mathbf{o}_2 . The LOF

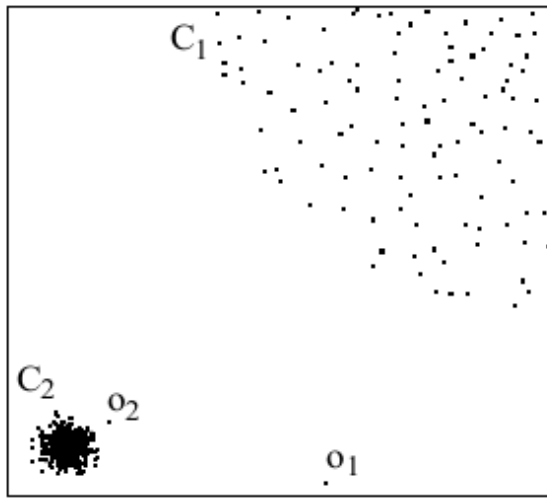


Figure 2.2. Example data set [27].

method overcomes this drawback by considering the difference in local densities around an instance as a measure of being an outlier. If the density around instance \mathbf{o} is highly different from the densities around its neighbors, LOF of \mathbf{o} will be higher.

$\mathcal{X} = \{(\mathbf{x}^{(t)}, \mathbf{r}^{(t)})\}_{t=1}^N$ denotes the input data set, \mathbf{x} , $\mathbf{x}^{(i)}$ and $\mathbf{x}^{(j)}$ represent instances from data set and $d(\mathbf{x}, \mathbf{x}^{(i)})$ denotes distance between \mathbf{x} and $\mathbf{x}^{(i)}$. The k -distance of an instance \mathbf{x} , denoted by k -distance(\mathbf{x}), gives the distance of instance \mathbf{x} to its k^{th} nearest neighbor:

$$k\text{-distance}(\mathbf{x}) \equiv d(\mathbf{x}, \mathbf{x}^{(i)}) \text{ such that} \quad (2.9)$$

$$d(\mathbf{x}, \mathbf{x}^{(j)}) \leq d(\mathbf{x}, \mathbf{x}^{(i)}) \text{ for at least } k \text{ instances}$$

$$d(\mathbf{x}, \mathbf{x}^{(j)}) < d(\mathbf{x}, \mathbf{x}^{(i)}) \text{ for at most } k - 1 \text{ instances}$$

The k -distance neighborhood of an instance \mathbf{x} , denoted by $\mathcal{N}_k(\mathbf{x})$, contains all the instances that are closer to \mathbf{x} than its k -distance(\mathbf{x}) value:

$$\mathcal{N}_k(\mathbf{x}) = \{\mathbf{x}^{(t)} \in \mathcal{X} \setminus \{\mathbf{x}\} | d(\mathbf{x}, \mathbf{x}^{(t)}) < k\text{-distance}(\mathbf{x})\} \quad (2.10)$$

The reachability distance of an instance \mathbf{x} with respect to another instance $\mathbf{x}^{(i)}$ is the distance between the two instances, but in order to prevent unnecessary fluctuations, reachability distances are smoothed in k -distance neighborhoods by assigning the same reachability distance to instances that are in the neighborhood of $\mathbf{x}^{(i)}$:

$$\text{reachdist}_k(\mathbf{x}, \mathbf{x}^{(i)}) = \max\{k\text{-distance}(\mathbf{x}^{(i)}), d(\mathbf{x}, \mathbf{x}^{(i)})\} \quad (2.11)$$

The local reachability density measures how easy it is to reach a certain instance and is calculated as the inverse of the average reachability distances of instances in the k -distance neighborhood:

$$\text{lrd}_k(\mathbf{x}) = \frac{|\mathcal{N}_k(\mathbf{x})|}{\sum_{\mathbf{x}^{(i)} \in \mathcal{N}_k(\mathbf{x})} \text{reachdist}_k(\mathbf{x}, \mathbf{x}^{(i)})} \quad (2.12)$$

After defining the local reachability density, we may move on to the final step where we calculate the local outlier factor for each instance. We expect instances with high variance between local reachability densities of its neighbors to take higher LOF values:

$$\text{LOF}_k(\mathbf{x}) = \frac{\sum_{\mathbf{x}^{(i)} \in \mathcal{N}_k(\mathbf{x})} \frac{\text{lrd}_k(\mathbf{x}^{(i)})}{\text{lrd}_k(\mathbf{x})}}{|\mathcal{N}_k(\mathbf{x})|} \quad (2.13)$$

Each specific problem requires a separate parameter search step to find the optimum k value. Moreover, the LOF values are quite sensitive to the value of k and may exhibit unstable behavior as k changes. In order to minimize the instability of the LOF values, authors propose calculating LOF values for various k values and taking the maximum of them for each instance. Although, it is possible to apply different heuristics to combine multiple LOF values, taking the maximum gives more impor-

tance to the LOF values individually and does not risk missing any possible outliers.

Figure 2.3 lists the algorithm for the LOF method. By iterating over all the instances and the k values, the algorithm calculates the LOF of each instance for all values of k and takes the maximum. The algorithm returns the scores for each data instance and how these scores will be utilized is left to be handled by the specific problem that the LOF method is applied to as with other outlier detection algorithms, a cut-off threshold may be finetuned using a separate validation set or the top n outliers may be reported by sorting the scores.

```

LOF(Input data set  $\mathcal{X} = \{\mathbf{x}^{(t)}\}_{t=1}^N$ , Minimum neighbors  $k_{min}$ , Maximum
neighbors  $k_{max}$ )
for  $t = 1$  to  $N$  do
  for  $k = k_{min}$  to  $k_{max}$  do
    Find  $k$ -distance( $\mathbf{x}^{(t)}$ ) from Equation 2.9
    Find  $k$ -distance neighborhood,  $\mathcal{N}_k$  of  $\mathbf{x}^{(t)}$  from Equation 2.10
    Calculate reachdist $_k(\mathbf{x}^{(t)}, \mathbf{x}^{(i)})$  for instance pairs  $\mathbf{x}^{(t)}$  and  $\mathbf{x}^{(i)} \in \mathcal{N}_k(\mathbf{x}^{(t)})$  from
    Equation 2.11
    Calculate lrd $_k(\mathbf{x}^{(i)})$  for  $\mathbf{x}^{(i)} \in \{\mathbf{x}^{(t)}\} \cup \mathcal{N}_k(\mathbf{x}^{(t)})$  from Equation 2.12
    Calculate LOF $_k(\mathbf{x}^{(t)})$  from Equation 2.13
  end for
  LOF( $\mathbf{x}^{(t)}$ ) = max(LOF $_{k_{min}}, \dots, \text{LOF}_{k_{max}}$ )
end for
return LOF

```

Figure 2.3. LOF method algorithm.

2.2.1. Feature Bagging for Outlier Detection

Bagging [30], based on the idea of training multiple classifiers on random subsets of data, is a widely employed statistical method to improve the accuracy of learners. In feature bagging, or more popularly random forests, multiple classifiers are trained

on random feature subsets of data [31]. By using random subspaces, high dimensional data can be more easily processed and the accuracy of the learner will be less affected by the noisy features in the data set. Lazarevic *et al.* apply feature bagging to the outlier detection problem and propose two alternatives to combine the outlier scores [32]. These scores need not come from the same outlier detection method, since only outlier scores or ranks are necessary for each instance. Denoting the number of outlier detection methods by M , Feature Bagging selects M random feature subsets of the data in random sizes between $\lfloor d/2 \rfloor$ and $(d - 1)$ and presents these to outlier detection methods. Each outlier detection method outputs an outlier score vector $\mathbf{y}_m, m = 1, \dots, M$ that contains the scores for instances in the input data set $\mathcal{X} = \{\mathbf{x}^{(t)}\}_{t=1}^N$. Afterwards, these outlier scores $\mathbf{y}_m, m = 1, \dots, M$ are combined to obtain the final outlier scores for each instance. The algorithm can be seen in Figure 2.4.

```

FeatureBagging(Outlier Detection Method  $g_o$ , Number of methods  $M$ ,
Input data set  $\mathcal{X} = \{\mathbf{x}^{(t)}\}_{t=1}^N$  where  $\mathbf{x}^{(t)} = \{x_1^{(t)}, \dots, x_d^{(t)}\}$  )
for  $m = 1$  to  $M$  do
     $d_m =$  Random integer in interval  $[\lfloor d/2 \rfloor, (d - 1)]$ 
    Randomly pick  $d_m$  features to create subset  $\mathcal{X}_m$ 
    Calculate outlier scores  $\mathbf{y}_m$  using method  $g_o$ ,  $\mathbf{y}_m = g_o(\mathcal{X}_m)$ 
end for
Combine scores,  $\mathbf{y}_{final} = \text{COMBINE}(\mathbf{y}_m), m = 1, \dots, M$ 
return  $\mathbf{y}_{final}$ 

```

Figure 2.4. Feature bagging method algorithm.

In breadth-first combination, whose pseudo-code is given in Figure 2.5, the outlier scores \mathbf{y}_m are sorted in descending order to obtain the indices of instances \mathbf{Ind}_m from the highest scored outlier to the lowest ones. The outlier scores are merged into a final list in a breadth-first manner by taking the first indices from each method's sorted score vector, then the second ones and so on. With this approach, each instance gets the outlier score that puts it to the highest rank among methods. It should be noted that this scheme of combination is not equivalent to taking the maximum outlier score

for each instance, since the outlier score intervals among methods may and most of the time will differ. In certain scenarios, it might be rational to normalize each score vector to the same scale to prevent such an effect.

```

COMBINE-BreadthFirst(Outlier Scores  $\mathbf{y}_m, m = 1, \dots, M$  where  $\mathbf{y}_m =$ 
 $\{y_m^1, y_m^2, \dots, y_m^N\}$  )
Sort all score vectors to obtain sorted vector;  $\mathbf{s}_m$  and indices of instances in sorted
vector  $\mathbf{Ind}_m$ 
Initialize empty  $\mathbf{y}_{final}$  and  $\mathbf{Ind}_{final}$ 
for  $n = 1$  to  $N$  do
  for  $m = 1$  to  $M$  do
    if  $\mathbf{Ind}_m(n) \notin \mathbf{Ind}_{final}$  then
      Append  $\mathbf{Ind}_m(n)$  to  $\mathbf{Ind}_{final}$ 
      Append  $\mathbf{s}_m(n)$  to  $\mathbf{y}_{final}$ 
    end if
  end for
end for
return  $\mathbf{Ind}_{final}$  and  $\mathbf{y}_{final}$ 

```

Figure 2.5. Feature bagging breadth-first combination algorithm.

In cumulative sum combination, the individual scores for each instance are summed to obtain the final outlier score. However, summing the scores may prove to be more useful when the outliers can only be detected in certain feature subsets. The pseudo code of the algorithm is given in Figure 2.6.

```

COMBINE-CumulativeSum(Outlier Scores  $\mathbf{y}_m, m = 1, \dots, M$  where  $\mathbf{y}_m =$ 
 $\{y_m^1, y_m^2, \dots, y_m^N\}$  )
for  $n = 1$  to  $N$  do
     $\mathbf{y}_{final} = \sum_{m=1}^M \mathbf{y}_m^{(n)}$ 
end for
return  $\mathbf{y}_{final}$ 

```

Figure 2.6. Feature bagging cumulative-sum combination algorithm.

2.3. One-Class Support Vector Machine

One-Class Support Vector Machine by Schölkopf *et al.* [12] is an unsupervised variant of the Support Vector Machine (SVM) [33]. SVM is a classification algorithm that finds the hyperplane that separates two classes with maximum margin. It is generally used with the kernel trick to map input data to a non-linear feature space. One-Class Support Vector Machine extends this algorithm to unsupervised case by finding the plane that separates the input data in feature space from the origin with maximum margin. It solves the problem of finding a binary function that gives 1 in regions where $p(x)$ is high and -1 where $p(x)$ is low, i.e., estimates the support of the distribution p . The problem is regularized by adding a smoothness constraint on the estimated function. When considered from the perspective of outlier detection, estimating the support is an easier and less general problem than density estimation.

Let $x^{(t)} \in \mathcal{X}, t = 1 \dots N$, drawn from distribution $p(x)$ be our input data. \mathcal{H} is the set of subsets of \mathcal{X} and λ is a real valued function defined on \mathcal{H} . The quantile function U is defined as

$$U(\alpha) = \inf\{\lambda(H) : p(H) \geq \alpha, H \in \mathcal{H}\}, \quad 0 \leq \alpha \leq 1. \quad (2.14)$$

The subset H that achieves the infimum for a certain α is denoted by $H(\alpha)$. If λ is chosen to be the volume of the input set, $H(\alpha)$ is the minimum volumed set that con-

tains a fraction α of the probability mass. For $\alpha = 1$, $H(1)$ contains the support of the distribution p . If we can find the subset H for a specified α value, we can predict if a test instance is an outlier by checking if it is out of H .

One-Class Support Vector algorithm chooses a λ measure that controls the smoothness of the estimated function instead of the volume of the set. The subset H is defined by the function f that depends on the parameter of the hyperplane w , $H_w = \{\mathbf{x} : f_w(\mathbf{x}) \geq \rho\}$, and the magnitude of the weight vector w is minimized, $\lambda(H_w) = \|\mathbf{w}\|^2$. Here, ρ is an offset parameterizing the hyperplane. The input data is mapped to a non-linear space by function $\phi : \mathcal{X} \rightarrow F$ and the inner product in this new space defines a kernel function $K(\mathbf{x}^{(i)}, \mathbf{x}^{(j)}) = \phi(\mathbf{x}^{(i)})^T \phi(\mathbf{x}^{(j)})$. The aim is to find a function f that returns 1 in a small region capturing most of the data and -1 elsewhere. This is achieved by mapping the input data to the feature space and separating it from the origin with maximum margin. The value of f for a test point is determined by the side of the hyperplane it falls on in feature space. The binary function f is found by solving the following quadratic program:

$$\begin{aligned} \min_{\mathbf{w}, \xi, \rho} \quad & \frac{1}{2} \|\mathbf{w}\|^2 + \frac{1}{\nu N} \sum_i \xi_i - \rho \\ \text{subject to} \quad & (\mathbf{w}^T \phi(\mathbf{x}^{(i)})) \geq \rho - \xi_i, \quad \xi_i \geq 0. \end{aligned} \quad (2.15)$$

Here, $\nu \in (0, 1]$ is a trade-off parameter that controls the effect of smoothness and the error on the estimated function. The decision function f is then given as:

$$f(\mathbf{x}) = \text{sgn}(\mathbf{w}^T \phi(x) - \rho) \quad (2.16)$$

where $\text{sgn}(x)$ is the sign function that equals 1 for $x \geq 0$. We write the Lagrangian by using the multipliers $\alpha_i, \beta_i \geq 0$:

$$\mathcal{L}(\mathbf{w}, \xi, \rho, \boldsymbol{\alpha}, \boldsymbol{\beta}) = \frac{1}{2} \|\mathbf{w}\|^2 + \frac{1}{\nu N} \sum_i \xi_i - \rho - \sum_i \alpha_i (\mathbf{w}^T \phi(x^{(i)}) - \rho + \xi_i) - \sum_i \beta_i \xi_i. \quad (2.17)$$

We set the derivatives with respect to \mathbf{w} , ξ and ρ equal to zero and get

$$\mathbf{w} = \sum_i \alpha_i \phi(\mathbf{x}^{(i)}) \quad (2.18)$$

$$\alpha_i = \frac{1}{\nu N} - \beta_i, \quad \sum_i \alpha_i = 1. \quad (2.19)$$

All training instances $\mathbf{x}^{(i)}$ that have $\alpha_i \geq 0$ are called support vectors and they define the hyperplane along with ρ . If we substitute \mathbf{w} into the decision function f , we get

$$f(\mathbf{x}) = \text{sgn} \left(\sum_i \alpha_i K(\mathbf{x}^{(i)}, \mathbf{x}) - \rho \right). \quad (2.20)$$

The support vectors are the instances that lie on the hyperplane and their ξ_i values are zero. Therefore, we can calculate the value of ρ from any of the support vectors by

$$\rho = \mathbf{w}^T \phi(\mathbf{x}^{(i)}) = \sum_j \alpha_j K(\mathbf{x}^{(j)}, \mathbf{x}^{(i)}). \quad (2.21)$$

As we have pointed out earlier, ν controls the trade-off between error and smoothness. If ν approaches zero, all the training instances are forced to lie on the same side of the hyperplane since errors are punished severely. However, as ν increases, the smoothness of the decision function becomes more and more important and more margin errors are allowed. Schölkopf *et al.* show that ν is an upper bound on the fraction of outliers, i.e., training instances that are not covered by the decision function [12]. It is also a lower bound on the fraction of support vectors.

2.4. Parzen Windows

Parzen Windows (PW) is a non-parametric density estimation method [14]. While a naive estimation for the density around an instance \mathbf{x} can be calculated by counting the number of instances that fall into the same neighborhood with it, Parzen Windows

uses a kernel function to obtain soft counts. In that case, all $\mathbf{x}^{(t)}$ have an effect on the density around \mathbf{x} but this effect decreases smoothly as $\|\mathbf{x} - \mathbf{x}^{(t)}\|$ increases [1]:

$$\hat{p}(\mathbf{x}) = \frac{1}{Nw} \sum_{t=1}^N K\left(\frac{\mathbf{x} - \mathbf{x}^{(t)}}{w}\right) \quad (2.22)$$

Here, w is the size of the bin and $K : \mathbb{R}^d \rightarrow \mathbb{R}$ is a kernel function that takes maximum value when its argument is 0 and decreases symmetrically as it increases. The Gaussian kernel is widely used:

$$K_{Gaussian}(\mathbf{u}) = \left(\frac{1}{2\pi}\right)^d \exp\left(\frac{-\|\mathbf{u}\|^2}{2}\right) \quad (2.23)$$

A nice property of Parzen Windows is that $\hat{p}(\mathbf{x})$ inherits all the continuity and differentiability characteristics of the kernel function. However, determining an optimum bin size is difficult and a problem specific parameter search needs to be done. Furthermore, a fixed value of bin size for the whole input space may not work well if local densities vary greatly.

Parzen Windows can be used for outlier detection by estimating the density from training set around a test instance and the inverse of this density can be used a measure of being an outlier. These outlier scores can be converted to hard decisions by using a threshold or reporting the top scored instances as outliers. Though an unsupervised method in nature, Parzen Windows can work in a semi-supervised manner by estimating the density from only the typical instances if labels are available. The pseudo-code of algorithm is given in Figure 2.7. The density for each input instance is calculated from Equation 2.22 and these are normalized to $[0, 1]$. Outlier scores are given by subtracting density values from 1.

```
ParzenWindows(Input data set  $\mathcal{X} = \{\mathbf{x}^{(t)}\}_{t=1}^N$ , Bin Size  $w$ , Kernel Function  $K$  )  
for  $i = 1$  to  $N$  do  
     $p_i = \frac{1}{Nh} \sum_{t=1}^N K\left(\frac{\mathbf{x}^{(i)} - \mathbf{x}^{(t)}}{w}\right)$   
end for  
Normalize  $p_i = \frac{p_i}{\sum_{j=1}^N p_j}$   
Convert density to outlier score,  $os_i = 1 - p_i$   
return  $os$ 
```

Figure 2.7. Parzen Windows algorithm.

3. SPECTRAL METHODS

Spectral methods are unsupervised learning techniques that reveal low dimensional structure in dimensional data [34]. These methods use the spectral decomposition of specially constructed matrices to reduce dimensionality and transform the input data to a new space.

We define the following problem. Let us assume that we have $N \times d$ data matrix $\mathbf{X} = [\mathbf{x}^{(t)}]_{t=1}^N$ where $\mathbf{x}^{(t)} \in \mathbb{R}^d$. We want to reach a lower dimensional representation $\mathbf{Z}_{N \times m}$ for the N instances such that $\mathbf{z}^{(t)} \in \mathbb{R}^m$ where $m < d$. We assume, without loss of generality, that \mathbf{X} is centered, i.e., $\sum_t \mathbf{x}^{(t)} = \mathbf{0}$.

Spectral methods find \mathbf{Z} by first constructing a similarity matrix \mathbf{S} or distance matrix \mathbf{E} . Let us say that we have a similarity matrix \mathbf{S} . Then, its spectral decomposition $\mathbf{S} = \mathbf{W}\mathbf{\Lambda}\mathbf{W}^T$ is calculated, where \mathbf{W} is a $N \times d$ matrix whose columns are the eigenvectors of \mathbf{S} and $\mathbf{\Lambda}$ is a $d \times d$ diagonal matrix whose entries are the corresponding eigenvalues. Assuming that eigenvalues are sorted in ascending order, we take the last m eigenvectors from \mathbf{W} to be our transformed data \mathbf{Z} for dimensionality reduction. If we use a distance matrix, we take the first m eigenvectors. Before reviewing various spectral methods, we analyze this generic algorithm in order to understand why this approach works and what it minimizes as the cost function. We carry out the following analysis with a similarity matrix \mathbf{S} but it is equally valid for a distance matrix since every distance matrix \mathbf{E} can be used as a similarity matrix by setting simply $\mathbf{S} = -\mathbf{E}$.

Let us say that we want to find a lower dimensional representation $\mathbf{Z}_{N \times m}$ for input data where the dot products in this new space matches the similarities as closely as possible. In other words, we need to minimize the following cost function:

$$C_{generic} \equiv \|\mathbf{S} - \mathbf{Z}\mathbf{Z}^T\|_F^2 = \text{tr}[(\mathbf{S} - \mathbf{Z}\mathbf{Z}^T)^T(\mathbf{S} - \mathbf{Z}\mathbf{Z}^T)] = \sum_{i,j} [(S_{ij} - (\mathbf{z}^{(i)})^T(\mathbf{z}^{(j)}))]^2 \quad (3.1)$$

Equation 3.1 is known as *low rank matrix approximation problem* and its solution is given by the singular value decomposition of $\mathbf{S} = \mathbf{U}\mathbf{\Sigma}\mathbf{V}^T$ [35]. Hence, taking the m left singular vectors with the greatest singular values from \mathbf{V} gives \mathbf{Z} (in order for the actual dot product values in the new space to match \mathbf{S} values, we need to take $\mathbf{Z} = \mathbf{U}\mathbf{\Sigma}^{1/2}$ but this is not necessary as $\mathbf{\Sigma}$ is only a scaling matrix and does not affect the transformation). The cost function in Equation 3.1 can also be reformulated as:

$$\sum_{i,j} (S_{ij} - (\mathbf{z}^{(i)})^T (\mathbf{z}^{(j)}))^2 = \text{tr}(\mathbf{S}\mathbf{S}^T) - \text{tr}(2\mathbf{Z}^T\mathbf{S}\mathbf{Z}) + \text{tr}(\mathbf{Z}\mathbf{Z}^T\mathbf{Z}\mathbf{Z}^T) \quad (3.2)$$

If we add the constraint $\mathbf{Z}^T\mathbf{Z} = \mathbf{I}$ to remove the effect of arbitrary scaling and note that $\text{tr}(\mathbf{Z}\mathbf{Z}^T) = \text{tr}(\mathbf{Z}^T\mathbf{Z})$, $\text{tr}(\mathbf{S}\mathbf{S}^T)$ is constant and does not depend on \mathbf{Z} , minimization of Equation 3.1 is equivalent to the maximization of

$$C_{generic_2} \equiv \text{tr}(\mathbf{Z}^T\mathbf{S}\mathbf{Z}) \quad (3.3)$$

This is a *trace maximization problem* and its solution is given by the eigenvectors of \mathbf{S} with the greatest eigenvalues [36]. Therefore, using spectral decomposition of a similarity matrix corresponds to assuming that the matrix gives the dot products of instances and we minimize the cost function of Equation 3.1 or maximize the Equation 3.3 to approximate these values in the new space as closely as possible.

3.1. Principal Components Analysis

Principal Components Analysis (PCA) is a well-known dimensionality reduction method that minimizes the projection error [37]. We have a transformation matrix $\mathbf{W}_{d \times m}$ that is orthonormal $\mathbf{W}^T\mathbf{W} = \mathbf{I}$ and our transformed data is $\mathbf{Z} = \mathbf{X}\mathbf{W}$. We project \mathbf{Z} back to the original space as $\hat{\mathbf{X}} = \mathbf{Z}\mathbf{W}^T$ and then minimize the reconstruction error:

$$C_{PCA} \equiv \|\mathbf{X} - \hat{\mathbf{X}}\|_F^2 = \|\mathbf{X} - \mathbf{Z}\mathbf{W}^T\|_F^2 \quad (3.4)$$

By expanding this cost function, we can show that the minimization of the projection error is equivalent to variance maximization in the transformed space:

$$\begin{aligned}
\|\mathbf{X} - \mathbf{Z}\mathbf{W}^T\|_F^2 &= \text{tr}[(\mathbf{X} - \mathbf{Z}\mathbf{W}^T)(\mathbf{X} - \mathbf{Z}\mathbf{W}^T)^T] \\
&= \text{tr}(\mathbf{X}^T\mathbf{X} - \mathbf{X}\mathbf{W}\mathbf{Z}^T - \mathbf{Z}\mathbf{W}^T\mathbf{X}^T + \mathbf{Z}\mathbf{W}^T\mathbf{W}\mathbf{Z}^T) \\
&= \text{tr}(\mathbf{X}^T\mathbf{X} - \mathbf{Z}\mathbf{Z}^T - \mathbf{Z}\mathbf{Z}^T + \mathbf{Z}\mathbf{Z}^T) \\
&= \text{tr}(\mathbf{X}^T\mathbf{X}) - \text{tr}(\mathbf{Z}^T\mathbf{Z})
\end{aligned}$$

Therefore, an alternative formulation for the cost function is as follows:

$$C_{PCA_2} \equiv \text{tr}(\mathbf{W}^T\mathbf{X}^T\mathbf{X}\mathbf{W}) \quad (3.5)$$

Hence, the transformation matrix \mathbf{W} that minimizes the projection error and maximizes the variance is given by the m greatest eigenvectors of $\mathbf{X}^T\mathbf{X}$, which is the covariance matrix when $\mathbb{E}[\mathbf{X}] = 0$.

In practice, for very high dimensional and low size samples PCA is carried out with the Gramian matrix $\mathbf{G} = \mathbf{X}\mathbf{X}^T$ instead of the covariance matrix. In that case, the eigenvectors of \mathbf{G} gives directly the transformed data \mathbf{Z} because (\mathbf{w} is an eigenvector and λ is its eigenvalue):

$$\begin{aligned}
(\mathbf{X}^T\mathbf{X})\mathbf{w} &= \lambda\mathbf{w} \quad (\text{multiply from left with } \mathbf{X}) \\
(\mathbf{X}\mathbf{X})^T\mathbf{X}\mathbf{w} &= \lambda\mathbf{X}\mathbf{w}
\end{aligned}$$

3.2. Kernel Principal Components Analysis

Kernel Principal Components Analysis (KPCA) is a non-linear generalization of PCA [38]. It is motivated by the desire to apply PCA in the feature space F which is possibly infinite dimensional and the mapping function $\phi : \mathbb{R}^d \rightarrow F$ defines this nonlinear transformation. If we have a kernel function $K : \mathbb{R}^d \times \mathbb{R}^d \rightarrow \mathbb{R}$ where

$K(\mathbf{x}^{(i)}, \mathbf{x}^{(j)}) = \phi(\mathbf{x}^{(i)})^T \phi(\mathbf{x}^{(j)})$, we can apply PCA by taking the eigenvectors as our transformed points (in that case we do not have an explicit transformation matrix but only the transformed data):

$$\begin{aligned} (\phi(\mathbf{X})^T \phi(\mathbf{X}))\mathbf{w} &= \lambda\mathbf{w} \quad (\text{multiply from left with } \phi(\mathbf{X})) \\ (\phi(\mathbf{X})\phi(\mathbf{X})^T)\phi(\mathbf{X})\mathbf{w} &= \lambda\phi(\mathbf{X})\mathbf{w} \\ \mathbf{K}\mathbf{z} &= \lambda\mathbf{z} \end{aligned}$$

Therefore, the spectral decomposition of \mathbf{K} gives us our transformed points, \mathbf{Z} . When $\phi(\mathbf{x}) = \mathbf{x}$, KPCA reduces to PCA. This is equivalent to using \mathbf{K} as our similarity matrix. Hence, KPCA tries to find a low dimensional representation where dot products in the new space closely matches the dot products in the feature space. The cost function minimized by KPCA is:

$$C_{KPCA} \equiv \sum_{i,j} (\phi(\mathbf{x}^{(i)})^T \phi(\mathbf{x}^{(j)}) - (\mathbf{z}^{(i)})^T (\mathbf{z}^{(j)}))^2 \quad (3.6)$$

Although, the input data is centered, it may not be in the feature space. However, we do not have the data in the feature space explicitly, meaning that we cannot simply calculate the mean and subtract it. Instead, we write $\tilde{\phi}(\mathbf{x}) = \phi(\mathbf{x}) - (1/N) \sum_t \phi(\mathbf{x}^{(t)})$ and $\tilde{\mathbf{K}} = \tilde{\phi}(\mathbf{x})^T \tilde{\phi}(\mathbf{x})$ to reach the following normalization to center \mathbf{K} where $\mathbf{1}_N$ is an $N \times N$ matrix with $(\mathbf{1}_N)_{ij} := 1/N$ [39]:

$$\tilde{\mathbf{K}} = \mathbf{K} - \mathbf{1}_N \mathbf{K} - \mathbf{K} \mathbf{1}_N + \mathbf{1}_N \mathbf{K} \mathbf{1}_N \quad (3.7)$$

The mean subtraction step augments the minimized cost function:

$$C_{KPCA_{mc}} \equiv \sum_{i,j} ((\phi(\mathbf{x}^{(i)}) - \tilde{\phi}(\mathbf{x}))^T (\phi(\mathbf{x}^{(j)}) - \tilde{\phi}(\mathbf{x})) - (\mathbf{z}^{(i)})^T (\mathbf{z}^{(j)}))^2 \quad (3.8)$$

3.3. Multidimensional Scaling

Multidimensional Scaling (MDS) is a family of dimensionality reduction methods with many variants. Here, we discuss the *Classical (or Metric) MDS* where the aim is to preserve the Euclidean distances in the projected space as closely as possible [40]. MDS uses the distance matrix $\mathbf{E}_{N \times N}$ where E_{ij} is assumed to be the Euclidean distance between $\mathbf{x}^{(i)}$ and $\mathbf{x}^{(j)}$: $\|\mathbf{x}^{(i)} - \mathbf{x}^{(j)}\|$. In order to find the best low dimensional representation that approximates the pairwise Euclidean distances as well as possible, the dot product matrix $\mathbf{B} = \mathbf{X}\mathbf{X}^T$ is obtained from \mathbf{E} [1]:

$$\mathbf{B} = -\frac{1}{2}(\mathbf{E} - \mathbf{1}_N\mathbf{E} - \mathbf{E}\mathbf{1}_N + \mathbf{1}_N\mathbf{E}\mathbf{1}_N) \quad (3.9)$$

We use the spectral decomposition of \mathbf{B} to get our transformed data \mathbf{Z} by taking the desired number of eigenvectors of \mathbf{B} starting from the ones with the greatest eigenvalues again. It is clear that we are trying to match the dot products of the transformed instances \mathbf{z} to the actual values in \mathbf{B} . In addition, since \mathbf{B} is obtained from the Euclidean distance matrix \mathbf{E} , the Euclidean distances between the points in the new space approximate the original distances in \mathbf{E} . MDS minimizes the cost function:

$$C_{MDS} \equiv \sum_{i,j} (\|\mathbf{x}^{(i)} - \mathbf{x}^{(j)}\|^2 - \|\mathbf{z}^{(i)} - \mathbf{z}^{(j)}\|^2)^2 \quad (3.10)$$

If \mathbf{E} contains the actual Euclidean distances calculated in the original space, MDS is equivalent to PCA.

3.4. Laplacian Eigenmaps

Laplacian Eigenmaps (LEM) assumes that each input instance denotes a node in a graph and uses the adjacency matrix as a similarity matrix [41]. Each instance is connected to only a small number of nearby instances resulting in a sparse adjacency matrix. Edges between connected instances S_{ij} are given constant weight or are weighted by a Gaussian kernel. However, we may use any similarity measure for

weighting the edges. LEM solves the following generalized eigenvalue problem to transform the input data where $\mathbf{D}_{N \times N}$ is the diagonal matrix of column (or row) sums of \mathbf{S} , $D_{ii} = \sum_j S_{ij}$.

$$(\mathbf{D} - \mathbf{S})\mathbf{z} = \lambda\mathbf{D}\mathbf{z} \quad (3.11)$$

We omit the eigenvector with the eigenvalue 0 and take the desired number of eigenvectors starting from the ones with smallest eigenvalues to obtain our transformed data \mathbf{z} . It is known that LEM minimizes the following cost function:

$$C_{LEM} \equiv \sum_{i,j} \|\mathbf{z}^{(i)} - \mathbf{z}^{(j)}\|^2 S_{ij} \quad (3.12)$$

Let us assume that the new \mathbf{z} are one dimensional. Then, \mathbf{z} is a $N \times 1$ vector where

$$\begin{aligned} \sum_{i,j} (\mathbf{z}^{(i)} - \mathbf{z}^{(j)})^2 S_{ij} &= \sum_{i,j} ((\mathbf{x}^{(i)})^2 + (\mathbf{x}^{(j)})^2 - 2\mathbf{x}^{(i)}\mathbf{x}^{(j)}) S_{ij} \\ &= \sum_i (\mathbf{x}^{(i)})^2 D_{ii} + \sum_j (\mathbf{x}^{(j)})^2 D_{jj} - 2 \sum_{i,j} \mathbf{x}^{(i)}\mathbf{x}^{(j)} S_{ij} \\ &= 2\mathbf{z}^T (\mathbf{D} - \mathbf{S})\mathbf{z} \end{aligned}$$

Therefore, in order to minimize Equation 3.12, we need to minimize $\mathbf{z}^T (\mathbf{D} - \mathbf{S})\mathbf{z}$. We add the constraint $\mathbf{z}^T \mathbf{D}\mathbf{z} = 1$ to remove the effect of arbitrary scaling in the solution. This optimization problem is solved by the generalized eigenvalue problem given in Equation 3.11.

3.5. Discussion

In Table 3.1, we list the cost functions minimized/maximized by the dimensionality reduction methods. We assume that the reduced number of dimensions is 1, $m = 1$, in order to get rid of trace operators for the sake of simplicity.

Table 3.1. Comparison of cost functions optimized by dimensionality reduction methods.

Method	Minimized/Maximized Cost Function
PCA	$\max \mathbf{W}^T (\mathbf{X}^T \mathbf{X}) \mathbf{W}$ $\min \ \mathbf{X} - \mathbf{Z}\mathbf{W}^T\ _F^2$
KPCA	$\max \mathbf{Z}^T (\mathbf{K}) \mathbf{Z}$ $\min \ \mathbf{K} - \mathbf{Z}\mathbf{Z}^T\ _F^2$ $\min \sum_{i,j} (\phi(\mathbf{x}^{(i)})^T \phi(\mathbf{x}^{(j)}) - (\mathbf{z}^{(i)})^T (\mathbf{z}^{(j)}))^2$
KPCA-MC	$\max \mathbf{Z}^T (\tilde{\mathbf{K}}) \mathbf{Z}$ $\min \ \tilde{\mathbf{K}} - \mathbf{Z}\mathbf{Z}^T\ _F^2$ $\min \sum_{i,j} ((\phi(\mathbf{x}^{(i)}) - \tilde{\phi}(\mathbf{x}))^T (\phi(\mathbf{x}^{(j)}) - \tilde{\phi}(\mathbf{x})) - (\mathbf{z}^{(i)})^T (\mathbf{z}^{(j)}))^2$
LEM	$\min \mathbf{Z}^T (\mathbf{D} - \mathbf{S}) \mathbf{Z}$ $\min \sum_{i,j} \ \mathbf{z}^{(i)} - \mathbf{z}^{(j)}\ ^2 \mathbf{S}_{ij}$
MDS	$\max \mathbf{Z}^T (\mathbf{B}) \mathbf{Z}$ $\min \sum_{i,j} (\ \mathbf{x}^{(i)} - \mathbf{x}^{(j)}\ ^2 - \ \mathbf{z}^{(i)} - \mathbf{z}^{(j)}\ ^2)^2$

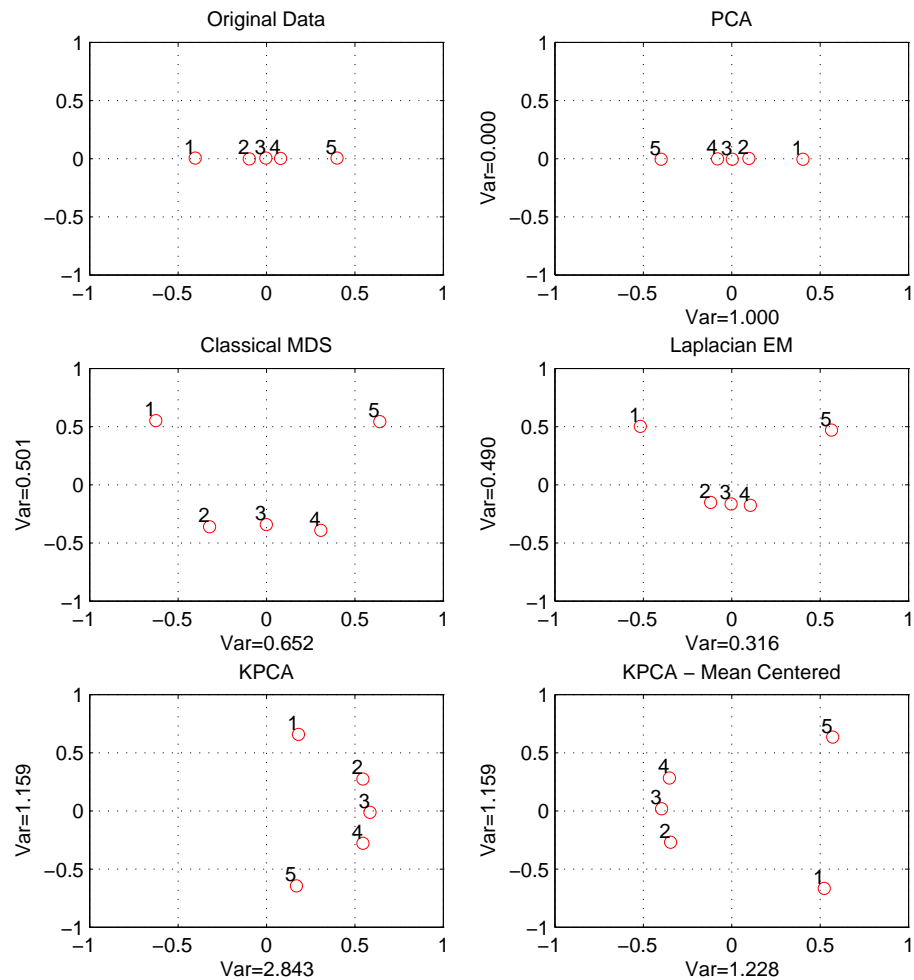


Figure 3.1. LEM, KPCA, KPCA-Mean centered and MDS transformations of a synthetic sample with Gaussian kernel with $\sigma = .1$ and neighbor count $k = 2$.

3.5.1. Approximating Dot Products or Euclidean Distances

Simply using \mathbf{S} to reduce dimensionality amounts to matching dot products in the new space to similarity values given in \mathbf{S} . This is also the case for KPCA where no mean subtraction is performed; however, LEM and MDS deal with the Euclidean distances in the new space. Since \mathbf{S} is a similarity matrix with no negative elements, all the dot products of $\mathbf{z}^{(i)}$ vectors need to be non-negative, thus forcing all $\mathbf{z}^{(i)}$ to the same half-space as seen under KPCA in Figure 3.1.

3.5.2. Mean Centered KPCA is Equivalent to Classical MDS

It is apparent that the mean subtraction step in KPCA is identical to the extraction of dot products from the Euclidean matrix \mathbf{E} . Similarity matrix \mathbf{S} can be used as a distance matrix as $\mathbf{E} = -\mathbf{S}$, then mean-centered KPCA is identical to MDS. Therefore, we can claim that mean subtraction modifies the cost function to approximate Euclidean distances instead of dot products. A similar transition to the Euclidean distances from the dot products is achieved in LEM by using $\mathbf{D} - \mathbf{S}$ matrix. Whereas using spectral decomposition of \mathbf{S} approximates dot products, LEM minimizes the cost function in Equation 3.12 involving Euclidean distances by using $\mathbf{D} - \mathbf{S}$ matrix.

3.5.3. How LEM Differs from MDS and KPCA

The cost function minimized by MDS shows us that it approximates the distances in the original space with the Euclidean distances in the new space. LEM's cost function is different in the sense that it weights the Euclidean distances with similarity values paying more attention to keeping highly similar points close in the new space. For example in Figure 3.1, three points in the middle, which are more similar to each other, are mapped to relatively closer points by LEM, while this is not the case for MDS.

4. SPECTRAL OUTLIER DETECTION

4.1. The Idea

In this chapter, we propose our *spectral outlier detection* method that combines spectral decomposition with outlier detection. We argue that applying spectral decomposition on input data before outlier detection has various advantages.

Methods that rely on distances between instances, for instance, density estimation techniques for outlier detection such as LOF or Parzen Windows, perform poorly as the number of dimensions increases. The amount of instances that fall into a fixed size bin decreases dramatically as the dimensionality increases, thus, making it impossible to estimate a smooth density. Furthermore, distance functions lose their meaning in high dimensions since pairwise distances tend to be similar for all instances. Although not as vulnerable as density estimation methods, discriminative methods suffer from high dimensionality too. For instance, suppose that our method learns a tight boundary, like in Active-Outlier, then, it is possible to learn a tighter boundary in a lower dimensional space if data can be projected to lower dimensions with minimal loss of information. Moreover, processing a higher dimensional data requires more computation. Hence, reducing input dimensionality with a spectral method alleviates the effect of the curse of dimensionality and possibly improves outlier detection performance.

Spectral methods find low dimensional structures in data and transform possibly complicated patterns to smoother ones, therefore, making it possible for discriminative methods to fit simpler boundaries. In Figure 4.1, a circular data set is seen along with the boundaries learned by the Active-Outlier method. Different contours correspond to boundaries for a different threshold value Θ . After applying KPCA on this data set, we obtain the boundaries seen in Figure 4.2. It is clear that the nonlinear to linear transformation achieved by the spectral method makes it possible for Active-Outlier method to learn much simpler boundaries. This advantage of spectral methods is also

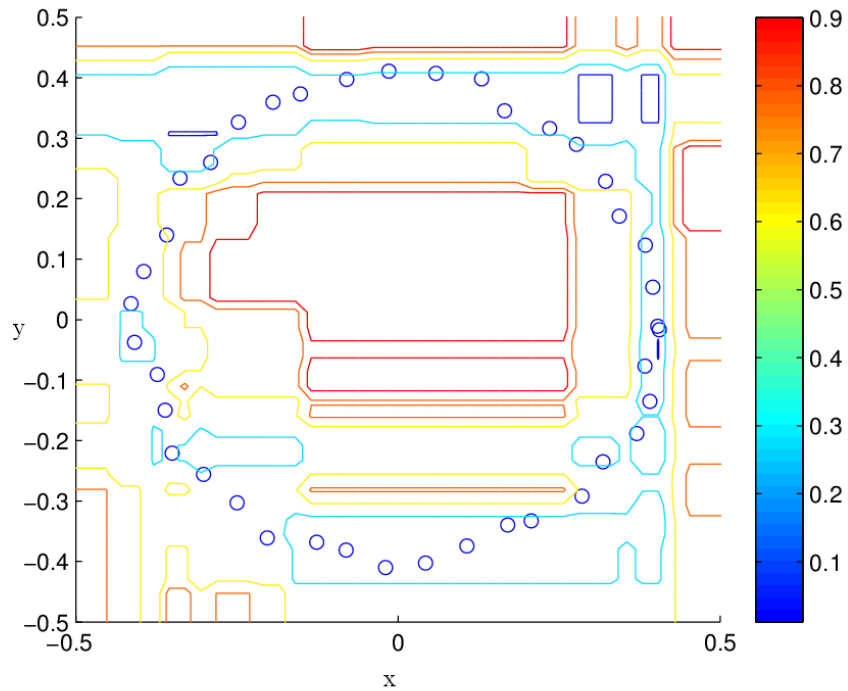


Figure 4.1. Boundary learned by Active-Outlier on a synthetic circular data set.

valid for density estimation as they are able to learn smoother densities. Furthermore, any outlier detection that relies on univariate information such as decision trees fail to consider combinations of attributes in their decisions. However, spectral methods reach a new representation for data where new attributes come from combinations of the original ones and applying decision trees on this new data will enable the learner to use multivariate splits.

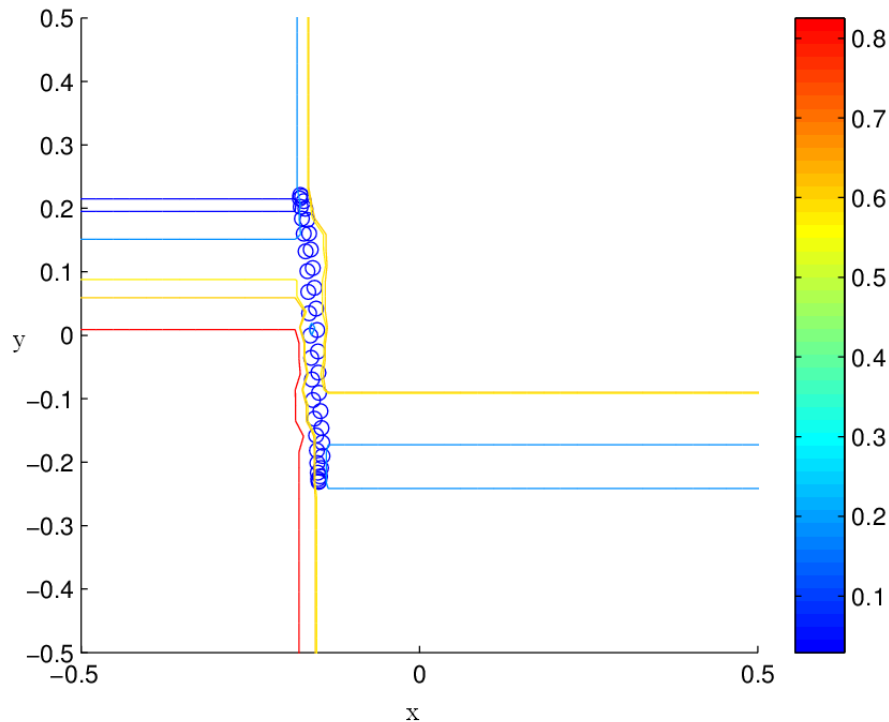


Figure 4.2. Boundary learned by Active-Outlier on a synthetic circular data set after KPCA with Gaussian kernel ($k = 2, \sigma = .4$).

4.2. Related Work

There are a few studies that have applied spectral methods for outlier detection, all using PCA. Shyu *et al.* [42] reduce the dimensionality of data with PCA and apply a classification method afterwards. They report better results than LOF and k nearest neighbor methods on *KDD99* data. Another method that uses PCA for intrusion detection is carried out by Wang *et al.* [43]. Parra *et al.* [44] also apply PCA on input data to decorrelate attributes and demonstrate their method on motor fault detection task. Another work based on PCA is done by Dutta *et al.* [45] for identifying outliers in astronomy catalogs. However, PCA is a linear method unable to cope with nonlinearity and is not good at revealing structures in the data. The success of PCA in outlier detection is mainly due to reduced dimensionality.

We argue that spectral methods such as LEM, MDS and KPCA can be of much more use due to their additional properties such as their non-linear nature and ability to uncover structure. In Figure 4.3, we give the pseudo code of our proposed method which is a meta-algorithm that combines a spectral technique with an outlier detection method.

```

SpectralOutlierDetection(Input data set  $\mathbf{X} = [\mathbf{x}^t]_{t=1}^N$ , Spectral Method
 $g_s$ , Spectral Method Parameters  $\gamma$ , Outlier Detection Method  $g_o$ , Outlier
Detection Method Parameters  $\theta$  )
 $\mathbf{Z} = g_s(\mathbf{X}, \gamma)$ 
 $\mathbf{os} = g_o(\mathbf{Z}, \theta)$ 
return  $\mathbf{os}$ 

```

Figure 4.3. Spectral outlier detection algorithm.

5. EXPERIMENTS

Much like the definition of outliers, the evaluation of outlier detection methods is also a problematic issue. In order to be able to calculate the performance of a method, it is necessary to have labeled data; however, due to the ambiguity of the outlier concept, there are various perspectives on evaluating outlier detection methods. In our experiments, we employ the widely-accepted and well-justified approach of considering outlier detection as a rare-class classification problem. Assuming that anomalous events take place much rarely than typical ones, we apply outlier detection methods to real life scenarios such as network intrusion detection, fault detection, face detection. By considering the rare classes as outliers, we form multiple data sets and evaluate the outlier detection methods by their accuracies obtained on these data sets. Apart from observing accuracies, we also analyze the behavior of the methods on synthetic data and try to assess these methods visually.

5.1. Evaluated Methods and Implementation Notes

In Active-Outlier (AO) method, we employ C4.5 decision tree [46] as the base learner and apply no conversion on categorical variables since C4.5 can handle discrete and numeric attributes together. An important point to note is that in order to reach high accuracies, learned decision trees should not overfit. Although a decision tree may be able to classify perfectly a specific data set, such classifiers do not achieve high accuracies when combined. This problem can be overcome by stopping splitting when a leaf contains fewer than a certain number of instances; this is known as prepruning. In our experiments, we observed that limiting the minimum number of instances in a leaf to $\lfloor N/16 \rfloor$ where N is the sample size leads to good results. For Local Outlier Factor (LOF) method, due to the high computational requirements of the method, we have modified it to calculate LOF values for k in the range of k_{min} to k_{max} . Instead of incrementing k from k_{min} to k_{max} one by one, we choose a step size s and increment k by s until we reach k_{max} . This strategy decreased running time significantly hopefully

without losing much from accuracy. In Parzen Windows (PW), densities are estimated with hyper spheric Gaussians with constant variance over the input space. The distance to the k^{th} neighbor is assumed to be two standard deviations to calculate the variance for a specific data set where the right value of k is found with parameter search for each problem. In One-Class Support Vector Machine (SVM), we employ three kernels, linear, quadratic and Gaussian, which are defined as follows;

$$K_{Linear}(\mathbf{x}^{(i)}, \mathbf{x}^{(j)}) = ((\mathbf{x}^{(i)})^T \mathbf{x}^{(j)}) \quad (5.1)$$

$$K_{Quadratic}(\mathbf{x}^{(i)}, \mathbf{x}^{(j)}) = [((\mathbf{x}^{(i)})^T \mathbf{x}^{(j)}) + 1]^2 \quad (5.2)$$

$$K_{Gaussian}(\mathbf{x}^{(i)}, \mathbf{x}^{(j)}) = \exp(-\gamma \|\mathbf{x}^{(i)} - \mathbf{x}^{(j)}\|^2) \quad (5.3)$$

In our experiments, we find the best parameter values by choosing $\nu \in \{.01, .05, .1, .2, .5\}$ and $\gamma \in \{2^{(-6)}, 2^{(-3)}, 1, 2^{(3)}, 2^{(6)}\}$. For all the methods except SVM, we use our own implementations. For SVM, we utilize the LIBSVM package [47].

5.2. Synthetic Data

Understanding how outlier scores change and observing the outlierness decision boundaries has the potential to reveal important insights into the properties of outlier detection methods. For this purpose, we generate two 2-D outlier detection problems where the first one is a relatively easy one with two Gaussians whereas the second data set exhibits non-linear behavior.

In the first synthetic outlier detection problem seen in Figure 5.1, there are two normally distributed clusters. Instances from the right cluster are considered typical and the left cluster represents the outlier class. Discriminants defined by the methods and the outlier scores of individual instances are observed as the sample size in the

outlier class is increased from 1 to 50. Figure 5.2 depicts the second synthetic outlier detection problem where instances outside are considered to be from the typical class while the instances in the center cluster are outliers. Again, we vary the number of instances in the outlier class to observe the change in the decision boundaries and the outlier scores. We analyze the algorithms in an unsupervised setting, meaning that we include outlier instances in the training set too.

As can be seen in Figure 5.3, the Active-Outlier method performs well for small number of outliers. For outlier counts 10 and 50, it starts to include outliers into the typical class boundaries. However, it is quite natural since as the number of instances in outlier class increases, these instances can no longer be assumed to be outliers. The decision boundaries drawn by the Active-Outlier method are smoother compared to the nearest neighbor or probabilistic methods but it should be noted that this is strictly related to the base learner. Therefore, for the method to generalize, the base learner should not be complex. As another property of the Active-Outlier method, we see that false positives occur near the boundaries of the typical class. Besides, the results on the second data set demonstrate that the method is immune to the distribution of the sample of typical instances since it is only interested in learning the boundaries of the typical class.

The LOF method experiences significant accuracy loss as the outlier count increases. However, it would be unjust to point this out as a weakness, because LOF assumes a low density of outlier instances. For outlier counts of 10 and 50, LOF includes outliers inside the typical class boundary, since they form a relatively uniform density cluster. As can be seen in Figure 5.4, the decision boundaries are quite jagged in all cases. This is caused by the fluctuations in the LOF value even with minor changes in the data. Since the LOF method requires no labeled data and utilizes local neighborhoods in finding outliers, it is of paramount importance for the outliers not to form a cluster. LOF method will not be of much use in scenarios where this assumption is violated. Analyzing the results on the second data set shows that LOF is able to operate on non-linearly distributed data by virtue of being a local method. Moreover,

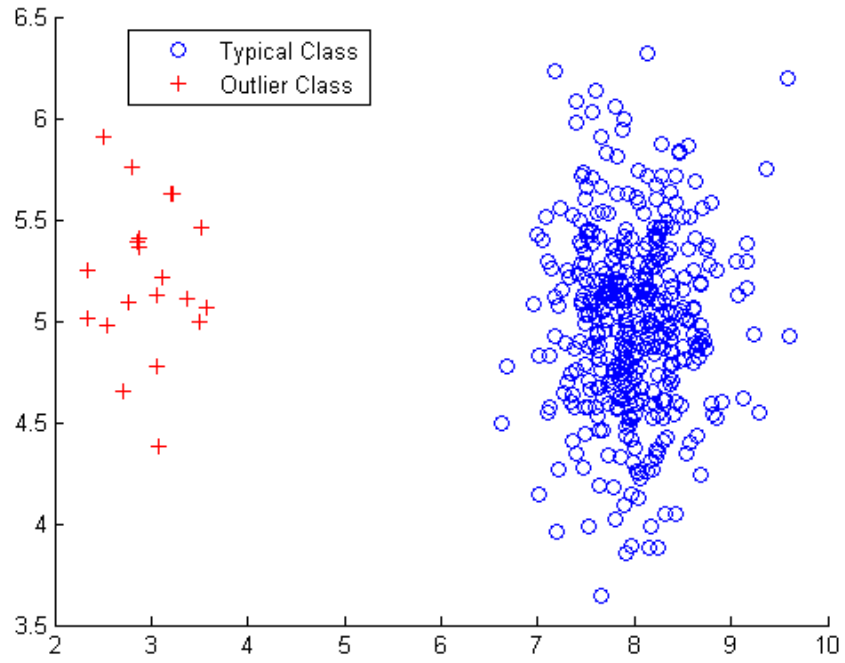


Figure 5.1. Synthetic data set 1.

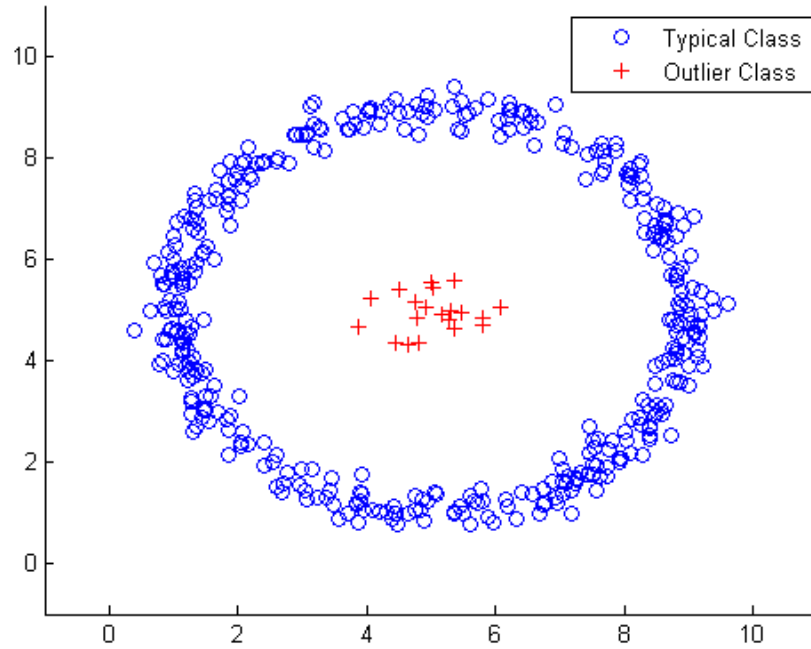


Figure 5.2. Synthetic data set 2.

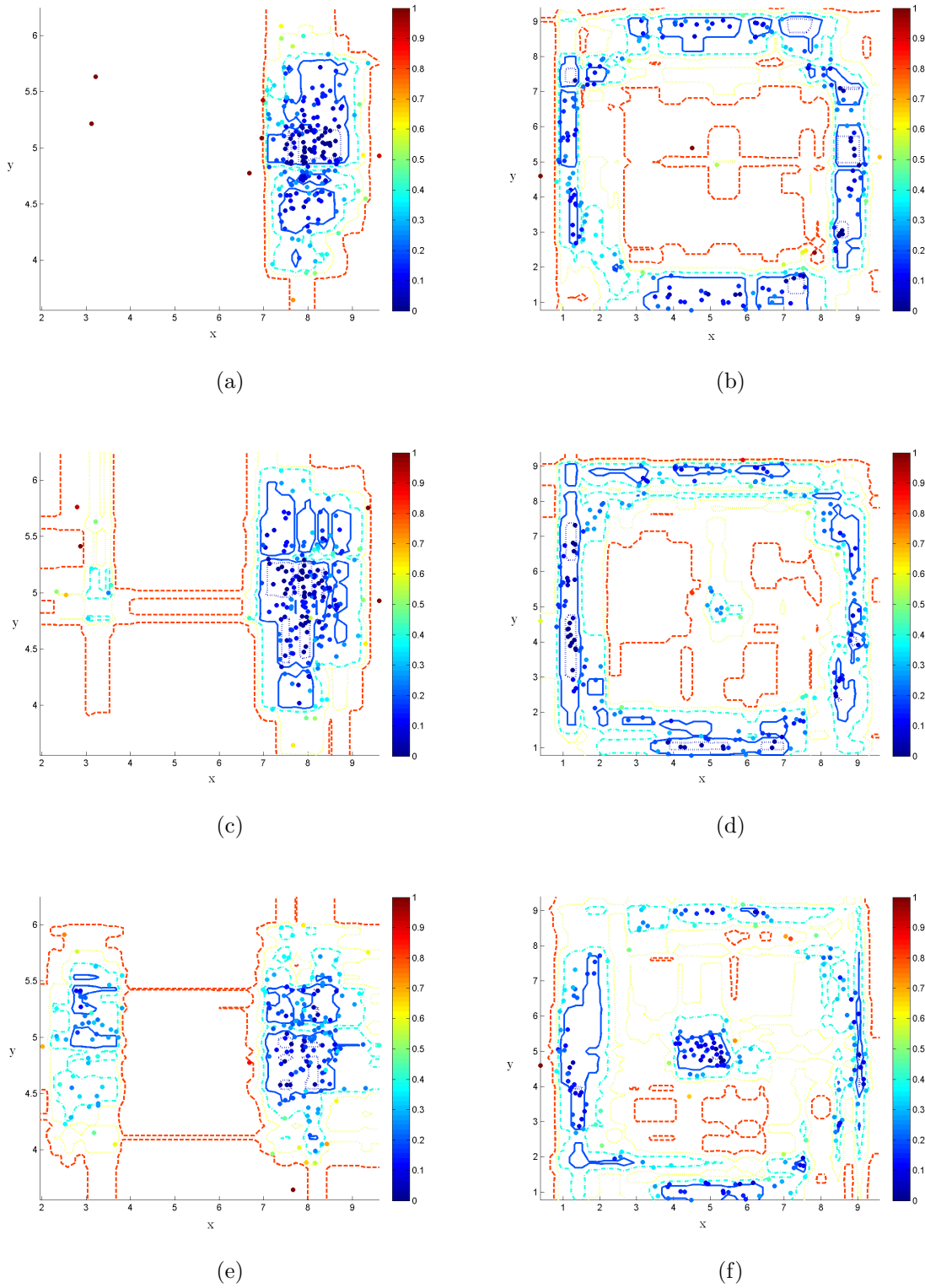


Figure 5.3. Outlier scores and discriminants for outlier count 2, 10, 50 on rows with the Active-Outlier method, synthetic data set 1 in the left column, synthetic data set 2 in the right column.

when compared to the Active-Outlier method, the LOF method is affected more by the quality of the training data. In Figure 5.4f, it is observed that the middle red point is deemed an outlier because it fell in a less dense neighborhood by chance, although we expect a method to be able to generalize and learn a smoother boundary around the middle cluster.

As can be expected from a probabilistic method, the Parzen Windows method performs with lower accuracy as the outlier count is increased. Although it fails to discriminate the outliers in all cases, the boundaries are always smooth and the outlier scores reflect the local density of the neighborhood. Like LOF, Parzen Windows assumes that outliers occur in low density regions, resulting in a significant drop in performance as the number of outliers increase. As a last note, we remark that because it is a local method, Parzen Windows method can work with non-linear data. Figure 5.6 shows the boundaries found by One-Class Support Vector Machine (SVM) method on both synthetic data sets. SVM is able to find smooth boundaries like PW and non-linearity can be achieved by kernel functions as seen in the second synthetic data set. Unsupervised setting makes it impossible for the method to push outliers to the other side of the boundary as the outlier count increases. However, distance to the decision boundary is usually a strong indicator of being an outlier. The ability to set the fraction of outliers by the parameter ν becomes important as one can tune the value of ν to leave the outliers out of the boundaries as seen in Figure 5.6d, although they are in the training set.

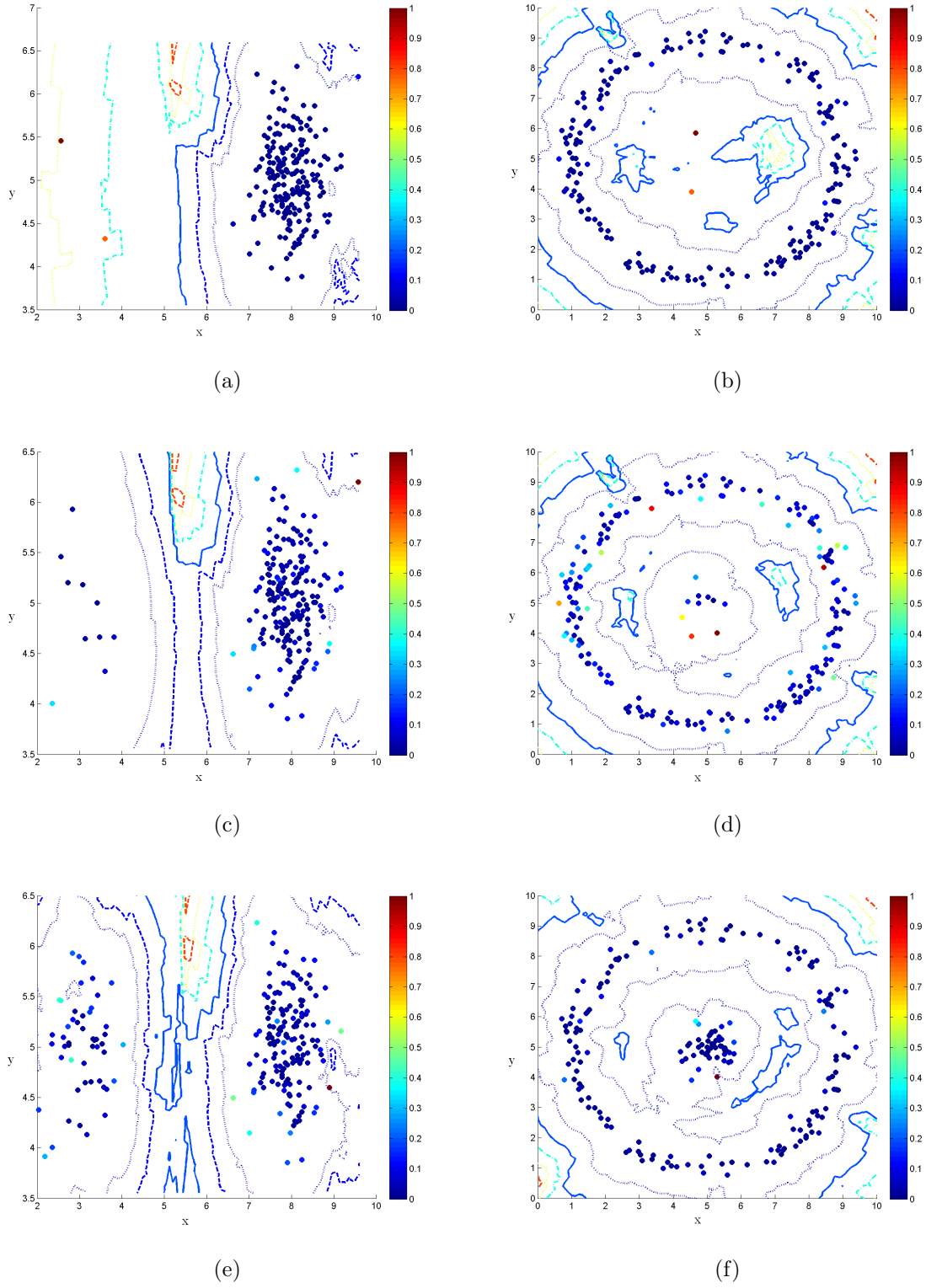


Figure 5.4. Outlier scores and discriminants for outlier count 2, 10, 50 with the LOF method, synthetic data set 1 in the left column, synthetic data set 2 in the right column.

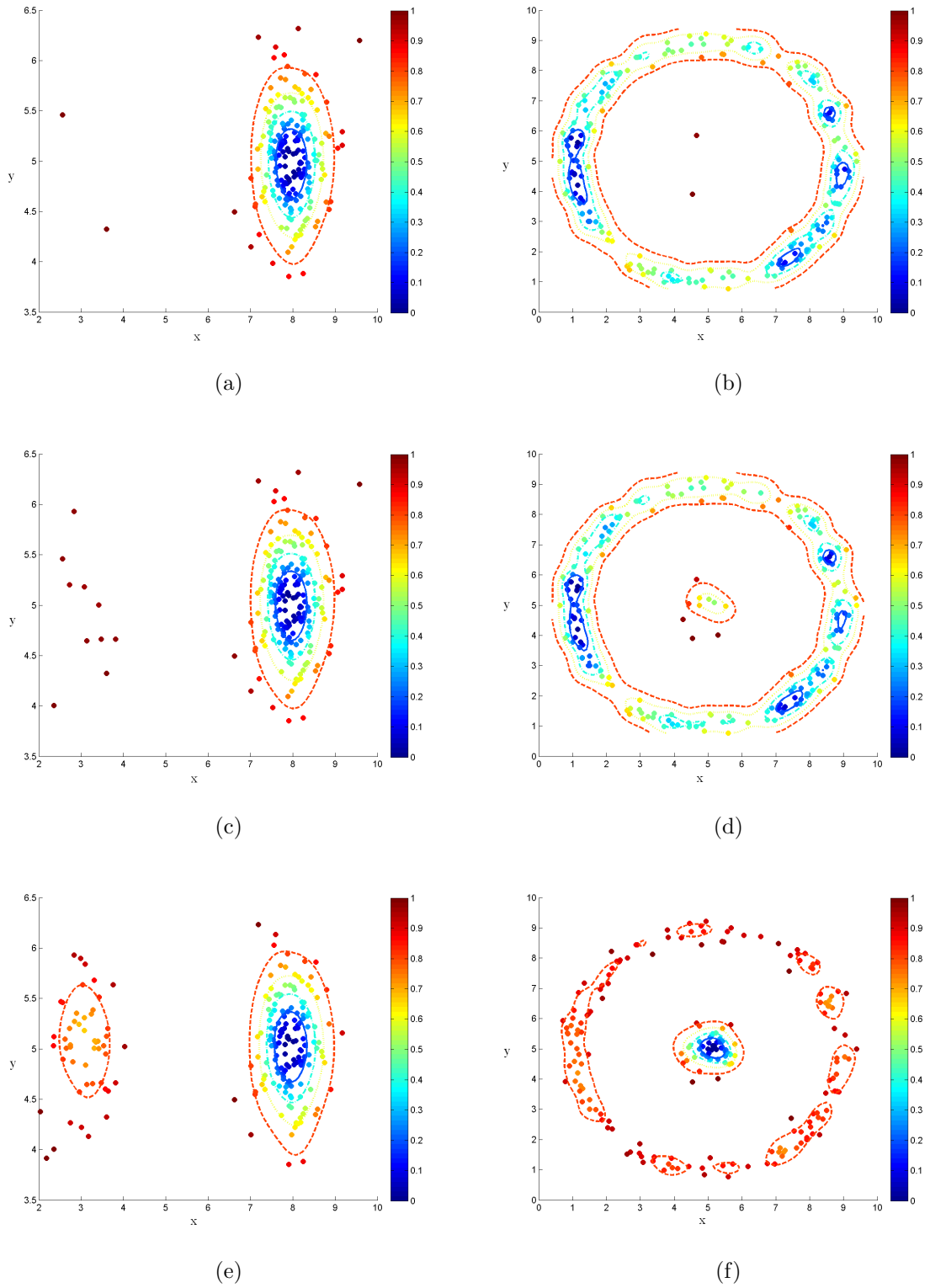


Figure 5.5. Outlier scores and discriminants for outlier count 2, 10, 50 with the Parzen Windows method, synthetic data set 1 in the left column, synthetic data set 2 in the right column.

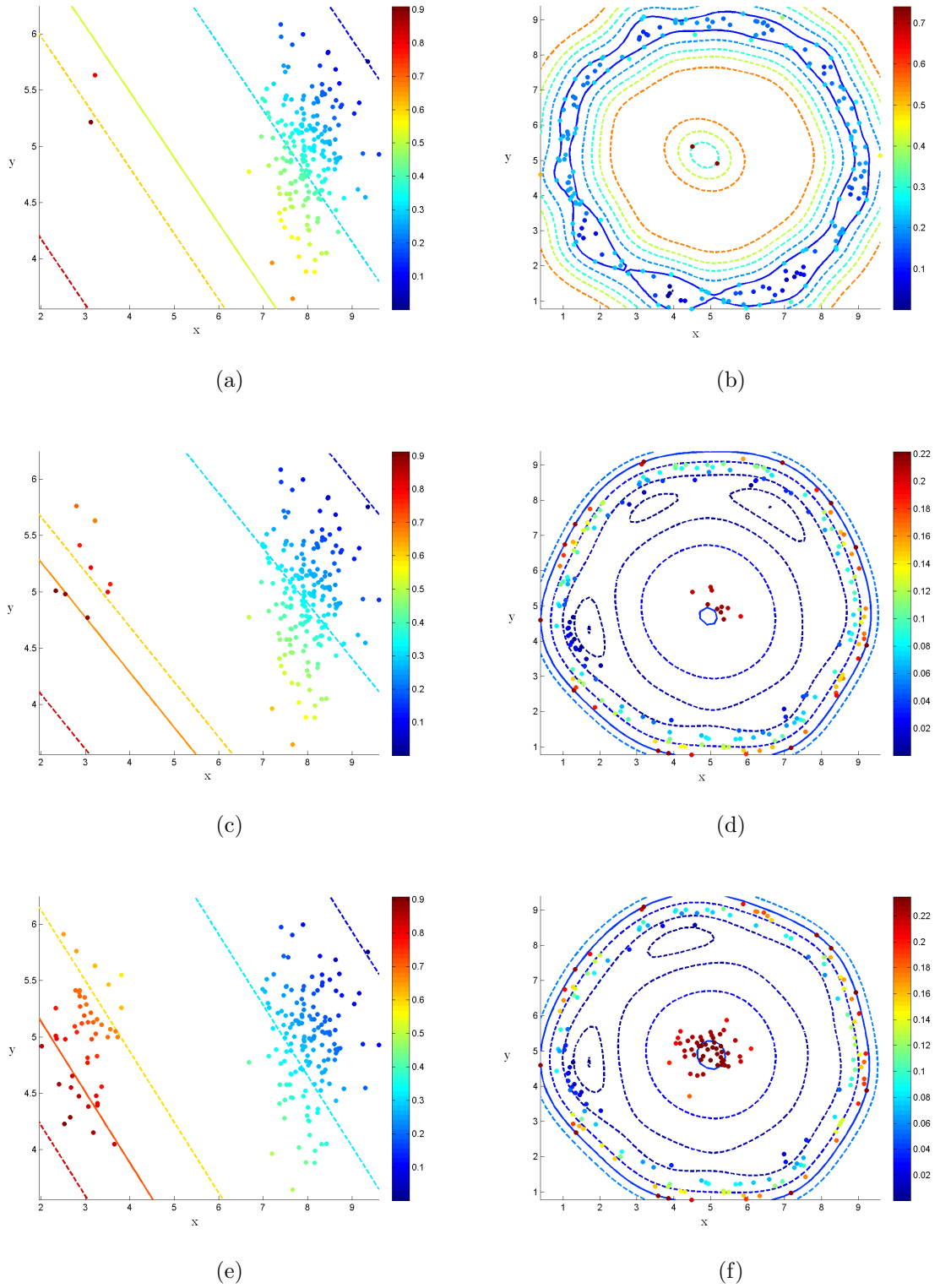


Figure 5.6. Outlier scores and discriminants for outlier count 2, 10, 50 with the One-Class Support Vector Machine, synthetic data set 1 in the left column, synthetic data set 2 in the right column.

5.3. Real Data

We evaluate the performances of Active-Outlier (AO), Local Outlier Factor (LOF), One-Class SVM (SVM) and Parzen Windows (PW) methods individually and combined with spectral methods on various real data sets. Since we approach the outlier detection problem from a rare-class classification perspective, we can use the classification accuracy as the performance measure. However, in settings where the class priors are heavily unbalanced, it is much more rational to evaluate methods with measures invariant under class priors. For this reason, we choose to use the area under the receiver operating characteristics (AUC) curve [1].

We use 2/3 of each data set as the training/validation set and the rest as the test set. We carry out a parameter search on the training/validation set to obtain the optimum values of the parameters specific to each method. We obtain 10 AUC values per data set for each method by applying 5×2 cross validation (CV) on training/validation sets and report the performance on the test set with the optimum parameters. We carry out two sets of experiments. For the unsupervised case, the training/validation set contains both the typical and the outlier sample and in the semi-supervised case, only the typical sample forms the training/validation set meaning that there are no outlier instances in the data set.

In our spectral detection algorithm, we combine each of the above methods with PCA, Laplacian Eigenmaps (LEM) and Multidimensional Scaling (MDS). We apply PCA on the covariance of the centered input data. LEM requires a similarity matrix \mathbf{W} calculated from the input data. W_{ij} denotes the similarity between inputs $\mathbf{x}^{(i)}$ and $\mathbf{x}^{(j)}$. For each instance, we calculate its similarity to its k neighbors and for the instances not in its k -neighborhood, W_{ij} is set to 0. In our experiments, we use three different kernels; constant, Gaussian and quadratic polynomial:

$$K_{Constant}(\mathbf{x}^{(i)}, \mathbf{x}^{(j)}) = 1 \quad (5.4)$$

$$K_{Gaussian}(\mathbf{x}^{(i)}, \mathbf{x}^{(j)}) = \exp\left(-\frac{\|\mathbf{x}^{(i)} - \mathbf{x}^{(j)}\|^2}{2\sigma^2}\right) \quad (5.5)$$

$$K_{Quadratic}(\mathbf{x}^{(i)}, \mathbf{x}^{(j)}) = [((\mathbf{x}^{(i)})^T \mathbf{x}^{(j)}) + 1]^2 \quad (5.6)$$

The variance for the Gaussian kernel, σ , is set to s , half of the average of distances to k th neighbors. The constant and quadratic kernels require no extra parameters. For MDS, we convert the similarity matrix \mathbf{W} to a distance matrix by negating it, $\mathbf{E} = -\mathbf{W}$. In our experiments, for the neighbor count, k , we try 3, 6, 12, 25 and 80. We also vary σ value to $s/2$, $2s$ and $4s$. In PCA, for the number of dimensions in the transformed space, we try the values that explain 80%, 90%, 95% and 99% of the variance. For LEM and MDS, we choose four values linearly spaced in the interval $[2, d]$ where d is the input dimensionality.

5.3.1. Data Sets

The attributes of the data sets used are summarized in Table 5.1.

- *Shuttle* data set is a low dimensional and large data set collected from the operation of a shuttle. Approximately 80% of data belongs to the typical class while the five rare classes have very few instances. We create an outlier detection problem from this data set by forming a binary classification problem between class 1 and one of the five rare classes, class 3.
- *Optdigits* data set contains 1024-dimensional images of handwritten digits from 10 classes [48]. We form a problem by taking all the instances from a certain class as the typical sample and adding a few instances from the other classes as outliers.
- *KDD99* data set [48] is about network intrusion detection and was provided by the annual International Knowledge Discovery and Data Mining Tools Competition as a contest problem in 1999. It contains 41 attributes denoting various properties of network activity and contains labeled network intrusions. Although there

are many intrusion classes, the smallest intrusion class, *u2r*, is chosen as the outlier class following the general approach in previous publications. The data set contains separate training and test splits which are known to come from different distributions. For this reason, we apply the outlier detection methods on two separate data sets; *KDD99Train* and *KDD99Test*.

- *Pageblocks* data set consists of 10 dimensional instances containing features extracted from blocks of the page layout of several documents. There are four classes; text, horizontal line, vertical line, picture and graphic. Nearly 90% of documents belong to the text class which is considered as the typical sample. We again discriminate between the typical class and one of the rare classes.
- *Abalone* data set contains physical measurements of abalones and the task is to predict the age. We take the class with the most instances to be the typical class and add a low sample sized class as outliers.
- In *Glass* data set, the properties of glasses are used to discriminate between different types. We take window glasses as the typical class and combine the others as the outliers.
- *Yeast* data set contains various properties of protein sequences and the class labels indicate their localization sites. Cytosolic sequences are considered to be typical whereas peroxisomal ones are the outliers.
- *Cardiotocography* data set consists of fetal cardiotocograms (CTG) where experts classified CTGs both with respect to the morphological pattern and the fetal state. We use the fetal state classification and try to discriminate between normal and pathologic instances.
- *Spam* data set contains various word and character frequency related attributes of e-mails from a large corpora and their labels. We assume that non-spam e-mails are typical and the spams are the outliers.
- *Ecoli* data set is very similar to *Yeast*, also concerning the localization sites of proteins. The class with the most instances is the typical one while the outer membrane proteins are considered to be the outliers.
- *Letter* data set is made up of the numerical attributes of the letters in the English alphabet obtained from black and white letter images. We choose one letter to

be typical and add a few instances from others to form the outlier class.

- *Satellite* data set consists of the multi-spectral values of pixels in 3×3 neighbourhoods in a satellite image and the classification of the region with respect to soil type. We take the largest class to be the typical one and one of the others as the outlier.
- *Wine* data set contains various attributes concerning the chemical properties of wines and each wine is classified with respect to its quality. We consider the medium quality to be typical and add poor quality instances as outliers.
- *Breast* and *Mammography* are cancer diagnosis data sets containing features extracted from images of breast masses and medical tests. We take the benign instances as the typical class and add the malignant instances as outliers.
- In *Pima* data set, patient information is used to decide whether the patient shows signs of diabetes. Healthy patients are considered typical and patients diagnosed with diabetes are the outliers.
- *Robot* data set contains force and torque measurements on a robot after failure detection in five different learning problems. We form the outlier detection problem by taking the normal instances from all problems against the collision instances from the first problem.
- *Vehicle* data set consists of shape features extracted from vehicle silhouettes and their classification into four classes. We group three classes into one and use it as the typical class where the bus class is the outlier class because it is relatively different than the other classes.
- *Secom* data set deals with fault detection in a semi-conductor manufacturing process. The features are gathered from sensors and each product is classified as pass or fail. We consider the faulty products to be outliers.

Whereas the Active-Outlier method can operate directly on categorical features, for other methods, we convert these features to continuous ones by replacing them with inverse document frequencies and in order to prevent the effect of different scales on methods relying on distances, data are normalized to the $[0, 1]$ interval.

Table 5.1. Data sets used in the experiments (d : input dimensionality, C: number of continuous features, D: number of discrete features, N : sample size).

Data Set Name	N	Normal/Outlier Class	d		% of outliers
			C	D	
Shuttle	45757	1/3	9	0	0.004%
Optdigits	313	1/2,3,7	1024	0	5.75%
KDD99Train	97308	normal/u2r	34	7	0.0003%
KDD99Test	60839	normal/u2r	34	7	0.004%
Pageblocks	5001	1/4	10	0	1.76%
Abalone	691	10/4	8	0	8.25%
Glass	214	1,2,3,4/5,6,7	9	0	23.83%
Yeast	483	1/9	8	0	4.14%
Cardiotocography	1831	1/3	21	0	9.61%
Spam	2927	0/1	57	0	4.75%
Ecoli	163	1/5	7	0	12.27%
Letter	2424	G,O,Q/X	16	0	4.74%
Satellite	1686	1/2	36	0	9.07%
Wine	2308	6/4	11	0	4.77%
Breast	393	B/M	30	0	9.16%
Mammography	568	0/1	5	0	9.15%
Pima	550	0/1	8	0	9.09%
Robot	119	normal/collision	90	0	14.29%
Vehicle	691	opel,van,saab/bus	18	0	9.12%
Secom	1567	-1/1	590	0	6.64%

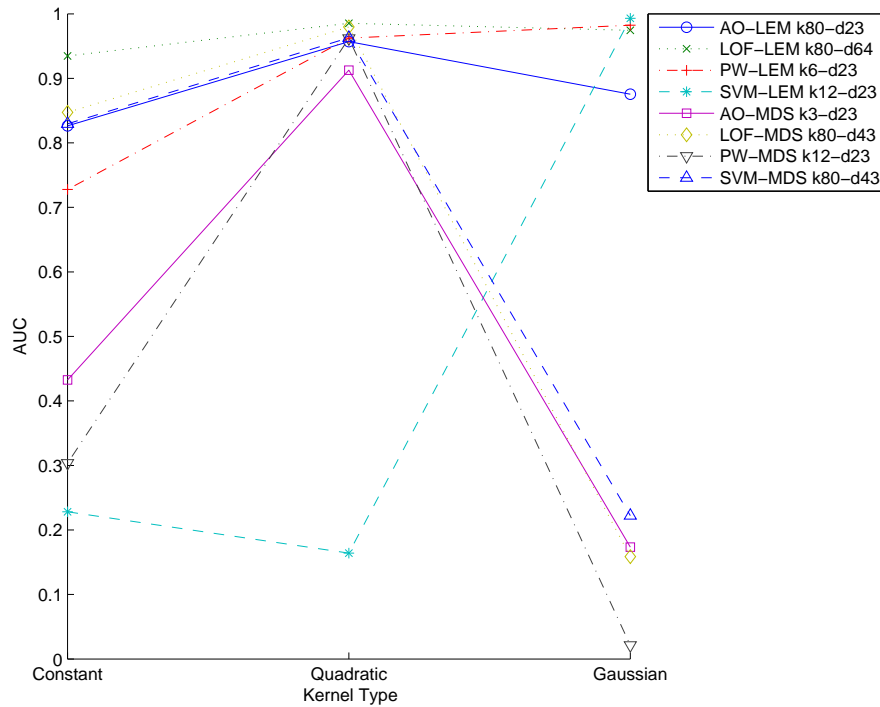


Figure 5.7. AUC vs. kernel type on *Optdigits* data set.

We carry out a set of experiments to analyze the effect of the kernel type, the neighbor count k and the input dimensionality d on our spectral outlier detection algorithm. Firstly, we look at the performances of each outlier detection combined with LEM and MDS using constant, Gaussian and quadratic kernels. For each spectral outlier detection method, we find the kernel type, k and d values that give the best performance and calculate the performances of other kernels with the same k and d values. Figures 5.7 and 5.8 show the AUC values for each kernel type on *Optdigits* and *Shuttle* data sets. We see that spectral outlier detection with LEM is most of the time less affected by the choice of kernel but there are significant differences between the performances of kernels with MDS; it suffers a great loss in performance with the Gaussian kernel. Our further investigations revealed that normalization of kernels decreased this performance gap but still, the quadratic kernel gave better results than the Gaussian for MDS.

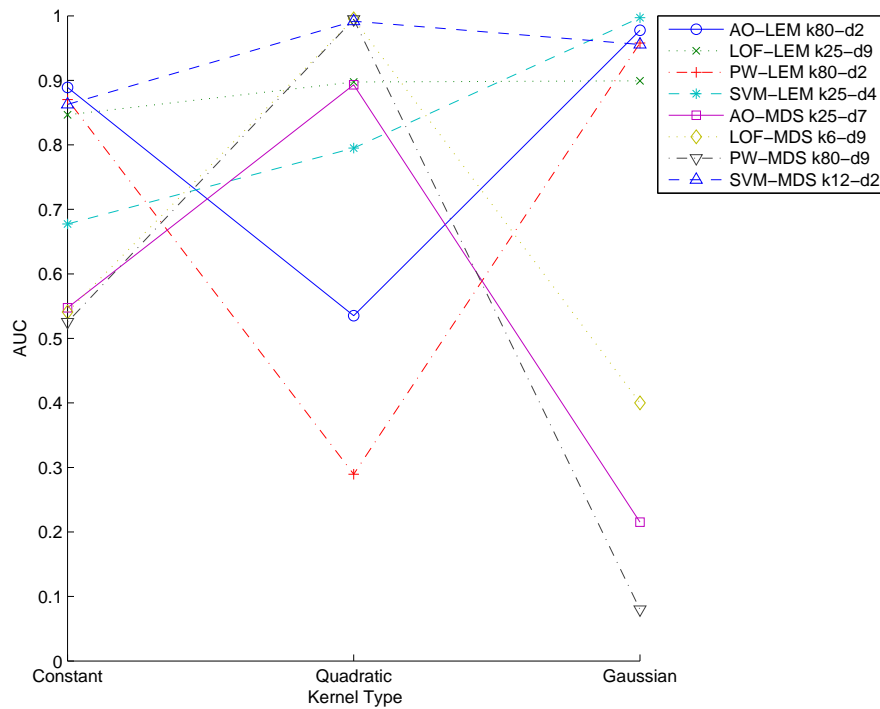


Figure 5.8. AUC vs. kernel type on *Shuttle* data set.

Next, we observe the effect of the neighbor count on spectral outlier detection algorithms. For each kernel and spectral outlier detection method, we find the best input dimensionality and calculate the AUC values for different neighbor counts. As seen in Figures 5.9 and 5.10, with constant kernel, LEM is not affected by the neighbor count as much as MDS. For LEM, AUC values increase until a point as neighbor count increases but remain close as k increases more. However, MDS's behavior is much more unpredictable. For the Gaussian kernel, results are seen in Figures 5.11 and 5.12. As we have seen in the previous analysis, the performance with MDS is significantly worse than with LEM. We again see that LEM is more robust to the choice of k . In the case of the quadratic kernel, we observe in Figures 5.13 and 5.14 that MDS's performance increases substantially and MDS with quadratic kernel is less affected by the neighbor count compared to other kernels. For all the three kernels, SVM's behavior with varying neighbor count is less stable and performance depends heavily on the choice of a good neighbor count.

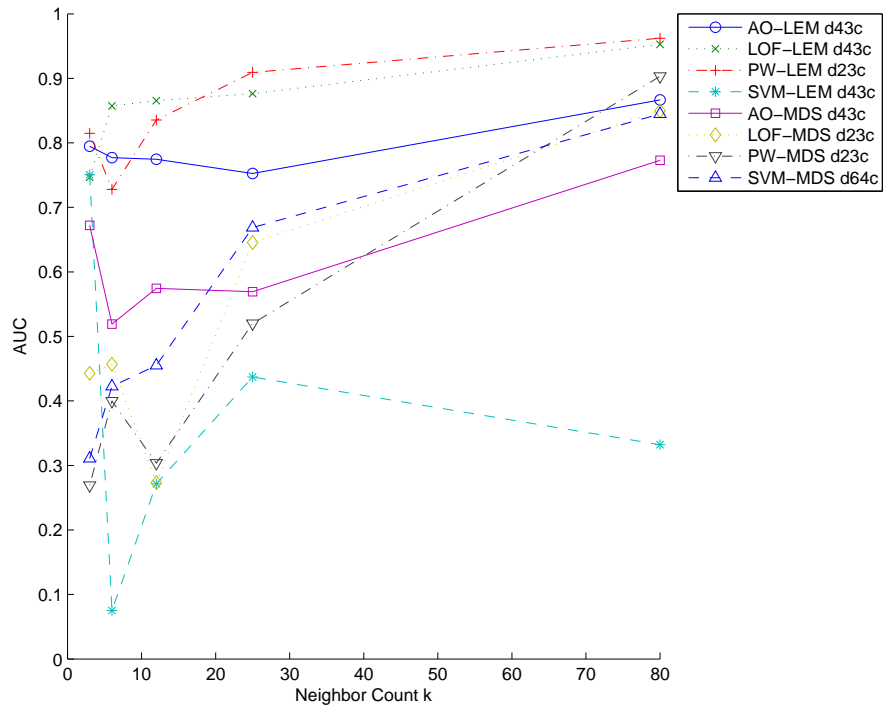


Figure 5.9. AUC vs. neighbor count on *Optdigits* data set with constant kernel.

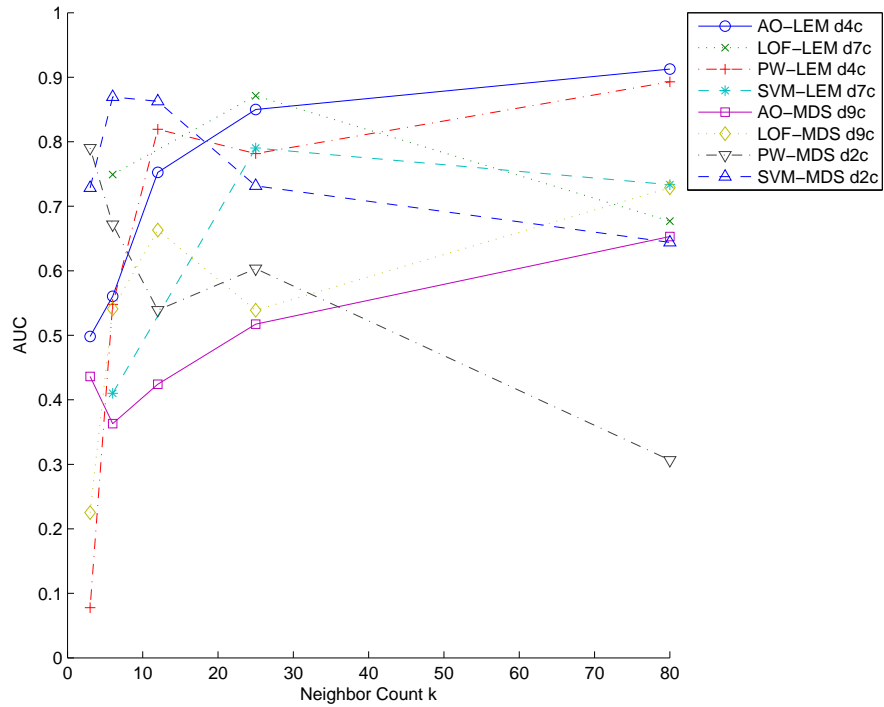


Figure 5.10. AUC vs. neighbor count on *Shuttle* data set with constant kernel.

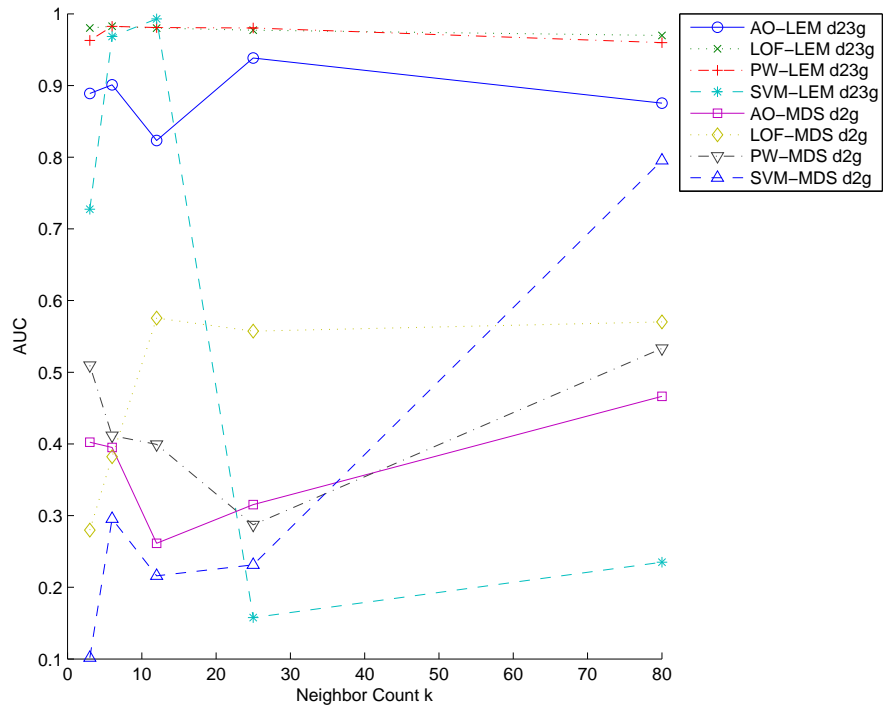


Figure 5.11. AUC vs. neighbor count on *Optdigits* data set with Gaussian kernel.

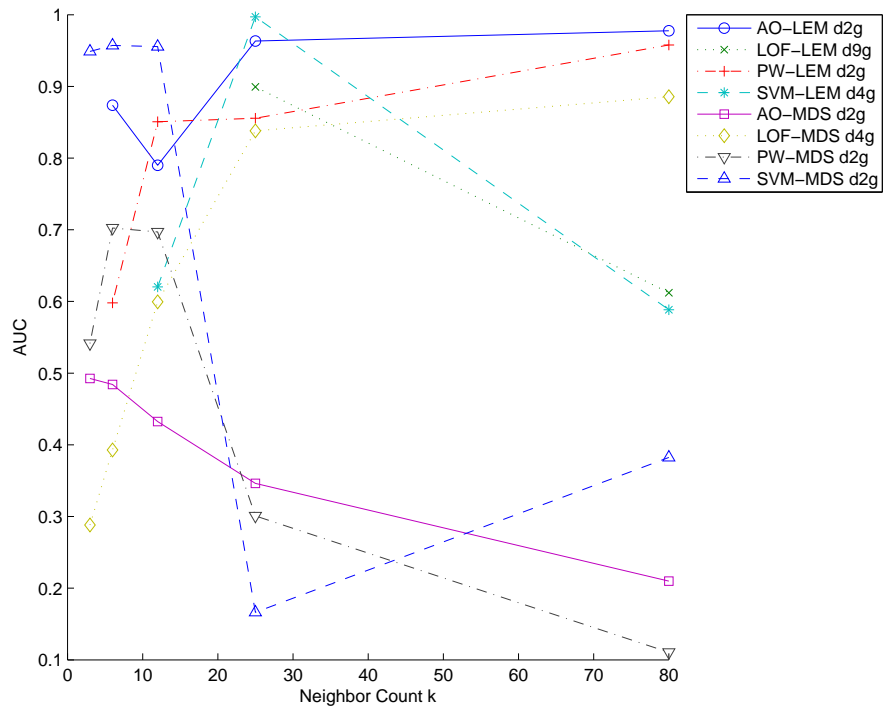


Figure 5.12. AUC vs. neighbor count on *Shuttle* data set with Gaussian kernel.

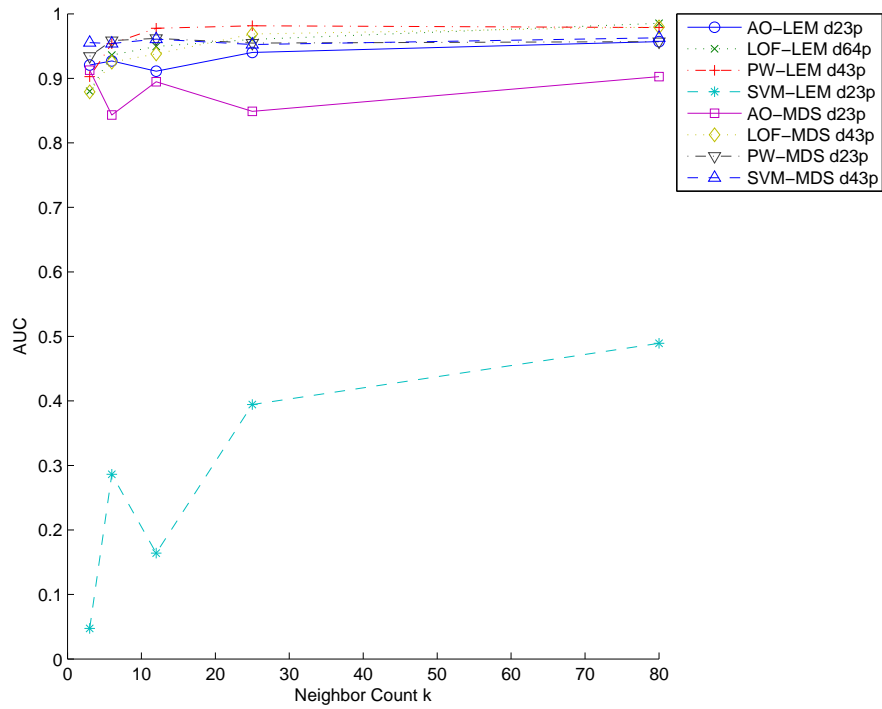


Figure 5.13. AUC vs. neighbor count on *Optdigits* data set with quadratic kernel.

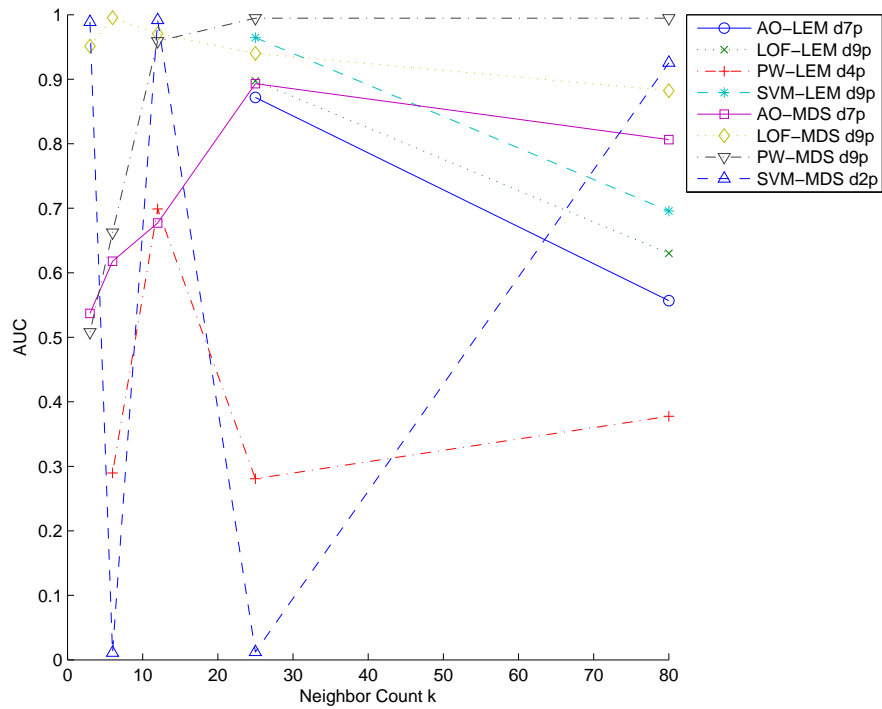


Figure 5.14. AUC vs. neighbor count on *Shuttle* data set with quadratic kernel.

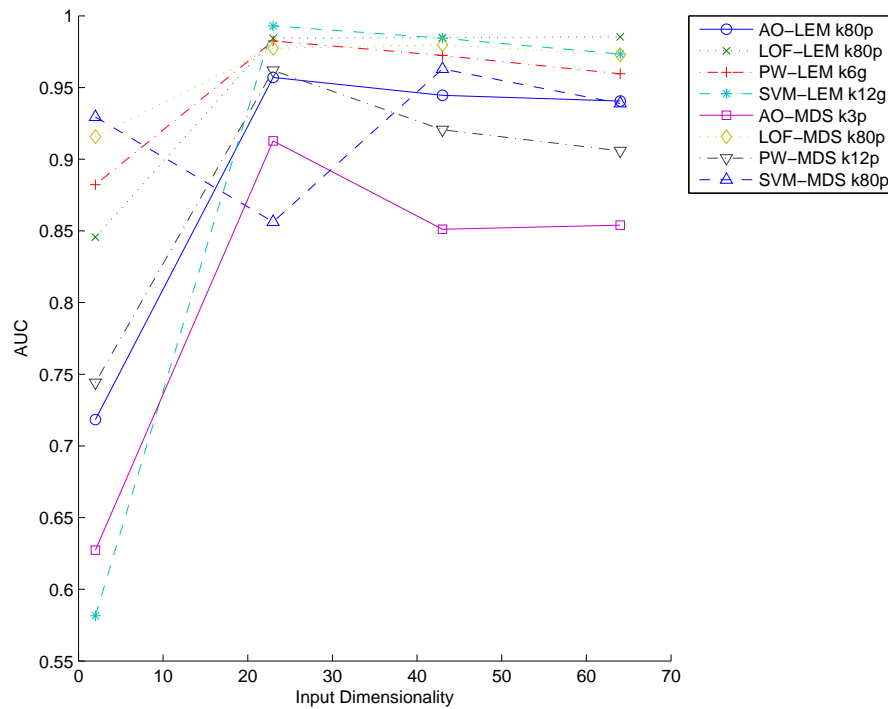


Figure 5.15. AUC vs. input dimensionality on *Optdigits* data set.

Lastly, we analyze how the performances of the spectral outlier detection methods are affected as the number of dimensions in the new space (d) changes. For each method, we plot the AUC values obtained by the best performing kernels with different number of dimensions. As seen in Figure 5.15, on *Optdigits* data set, both LEM and MDS reach their top performances at nearly the same dimensionality and after this point, adding more dimensions do not increase the accuracy much. Also, we again see that LEM is able to reach higher AUC values than MDS most of the time. Figure 5.16 shows the results on the *Shuttle* data set. We understand that the *Shuttle* data set is represented quite well in two dimensions with LEM and performances do not increase much with more dimensions. Except for SVM, performances do not change much as the number of dimensions increases. If we analyze the three experiments from the perspective of outlier detection methods, Active-Outlier, LOF, Parzen Windows and One-Class Support Vector Machine, we see that no single one is always the best and the performance relies on the spectral method heavily. We can also say that SVM is less robust to changes in parameter values.

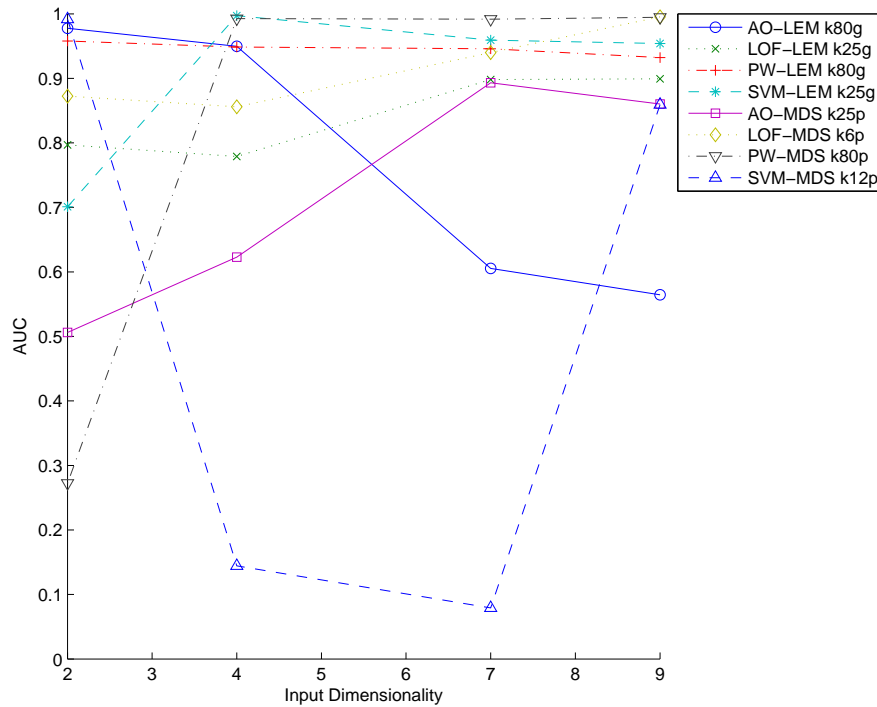


Figure 5.16. AUC vs. input dimensionality on *Shuttle* data set.

In the following paragraphs, we analyze each outlier detection method individually and with PCA, LEM and MDS on 20 data sets. Table 5.2 and 5.3 list the means and standard deviations of AUC values for each outlier detection method with no spectral transformation. We also plot the accuracies on each data set as seen in Figures 5.17 and 5.18. We apply various statistical tests to check for significant difference among the methods. As a start, we use Friedman’s test [49] which is the non-parametric equivalent of ANOVA [1], to check if any of the algorithms are significantly different from the others. The average ranks for each algorithm report no significant difference for the unsupervised case whereas SVM is significantly better than AO in the semi-supervised case. We also apply 5×2 cv F test [50] on pairs of algorithms and the number of wins of each algorithm can be seen in Table 5.4. The cells contain the number of times the method in the row wins against the method on the column. Any significant difference with sign test is indicated with bold typeface. No significance between the wins of methods are reported for both the semi-supervised and the unsupervised case. We also apply Wilcoxon’s signed rank test on the wins/ties/losses of algorithms, but it reports

Table 5.2. Average values and standard deviations of AUCs for the semi-supervised case.

	ActiveOutlier	LOF	ParzenWindow	Svm
shuttle2	1.00±0.0004	0.96±0.010	0.87±0.015	1.00±0.0003
optdigits2	0.93±0.023	0.99±0.006	1.00±0.002	0.99±0.005
kdd99Half	0.91±0.034	0.88±0.009	0.99±0.001	0.99±0.001
kdd99trainHalf	0.99±0.026	0.90±0.023	0.99±0.0003	0.99±0.002
pageblocks3	0.87±0.056	0.93±0.008	0.88±0.016	0.95±0.003
abalone	0.95±0.062	1.00±0.004	1.00±0.001	1.00±0.000
glass	0.89±0.055	0.97±0.009	0.96±0.007	0.98±0.004
yeast	0.60±0.122	0.66±0.023	0.62±0.008	0.71±0.014
cardiotocography	0.62±0.141	0.92±0.012	0.95±0.002	0.97±0.005
spam	0.79±0.064	0.67±0.005	0.74±0.013	0.83±0.003
ecoli	0.96±0.031	0.98±0.011	0.99±0.010	0.99±0.007
letter	0.79±0.050	0.98±0.005	0.87±0.004	0.97±0.005
satellite	1.00±0.001	1.00±0.000	1.00±0.000	1.00±0.000
wine	0.69±0.041	0.76±0.015	0.75±0.006	0.75±0.022
breast	0.89±0.034	0.94±0.015	0.94±0.006	0.93±0.010
mammography	0.72±0.052	0.58±0.048	0.72±0.017	0.70±0.004
pima	0.66±0.022	0.62±0.022	0.78±0.008	0.73±0.028
robot	0.89±0.138	0.99±0.020	0.66±0.046	0.95±0.039
vehicle	0.71±0.059	0.67±0.039	0.57±0.028	0.81±0.030
secom	0.54±0.021	0.58±0.012	0.56±0.009	0.56±0.017
Average Ranks	3.30	2.60	2.35	1.75

no significant differences either. Any significant difference according to Wilcoxon's test is marked with an asterisk.

We carry out the same statistical tests to check for differences between the outlier detection methods when combined with a spectral method. For PCA, Tables 5.5 and 5.6 list the accuracies and Figures 5.19 and 5.20 show the plots. The number of dimensions that give the best performance on each data set are given in parentheses. Friedman's test reports no significant differences in the semi-supervised case while SVM is significantly better than LOF in the unsupervised case. Sign test and Wilcoxon's signed rank test on the wins of methods, seen in Table 5.7, report no significant differences except SVM is better than LOF in the unsupervised case according to Wilcoxon's signed rank test. The results for LEM can be seen in Tables 5.8, 5.9, 5.10 and Figures

Table 5.3. Average values and standard deviations of AUCs for the unsupervised case.

	ActiveOutlier	LOF	ParzenWindow	Svm
shuttle2	1.00±0.0003	0.87±0.012	0.88±0.024	1.00±0.001
optdigits2	0.85±0.058	0.97±0.006	0.97±0.017	0.97±0.010
kdd99Half	0.90±0.022	0.77±0.050	0.96±0.002	0.99±0.0002
kdd99trainHalf	0.99±0.026	0.89±0.029	0.98±0.008	0.92±0.022
pageblocks3	0.74±0.096	0.76±0.044	0.73±0.009	0.92±0.005
abalone	0.71±0.159	0.57±0.088	0.49±0.061	0.99±0.001
glass	0.80±0.058	0.91±0.025	0.90±0.007	0.92±0.009
yeast	0.68±0.065	0.66±0.022	0.62±0.011	0.61±0.020
cardiotocography	0.51±0.006	0.70±0.026	0.92±0.004	0.93±0.003
spam	0.65±0.108	0.64±0.017	0.73±0.011	0.77±0.014
ecoli	0.72±0.243	0.95±0.007	0.94±0.013	0.95±0.006
letter	0.68±0.064	0.89±0.011	0.84±0.005	0.85±0.008
satellite	0.82±0.050	0.62±0.049	0.95±0.004	1.00±0.001
wine	0.68±0.049	0.75±0.023	0.74±0.009	0.70±0.041
breast	0.78±0.041	0.93±0.019	0.92±0.006	0.91±0.007
mammography	0.64±0.084	0.54±0.043	0.68±0.014	0.70±0.004
pima	0.62±0.028	0.61±0.026	0.77±0.008	0.71±0.013
robot	0.87±0.090	0.99±0.020	0.55±0.042	0.84±0.028
vehicle	0.64±0.065	0.57±0.047	0.48±0.035	0.71±0.047
secom	0.54±0.042	0.58±0.011	0.56±0.011	0.55±0.015
Average Ranks	2.95	2.55	2.60	1.90

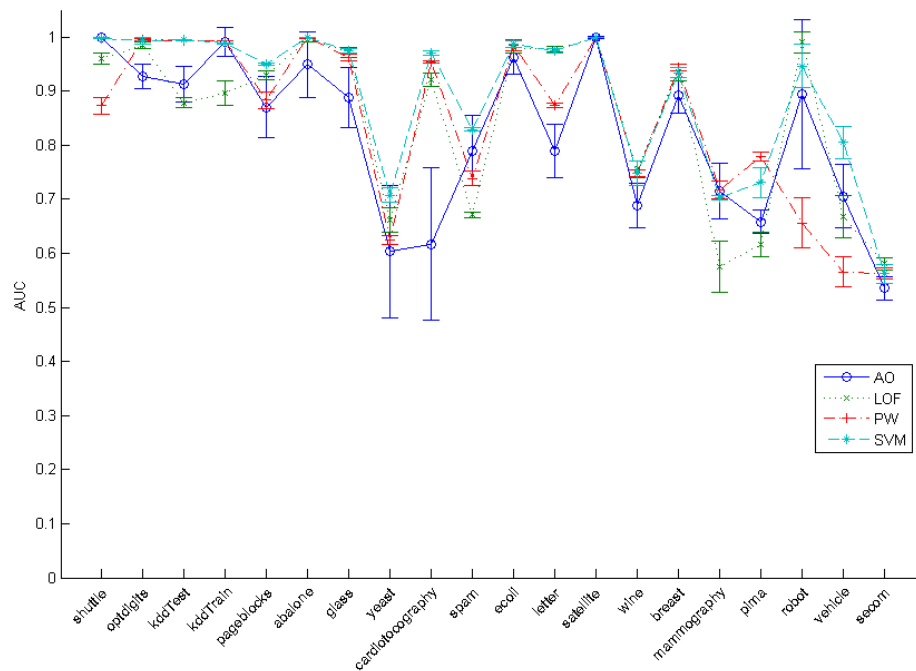


Figure 5.17. Plots of AUCs for the semi-supervised case.

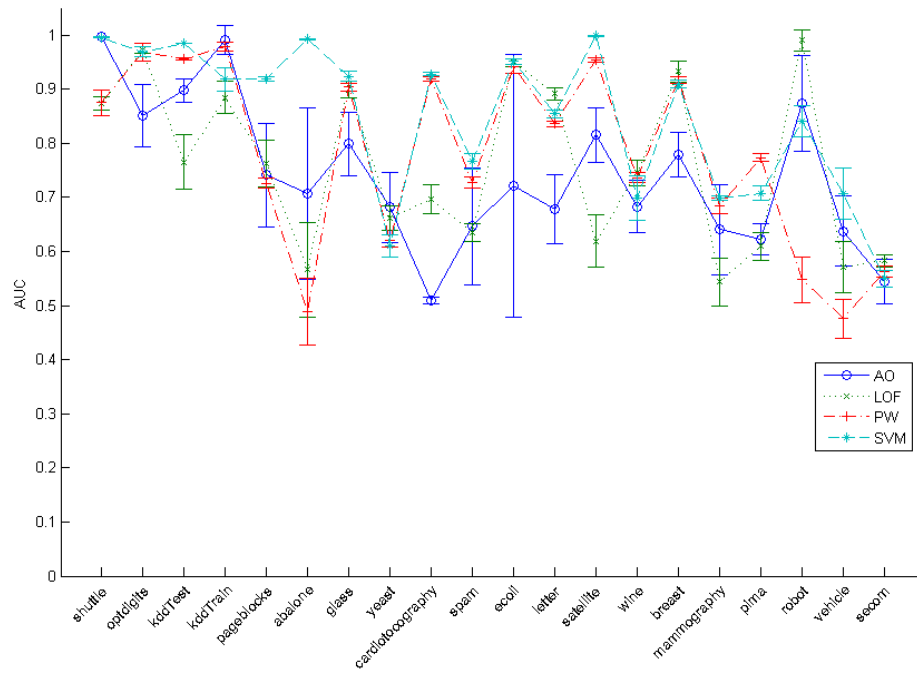


Figure 5.18. Plots of AUCs for the unsupervised case.

Table 5.4. Wins/ties/losses of each algorithm with 5×2 cv F test, a: semi-supervised, b: unsupervised.

(a)					(b)				
	AO	LOF	PW	SVM		AO	LOF	PW	SVM
AO					AO				
LOF	4/13/3				LOF	4/11/5			
PW	4/15/1	6/10/4			PW	8/8/4	7/10/3		
SVM	5/15/0	7/13/0	8/11/1		SVM	10/8/2	9/9/2	7/11/2	

Table 5.5. Average values and standard deviations of AUCs for spectral outlier detection with PCA, semi-supervised case (The numbers in parentheses show the original and best dimensionality chosen for each data set/method).

	ActiveOutlier	LOF	ParzenWindow	Svm
shuttle2 (9)	1.00±0.0001 (7)	0.96±0.007 (9)	0.89±0.029 (4)	0.91±0.002 (4)
optdigits2 (1024)	0.95±0.020 (21)	0.98±0.009 (39)	1.00±0.001 (38)	1.00±0.001 (38)
kdd99Half (41)	0.94±0.012 (4)	0.72±0.012 (12)	0.98±0.001 (12)	0.91±0.022 (12)
kdd99trainHalf (41)	0.96±0.030 (9)	0.67±0.021 (13)	0.96±0.003 (2)	0.94±0.003 (8)
pageblocks3 (10)	0.92±0.015 (3)	0.91±0.020 (6)	0.86±0.018 (6)	0.97±0.001 (3)
abalone (8)	0.98±0.017 (2)	1.00±0.003 (6)	1.00±0.000 (2)	1.00±0.000 (2)
glass (9)	0.93±0.028 (4)	0.98±0.012 (3)	0.95±0.007 (3)	0.96±0.013 (3)
yeast (8)	0.63±0.054 (8)	0.68±0.022 (8)	0.64±0.009 (8)	0.61±0.021 (8)
cardiotocography (21)	0.92±0.008 (11)	0.92±0.016 (15)	0.94±0.003 (15)	0.96±0.009 (15)
spam (57)	0.73±0.030 (50)	0.67±0.015 (50)	0.76±0.004 (50)	0.78±0.004 (2)
ecoli (7)	0.97±0.023 (5)	0.98±0.015 (4)	0.99±0.004 (4)	0.99±0.010 (4)
letter (16)	0.83±0.030 (14)	0.96±0.018 (14)	0.87±0.004 (14)	0.97±0.004 (14)
satellite (36)	1.00±0.003 (9)	1.00±0.00003(24)	1.00±0.0001 (9)	1.00±0.0002 (9)
wine (11)	0.71±0.032 (8)	0.77±0.021 (7)	0.74±0.007 (10)	0.77±0.002 (7)
breast (30)	0.88±0.048 (5)	0.92±0.016 (11)	0.89±0.017 (2)	0.93±0.009 (5)
mammography (5)	0.72±0.062 (5)	0.44±0.042 (3)	0.67±0.018 (3)	0.67±0.004 (2)
pima (8)	0.65±0.049 (8)	0.64±0.043 (7)	0.76±0.006 (7)	0.73±0.009 (8)
robot (90)	0.76±0.097 (24)	0.58±0.216 (10)	0.54±0.038 (24)	0.81±0.028 (24)
vehicle (18)	0.58±0.049 (2)	0.57±0.044 (2)	0.63±0.053 (2)	0.83±0.038 (10)
secom (590)	0.58±0.053(196)	0.56±0.010 (196)	0.56±0.003(196)	0.55±0.001(196)
Average Ranks	2.90	2.75	2.33	2.03

Table 5.6. Average values and standard deviations of AUCs for spectral outlier detection with PCA, unsupervised case (The numbers in parentheses show the original and best dimensionality chosen for the data set/method.).

	ActiveOutlier	LOF	ParzenWindow	Svm
shuttle2 (9)	1.00±0.0001(4)	0.88±0.010 (7)	0.88±0.029 (4)	0.91±0.002 (4)
optdigits2 (1024)	0.88±0.028(23)	0.97±0.009(27)	0.97±0.005 (23)	0.95±0.002(23)
kdd99Half (41)	0.95±0.011 (4)	0.69±0.036(14)	0.96±0.002 (14)	0.97±0.002 (2)
kdd99trainHalf (41)	0.97±0.011 (8)	0.67±0.046(13)	0.96±0.003 (2)	0.93±0.002(13)
pageblocks3 (10)	0.86±0.060 (6)	0.68±0.056 (6)	0.71±0.014 (6)	0.98±0.004 (3)
abalone (8)	0.73±0.067 (6)	0.56±0.070 (7)	0.76±0.041 (8)	1.00±0.0002(5)
glass (9)	0.75±0.067 (2)	0.91±0.015 (7)	0.91±0.005 (7)	0.98±0.002 (2)
yeast (8)	0.64±0.034 (8)	0.67±0.038 (7)	0.63±0.015 (2)	0.58±0.009 (7)
cardiotocography (21)	0.81±0.031 (9)	0.66±0.033 (2)	0.92±0.009 (9)	0.93±0.003 (9)
spam (57)	0.69±0.027(21)	0.65±0.015(40)	0.77±0.004 (32)	0.77±0.086 (2)
ecoli (7)	0.84±0.102 (5)	0.96±0.042 (2)	0.93±0.013 (2)	0.99±0.000 (2)
letter (16)	0.72±0.021 (9)	0.87±0.029 (9)	0.84±0.006 (9)	0.83±0.005 (9)
satellite (36)	0.81±0.039 (8)	0.64±0.049(22)	0.97±0.002 (22)	0.99±0.001 (8)
wine (11)	0.71±0.022 (5)	0.71±0.022 (5)	0.73±0.003 (9)	0.68±0.024(10)
breast (30)	0.80±0.055 (2)	0.90±0.020(10)	0.91±0.008 (2)	0.92±0.013 (2)
mammography (5)	0.62±0.035 (2)	0.48±0.054 (2)	0.66±0.019 (3)	0.67±0.006 (2)
pima (8)	0.67±0.029 (7)	0.61±0.028 (8)	0.77±0.006 (6)	0.70±0.036 (8)
robot (90)	0.83±0.060(30)	0.60±0.201(18)	0.80±0.032 (30)	0.81±0.040(18)
vehicle (18)	0.52±0.079 (2)	0.47±0.062 (2)	0.55±0.027 (2)	0.74±0.018(10)
secom (590)	0.60±0.037 (2)	0.60±0.035 (2)	0.57±0.005(133)	0.57±0.034 (2)
Average Ranks	2.70	3.15	2.25	1.90

Table 5.7. Wins/ties/losses of outlier detection methods combined with PCA with 5×2 cv F test, a: semi-supervised, b: unsupervised.

(a)					(b)				
	AO	LOF	PW	SVM		AO	LOF	PW	SVM
AO					AO				
LOF	1/15/4				LOF	2/12/6			
PW	1/16/3	5/14/1			PW	7/11/2	8/12/0		
SVM	4/15/1	7/11/2	4/13/3		SVM	8/9/3	10/9/1*	7/11/2	

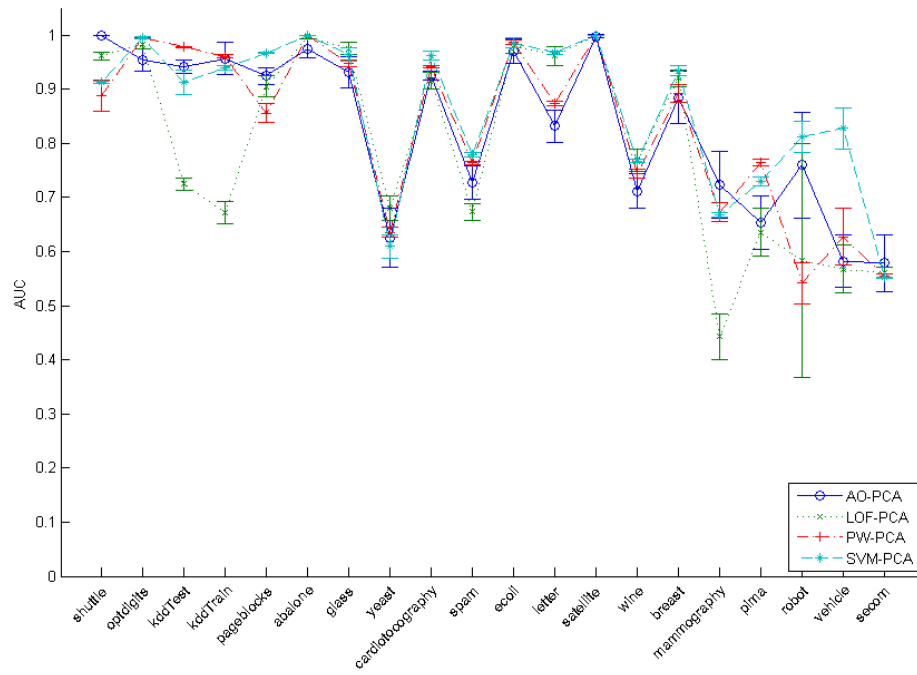


Figure 5.19. Plots of AUCs for spectral outlier detection with PCA for the semi-supervised case.

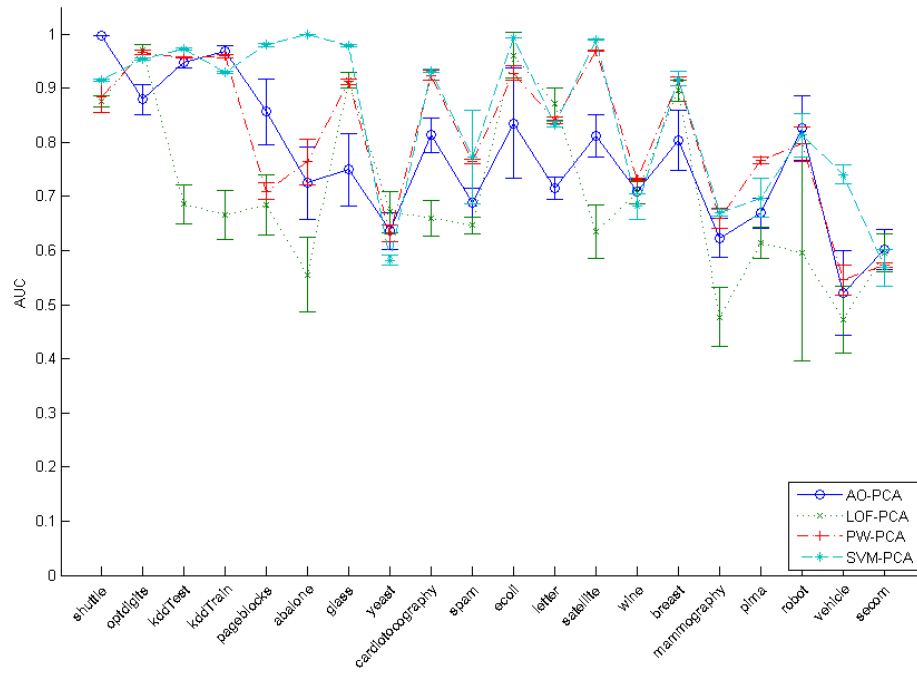


Figure 5.20. Plots of AUCs for spectral outlier detection with PCA for the unsupervised case.

5.21 and 5.22. In the semi-supervised case, SVM is significantly better than AO. In the unsupervised case, we see that the top performer SVM significantly outperforms PW and AO and LOF is significantly better than AO. The AUC values, their plots and ranks of each method for MDS are given in Table 5.11, 5.12 and Figures 5.23, 5.24. A significant difference appears between the outlier detection methods when combined with MDS. Nemenyi's post-hoc procedure [51] after Friedman's test shows that SVM, LOF and PW are significantly better than the Active-Outlier method for both cases. However, the reason for this difference is not that MDS increases the accuracy but the performance of the Active-Outlier method deteriorates significantly when combined with MDS. We summarize the average ranks in Table 5.14 and the results of Nemenyi's post-hoc procedure in Table 5.15 and 5.16. The methods are ranked from the left to the right. If two methods are underlined, there is no significant difference between them. Although none of the methods are significantly better than the others in all cases, on average, SVM ranks higher than other methods and AO is never the top performer either with no transformation or with PCA, LEM or MDS. Nevertheless, the fact that there is no clear statistical significance in the results leads us to argue that all of these methods perform comparably when assessed purely in terms of their accuracies. However, other criteria such as computational complexity may make some of them preferable in certain scenarios and SVM and AO are by far the most efficient ones from that perspective.

In order to test our hypothesis that combining outlier detection methods with non-linear dimensionality reduction methods increases performance, we run four sets of statistical tests for each outlier detection method with PCA, LEM and MDS. We plot the accuracies obtained by AO, LOF, SVM and PW and their combinations with spectral methods in Figures 5.25, 5.26, 5.27, 5.28, 5.29, 5.30, 5.31 and 5.32. The average ranks for the Friedman's test for each outlier method can be seen in Table 5.17 both for the semi-supervised and the unsupervised case. We also summarize the results of Nemenyi's tests on each outlier detection method with different spectral methods in Tables 5.18 and 5.19. In five of the eight cases, there is no significant difference among the spectral outlier detection methods. Similarly, sign test and Wilcoxon's signed rank

Table 5.8. Average values and standard deviations of AUCs for spectral outlier detection with LEM, semi-supervised, (k: neighbor count, d: number of dimensions.

Kernels are c: constant, g: Gaussian, p: quadratic.).

	ActiveOutlier	LOF	ParzenWindow	svm
shuttle2Lem	1.00±0.001 (k25-d4g)	1.00±0.001 (k80-d9g)	1.00±0.0004 (k12-d4g)	1.00±0.003 (k80-d9g)
optdigits2	0.99±0.010 (k6-d43p)	0.98±0.007 (k3-d23g)	0.99±0.003 (k12-d23p)	1.00±0.004 (k12-d23g)
kddLem	0.95±0.015 (k80-d2g)	0.95±0.007 (k12-d31p)	0.97±0.003 (k12-d19g)	0.98±0.003 (k80-d15g)
kddtrainLem	0.97±0.022 (k12-d2g)	0.94±0.006 (k80-d41p)	0.99±0.002 (k6-d33g)	0.99±0.001 (k6-d33g)
pageblocks3	0.98±0.010 (k12-d2g)	0.95±0.005 (k25-d5g)	0.93±0.004 (k6-d10g)	0.84±0.002 (k25-d7c)
abalone	1.00±0.002 (k25-d8g)	0.99±0.006 (k12-d8g)	1.00±0.0004 (k6-d6g)	0.99±0.008 (k6-d4g)
glass	0.95±0.011 (k6-d2g)	0.99±0.002 (k80-d4g)	0.97±0.001 (k80-d9p)	0.99±0.004 (k12-d2g)
yeast	0.64±0.056 (k12-d2g)	0.71±0.047 (k12-d2g)	0.70±0.027 (k25-d2g)	0.68±0.050 (k12-d2g)
cardiotocography	0.95±0.015 (k25-d8c)	0.96±0.004 (k25-d21g)	0.97±0.007 (k12-d15g)	0.95±0.009 (k12-d2g)
spam	0.64±0.072 (k80-d57c)	0.73±0.021 (k6-d2g)	0.80±0.012 (k80-d39c)	0.87±0.00001 (k80-d2g)
ecoli	0.98±0.012 (k3-d4g)	1.00±0.000 (k6-d2c)	1.00±0.000 (k3-d2c)	1.00±0.000 (k3-d2c)
letter	0.98±0.009 (k6-d11g)	0.97±0.011 (k3-d9g)	0.98±0.003 (k3-d13p)	0.99±0.002 (k6-d15g)
satellite	1.00±0.001 (k25-d13g)	1.00±0.000 (k6-d2g)	1.00±0.000 (k6-d13g)	1.00±0.000 (k6-d13g)
wine	0.61±0.020 (k25-d8c)	0.67±0.014 (k12-d11g)	0.54±0.011 (k12-d5p)	0.71±0.0004 (k3-d5p)
breast	0.91±0.036 (k3-d2g)	0.96±0.026 (k12-d2g)	0.96±0.010 (k12-d2c)	0.97±0.004 (k6-d2c)
mammography	0.80±0.041 (k3-d5g)	0.83±0.033 (k12-d2g)	0.84±0.014 (k3-d2g)	0.87±0.006 (k25-d3g)
pima	0.59±0.061 (k12-d4g)	0.67±0.053 (k25-d8g)	0.70±0.006 (k3-d2g)	0.58±0.052 (k3-d4g)
robot	0.85±0.087 (k25-d31g)	1.00±0.000 (k3-d61g)	1.00±0.005 (k12-d31c)	0.99±0.010 (k12-d31c)
vehicle	0.68±0.052 (k12-d7g)	0.63±0.050 (k12-d18g)	0.77±0.017 (k6-d18g)	0.77±0.026 (k12-d18g)
secom	0.54±0.033 (k12-d2p)	0.64±0.026 (k25-d2g)	0.52±0.001 (k6-d2p)	0.64±0.000 (k25-d2g)

Table 5.9. Average values and standard deviations of AUCs for spectral outlier detection with LEM, unsupervised case (k: neighbor count, d: number of dimensions and the kernel chosen. Kernels are c: constant, g: Gaussian, p: quadratic.).

	ActiveOutlier	LOF	ParzenWindow	Svm
shuttle2Lem	0.98±0.013 (k25-d4g)	0.98±0.003 (k12-d2g)	0.96±0.003 (k80-d2g)	0.99±0.001 (k25-d4g)
optdigits2	0.94±0.029 (k80-d23p)	0.98±0.004 (k12-d23g)	0.97±0.008 (k6-d23g)	0.92±0.003 (k12-d23g)
kddLem	0.89±0.014 (k12-d35g)	0.89±0.028 (k6-d20g)	0.87±0.003 (k80-d2g)	0.93±0.001 (k25-d14g)
kddtrainLem	0.94±0.018 (k12-d2g)	0.97±0.005 (k12-d2g)	0.93±0.004 (k80-d2g)	0.96±0.002 (k12-d2p)
pageblocks3	0.95±0.015 (k12-d2g)	0.95±0.005 (k12-d2g)	0.94±0.003 (k6-d5g)	0.98±0.00002 (k6-d5g)
abalone	0.76±0.137 (k6-d6p)	0.94±0.028 (k6-d4c)	0.89±0.014 (k3-d4g)	1.00±0.001 (k12-d4c)
glass	0.86±0.039 (k6-d2g)	0.97±0.002 (k6-d2g)	0.96±0.004 (k6-d2g)	0.98±0.001 (k80-d4p)
yeast	0.62±0.079 (k12-d2g)	0.70±0.040 (k12-d2g)	0.60±0.049 (k80-d2g)	0.70±0.018 (k80-d2g)
cardiotocography	0.89±0.030 (k12-d2g)	0.90±0.018 (k12-d15g)	0.95±0.003 (k6-d2g)	0.95±0.001 (k25-d2g)
spam	0.59±0.040 (k3-d18p)	0.73±0.008 (k3-d39g)	0.79±0.005 (k80-d57c)	0.87±0.0001 (k80-d2g)
ecoli	0.93±0.020 (k80-d7g)	0.99±0.010 (k6-d2c)	0.96±0.023 (k80-d7g)	1.00±0.000 (k3-d2c)
letter	0.94±0.029 (k6-d15g)	0.95±0.007 (k6-d11g)	0.93±0.004 (k25-d2g)	0.97±0.002 (k6-d11g)
satellite	0.90±0.078 (k80-d2g)	1.00±0.001 (k6-d13g)	1.00±0.003 (k6-d2g)	1.00±0.000 (k6-d2g)
wine	0.61±0.028 (k25-d5p)	0.65±0.012 (k12-d11g)	0.51±0.016 (k12-d5p)	0.72±0.002 (k80-d11g)
breast	0.91±0.069 (k12-d2g)	0.91±0.041 (k3-d2g)	0.97±0.002 (k12-d2g)	0.97±0.002 (k6-d2c)
mammography	0.76±0.044 (k3-d5g)	0.79±0.051 (k12-d2g)	0.82±0.014 (k3-d2g)	0.85±0.007 (k25-d3g)
pima	0.66±0.046 (k12-d8g)	0.62±0.026 (k25-d8g)	0.70±0.017 (k6-d2g)	0.77±0.028 (k12-d8g)
robot	0.85±0.104 (k25-d31p)	1.00±0.000 (k3-d61g)	0.98±0.021 (k12-d31c)	0.98±0.057 (k25-d2g)
vehicle	0.57±0.064 (k12-d18g)	0.60±0.038 (k6-d13g)	0.70±0.026 (k6-d13g)	0.60±0.010 (k6-d13p)
secom	0.51±0.045 (k12-d2p)	0.64±0.023 (k25-d2g)	0.52±0.002 (k6-d2p)	0.64±0.00002 (k25-d2g)

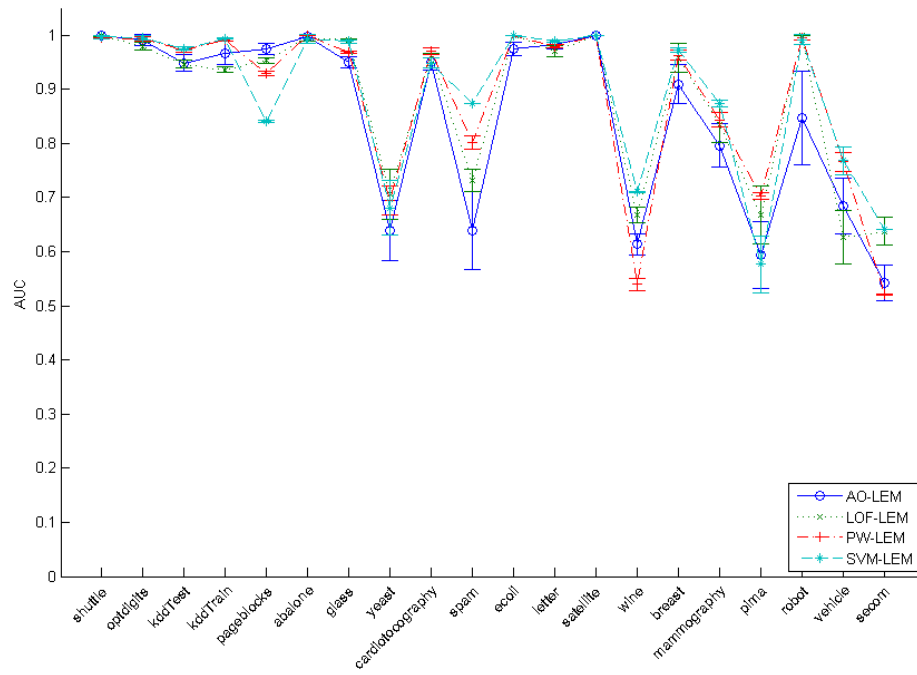


Figure 5.21. Plots of AUCs for spectral outlier detection with LEM for the semi-supervised case.

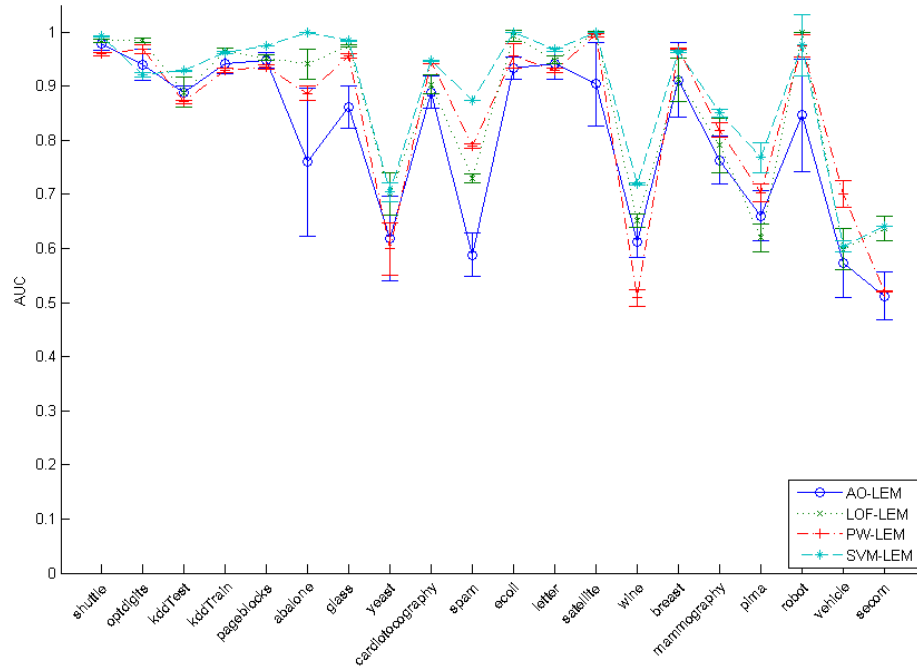


Figure 5.22. Plots of AUCs for spectral outlier detection with LEM for the unsupervised case.

Table 5.10. Wins/ties/losses of outlier detection methods combined with LEM with 5×2 cv F test, a: semi-supervised, b: unsupervised.

(a)					(b)				
	AO	LOF	PW	SVM		AO	LOF	PW	SVM
AO					AO				
LOF	3/17/0				LOF	4/16/0			
PW	3/15/2	3/13/4			PW	3/16/1	2/12/6		
SVM	6/13/1	5/14/1	4/14/2		SVM	10/10/0*	8/11/1	10/8/2	

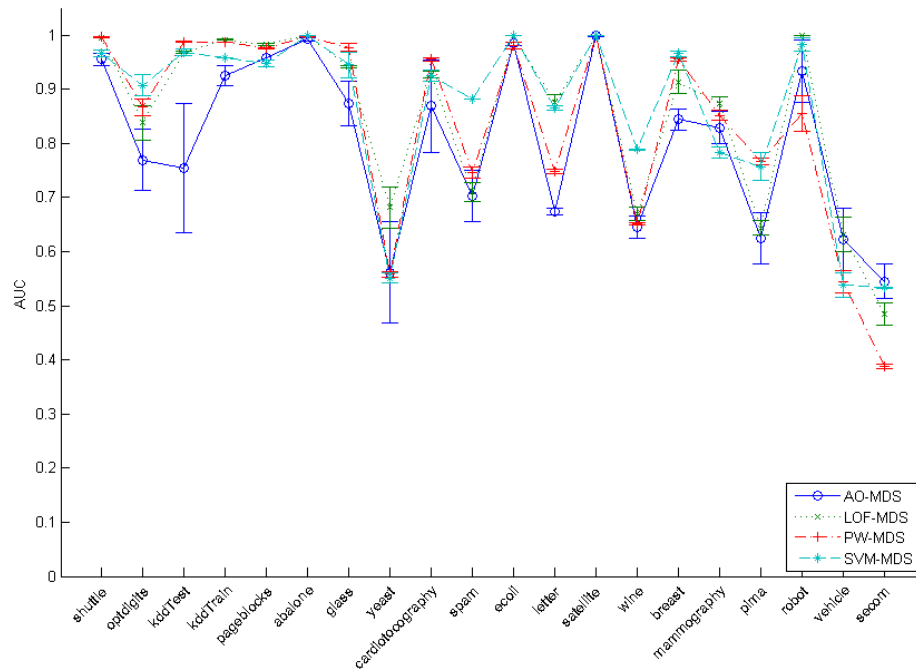


Figure 5.23. Plots of AUCs for spectral outlier detection with MDS for the semi-supervised case.

Table 5.11. Average values and standard deviations of AUCs for spectral outlier detection with MDS, semi-supervised, (k: neighbor count, d: number of dimensions.

Kernels are c: constant, g: Gaussian, p: quadratic.).

	ActiveOutlier	LOF	ParzenWindow	svm
shuttle2Lem	0.96±0.012 (k80-d9c)	1.00±0.001 (k6-d9p)	1.00±0.001 (k80-d9p)	0.97±0.007 (k80-d9p)
optdigits2	0.77±0.056 (k80-d23c)	0.84±0.032 (k80-d23c)	0.87±0.016 (k80-d23c)	0.91±0.019 (k80-d23c)
kddLem	0.75±0.119 (k12-d41p)	0.97±0.002 (k12-d41p)	0.99±0.001 (k80-d41p)	0.97±0.006 (k6-d41p)
kddtrainLem	0.93±0.018 (k25-d2c)	0.99±0.001 (k6-d2p)	0.99±0.001 (k12-d15p)	0.96±0.0001 (k3-d41p)
pageblocks3	0.96±0.016 (k25-d2c)	0.98±0.002 (k6-d10g)	0.98±0.001 (k25-d2c)	0.95±0.006 (k25-d2c)
abalone	0.99±0.003 (k6-d8p)	1.00±0.000 (k3-d8p)	1.00±0.000 (k25-d2p)	1.00±0.000 (k12-d4p)
glass	0.87±0.041 (k80-d9p)	0.94±0.002 (k80-d7p)	0.98±0.006 (k80-d7g)	0.95±0.024 (k80-d4g)
yeast	0.56±0.094 (k3-d4c)	0.68±0.038 (k80-d6p)	0.56±0.005 (k6-d4p)	0.55±0.009 (k80-d4p)
cardiotocography	0.87±0.085 (k80-d8p)	0.93±0.006 (k25-d8p)	0.96±0.003 (k25-d8p)	0.92±0.010 (k12-d15p)
spam	0.70±0.047 (k80-d39p)	0.71±0.017 (k12-d2p)	0.75±0.010 (k80-d20p)	0.88±0.0001 (k25-d2p)
ecoli	0.98±0.003 (k3-d4p)	1.00±0.000 (k3-d2c)	0.98±0.006 (k80-d2g)	1.00±0.000 (k3-d2c)
letter	0.67±0.006 (k6-d11p)	0.88±0.015 (k80-d16g)	0.75±0.004 (k3-d11g)	0.87±0.004 (k12-d7g)
satellite	1.00±0.0004 (k80-d2p)	1.00±0.00003 (k12-d13p)	1.00±0.000 (k25-d2p)	1.00±0.000 (k25-d2p)
wine	0.65±0.020 (k6-d11p)	0.67±0.012 (k3-d8p)	0.65±0.002 (k25-d5p)	0.79±0.0004 (k80-d5p)
breast	0.84±0.020 (k3-d11p)	0.91±0.021 (k3-d11p)	0.96±0.003 (k25-d2p)	0.97±0.005 (k12-d11c)
mammography	0.83±0.029 (k25-d2c)	0.87±0.012 (k12-d3c)	0.85±0.009 (k25-d2c)	0.78±0.010 (k25-d2g)
pima	0.63±0.048 (k25-d8p)	0.64±0.014 (k6-d2p)	0.77±0.006 (k25-d8p)	0.76±0.025 (k12-d2g)
robot	0.93±0.057 (k25-d2p)	1.00±0.000 (k3-d61g)	0.86±0.033 (k12-d61g)	0.98±0.012 (k6-d61g)
vehicle	0.62±0.058 (k3-d13c)	0.63±0.032 (k6-d13p)	0.55±0.021 (k3-d7g)	0.54±0.023 (k3-d2c)
secom	0.55±0.032 (k25-d590p)	0.49±0.021 (k12-d2p)	0.39±0.004 (k25-d590c)	0.53±0.001 (k3-d198c)

Table 5.12. Average values and standard deviations of AUCs for spectral outlier detection with MDS, unsupervised case (k: neighbor count, d: number of dimensions and the kernel chosen. Kernels are c: constant, g: Gaussian, p: quadratic.).

	ActiveOutlier	LOF	ParzenWindow	svm
shuttle2Lem	0.91±0.036 (k25-d7p)	0.99±0.001 (k6-d9p)	0.99±0.001 (k80-d9p)	0.99±0.000 (k12-d2p)
optdigits2	0.91±0.031 (k3-d23p)	0.97±0.009 (k80-d43p)	0.93±0.010 (k12-d23p)	0.96±0.007 (k80-d43p)
kddLem	0.78±0.086 (k12-d41p)	0.97±0.001 (k12-d41p)	0.98±0.001 (k80-d41p)	0.92±0.014 (k12-d41p)
kddtrainLem	0.90±0.049 (k25-d2c)	0.99±0.001 (k12-d2p)	0.98±0.002 (k12-d15p)	0.96±0.0003 (k3-d41p)
pageblocks3	0.96±0.014 (k25-d2c)	0.97±0.003 (k12-d5p)	0.96±0.002 (k25-d2c)	0.94±0.006 (k25-d2c)
abalone	0.99±0.002 (k25-d2p)	1.00±0.000 (k3-d8p)	0.99±0.001 (k25-d2p)	1.00±0.0001 (k25-d2p)
glass	0.77±0.102 (k25-d7p)	0.93±0.009 (k80-d7p)	0.92±0.017 (k80-d4p)	0.95±0.005 (k80-d4g)
yeast	0.60±0.047 (k6-d8c)	0.67±0.027 (k80-d6p)	0.56±0.010 (k6-d4p)	0.74±0.004 (k6-d8p)
cardiotocography	0.87±0.034 (k80-d15p)	0.91±0.012 (k12-d15p)	0.95±0.002 (k25-d8p)	0.94±0.002 (k80-d8p)
spam	0.63±0.062 (k80-d20p)	0.70±0.013 (k12-d2p)	0.74±0.009 (k80-d20p)	0.88±0.0001 (k25-d2p)
ecoli	0.89±0.189 (k12-d2p)	1.00±0.000 (k3-d2p)	1.00±0.000 (k3-d4p)	1.00±0.000 (k3-d2c)
letter	0.65±0.015 (k12-d11p)	0.91±0.017 (k80-d11g)	0.75±0.012 (k3-d11g)	0.87±0.004 (k12-d7g)
satellite	0.98±0.016 (k80-d2p)	1.00±0.0003 (k12-d13p)	1.00±0.000 (k80-d2p)	1.00±0.000 (k25-d2p)
wine	0.60±0.038 (k6-d11p)	0.66±0.008 (k3-d8p)	0.65±0.001 (k25-d5p)	0.79±0.0002 (k80-d5p)
breast	0.74±0.120 (k25-d2p)	0.91±0.021 (k3-d11p)	0.80±0.056 (k6-d11p)	0.98±0.000 (k3-d2p)
mammography	0.70±0.082 (k12-d3c)	0.70±0.008 (k3-d5p)	0.84±0.008 (k25-d2c)	0.79±0.011 (k25-d2g)
pima	0.62±0.041 (k12-d8p)	0.63±0.022 (k6-d2p)	0.76±0.011 (k25-d8p)	0.70±0.023 (k12-d2c)
robot	0.90±0.022 (k25-d2p)	1.00±0.000 (k3-d61g)	0.77±0.056 (k12-d61g)	0.98±0.013 (k6-d61g)
vehicle	0.60±0.027 (k3-d2g)	0.64±0.022 (k6-d13p)	0.53±0.006 (k3-d7g)	0.63±0.011 (k3-d2c)
secom	0.55±0.043 (k12-d590g)	0.48±0.024 (k12-d2p)	0.39±0.004 (k25-d590c)	0.54±0.001 (k3-d198c)

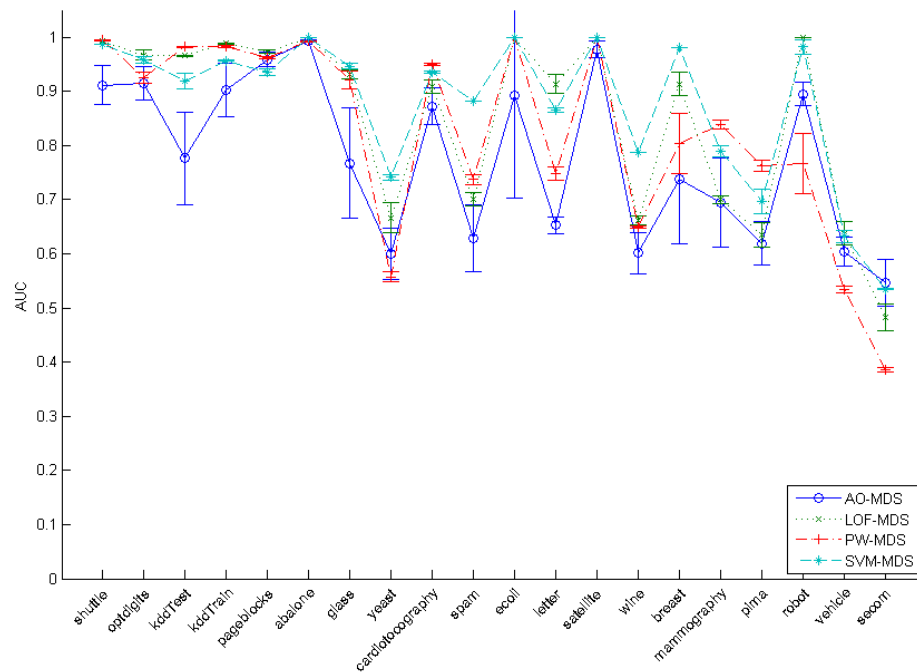


Figure 5.24. Plots of AUCs for spectral outlier detection with MDS for the unsupervised case.

Table 5.13. Wins/ties/losses of outlier detection methods combined with MDS, a: semi-supervised, b: unsupervised.

(a)					(b)				
	AO	LOF	PW	SVM		AO	LOF	PW	SVM
AO					AO				
LOF	8/12/0				LOF	6/14/0			
PW	7/12/1	4/7/9			PW	5/13/2	4/9/7		
SVM	9/11/0*	3/10/7	7/7/6		SVM	8/12/0	5/9/6	10/4/6	

Table 5.14. Average ranks of outlier detection methods, a: semi-supervised, b: unsupervised.

(a)					(b)				
	AO	LOF	PW	SVM		AO	LOF	PW	SVM
None	3.30	2.60	2.35	1.75	None	2.95	2.55	2.60	1.90
PCA	2.90	2.75	2.33	2.03	PCA	2.70	3.15	2.25	1.90
LEM	3.15	2.50	2.30	2.05	LEM	3.55	2.20	2.90	1.35
MDS	3.45	1.98	2.28	2.30	MDS	3.65	1.95	2.45	1.95
Average	3.20	2.46	2.32	2.03	Average	3.21	2.46	2.55	1.78

Table 5.15. Significant differences between outlier detection methods for each spectral method for the semi-supervised case.

None	SVM	PW	LOF	AO
PCA	SVM	PW	LOF	AO
LEM	SVM	PW	LOF	AO
MDS	LOF	PW	SVM	AO

Table 5.16. Significant differences between outlier detection methods for each spectral method for the unsupervised case.

None	SVM	LOF	PW	AO
PCA	SVM	PW	AO	LOF
LEM	SVM	LOF	PW	AO
MDS	SVM	LOF	PW	AO

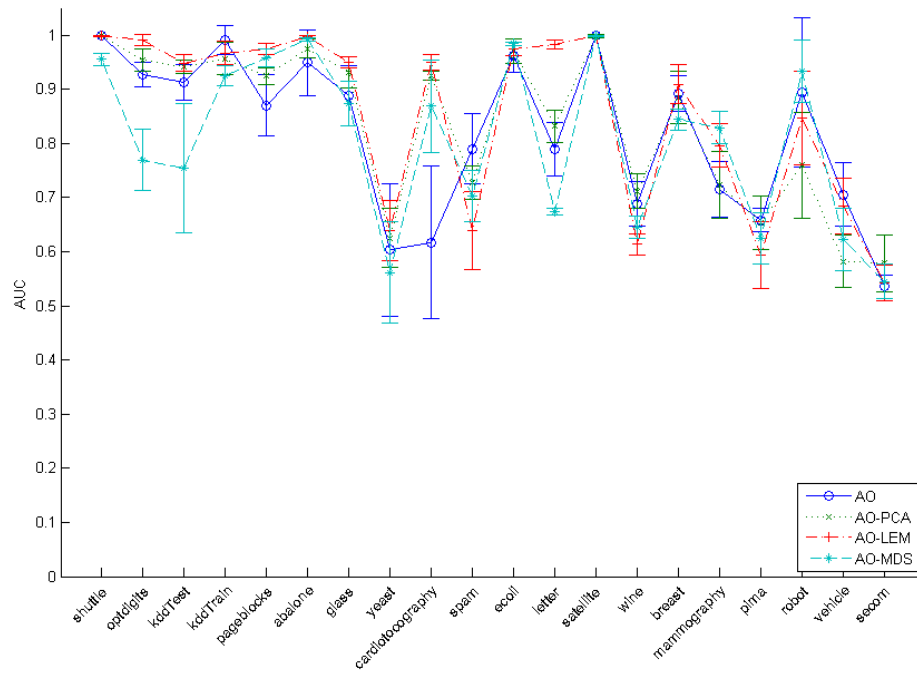


Figure 5.25. Plots of AUCs for AO with different spectral methods for the semi-supervised case.

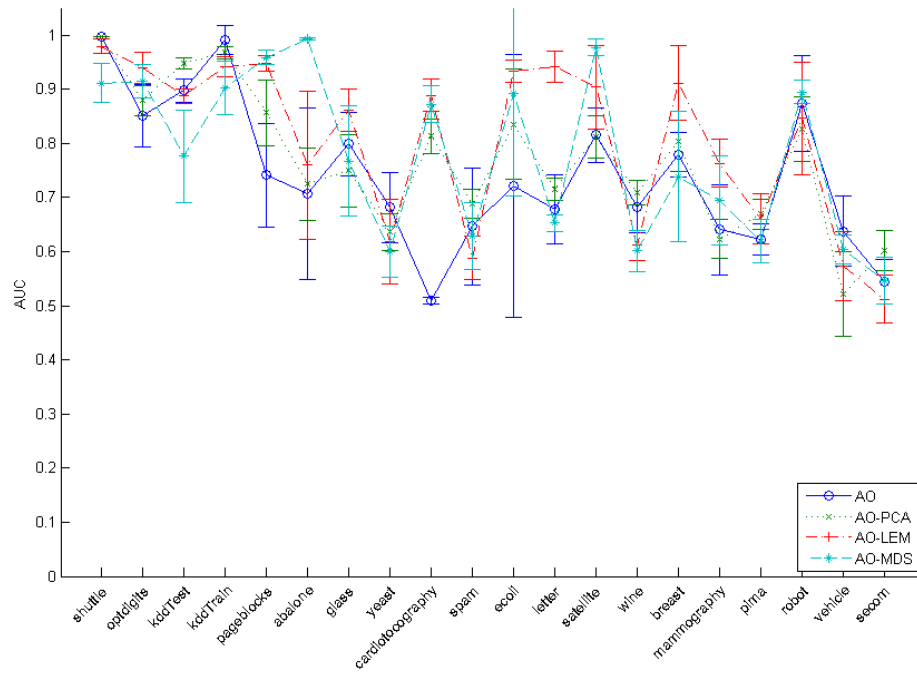


Figure 5.26. Plots of AUCs for AO with different spectral methods for the unsupervised case.

Table 5.17. Average ranks of spectral methods with respect to outlier detection methods, a: semi-supervised, b: unsupervised.

(a)					(b)				
	None	PCA	LEM	MDS		None	PCA	LEM	MDS
AO	2.65	2.45	1.95	2.95	AO	2.65	2.45	2.20	2.70
LOF	2.68	3.18	1.83	2.33	LOF	3.10	3.35	1.78	1.78
PW	2.45	2.90	2.00	2.65	PW	2.90	2.60	2.20	2.30
SVM	2.17	2.95	2.10	2.77	SVM	3.00	2.95	1.90	2.15
Average	2.49	2.87	1.97	2.68	Average	2.91	2.84	2.02	2.23

test on wins/ties/losses of algorithms find that none of the algorithms are better than the others in most cases. However, in the unsupervised case, there are significant differences for LOF and SVM methods. LEM and MDS are significantly better than PCA and no transformation for LOF and LEM outperforms PCA and no transformation for SVM. Also, according to Wilcoxon’s signed rank test, LOF with LEM significantly outperforms LOF with no transformation and with PCA. Although, there are no significance in the wins of SVM, with LEM and MDS, SVM has nearly significant number of wins against PCA and no transformation. In semi-supervised case, there are no significant differences between spectral methods for all the outlier detection methods except LOF. This leads us to argue that if we are able to provide only the typical instances in the training set, spectral transformations are not very useful. Because, for the semi-supervised case most outlier detection methods are able to perform comparably regardless of spectral method. However, in the unsupervised case, SVM and LOF gain significant accuracies when combined with LEM or MDS. If we were able to conclude from the previous analyses that LOF or SVM are always significantly better than other outlier detection methods, we would be able to argue that spectral outlier detection algorithm that combines LOF or SVM with LEM or MDS is a promising one. Nonetheless, if we just look at the ranks of each method, we can see that LEM takes the highest rank in all cases. MDS is the second best performer for four cases. Although there is no clear statistically significant difference, combining outlier detection methods with spectral methods, especially LEM, seems to increase performance slightly indicated by higher ranks of such methods.

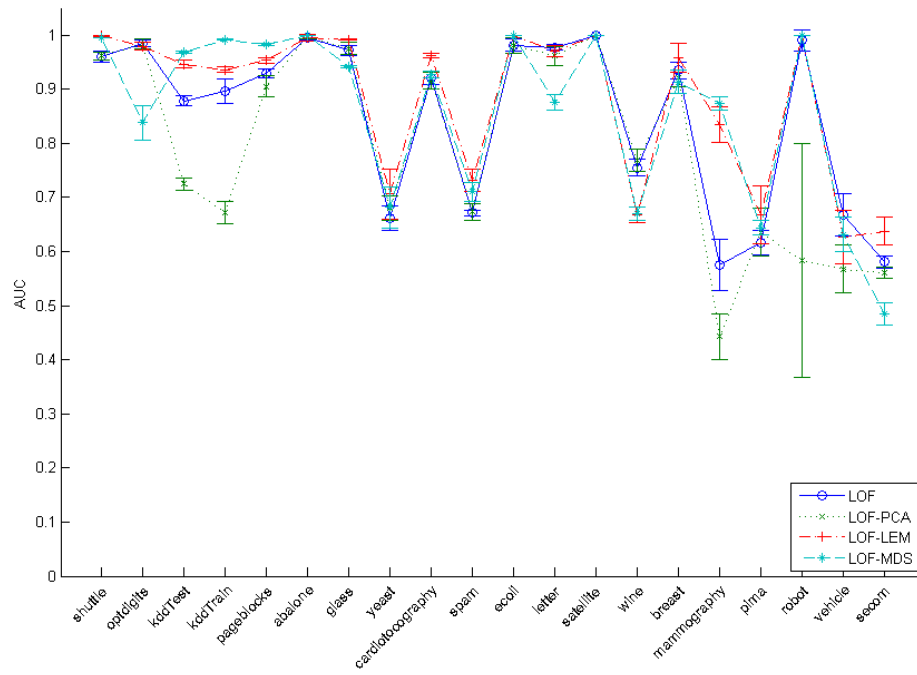


Figure 5.27. Plots of AUCs for LOF with different spectral methods for the semi-supervised case.

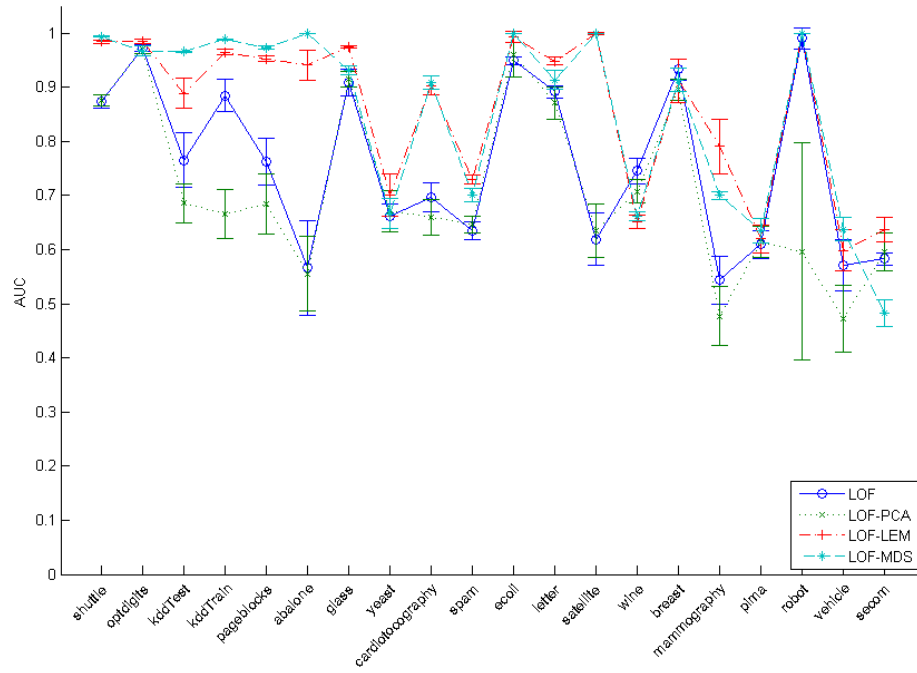


Figure 5.28. Plots of AUCs for LOF with different spectral methods for the unsupervised case.

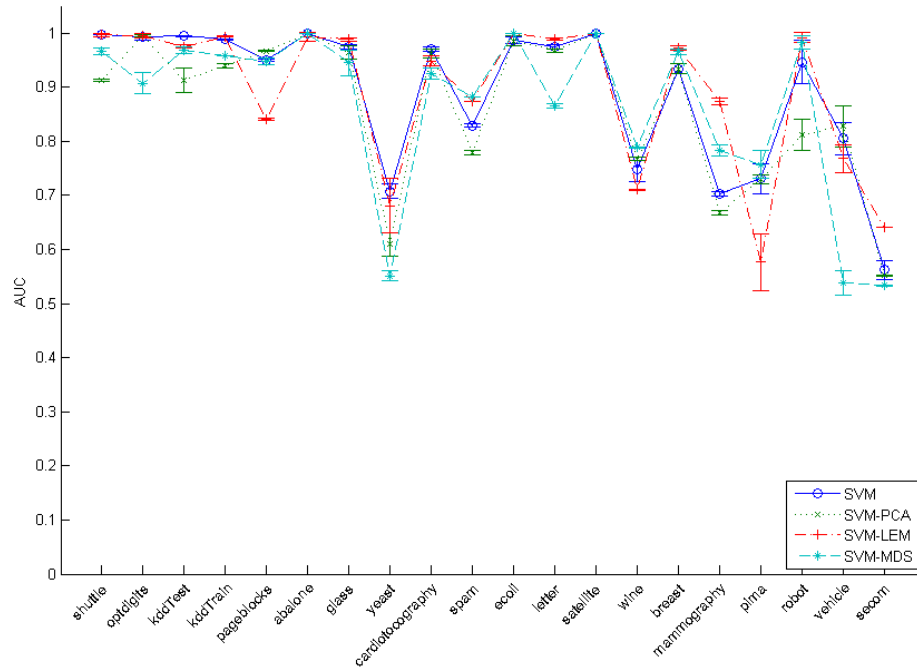


Figure 5.29. Plots of AUCs for SVM with different spectral methods for the semi-supervised case.

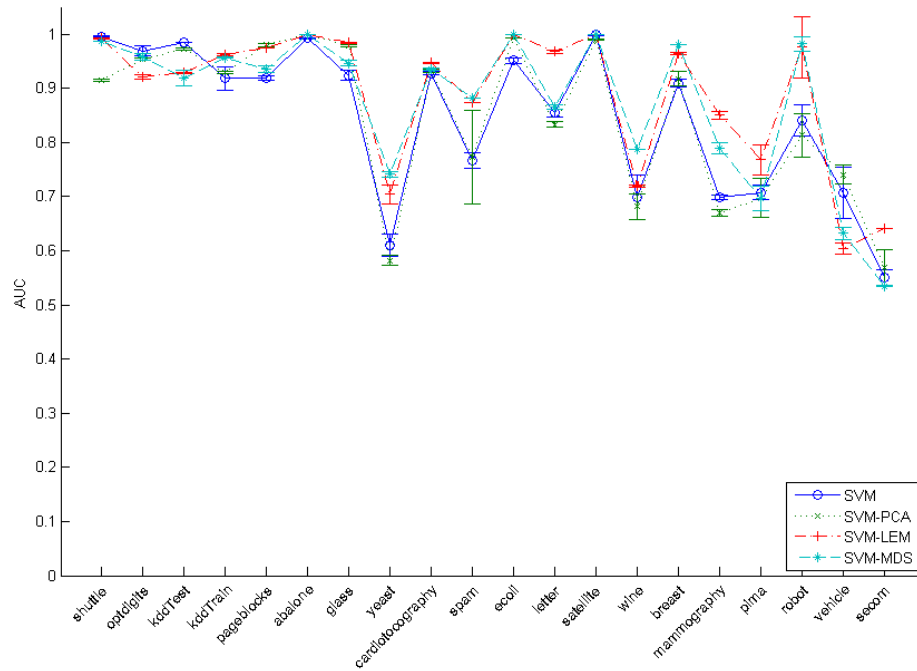


Figure 5.30. Plots of AUCs for SVM with different spectral methods for the unsupervised case.

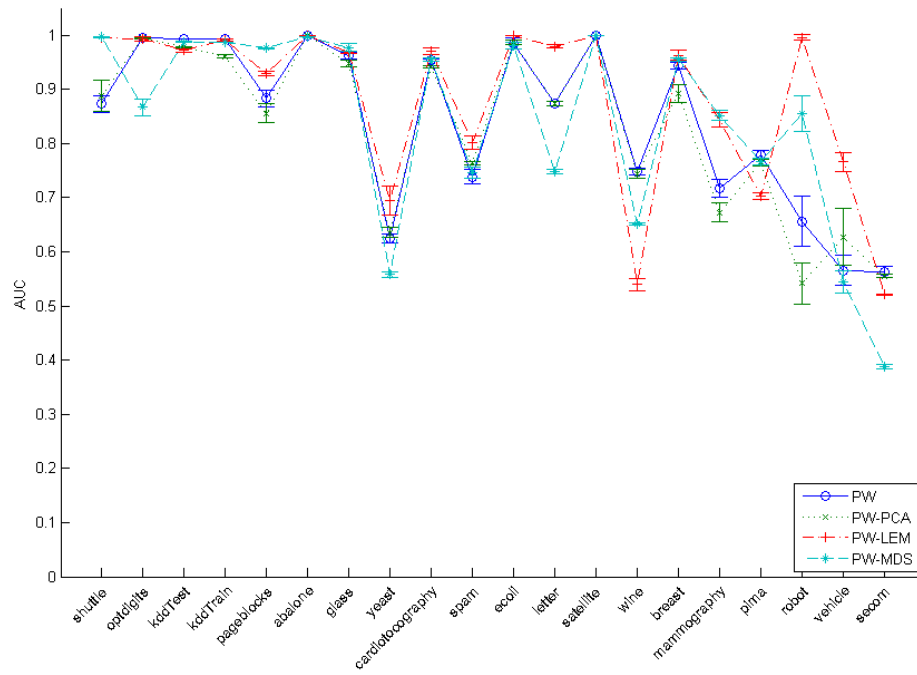


Figure 5.31. Plots of AUCs for PW with different spectral methods for the semi-supervised case.

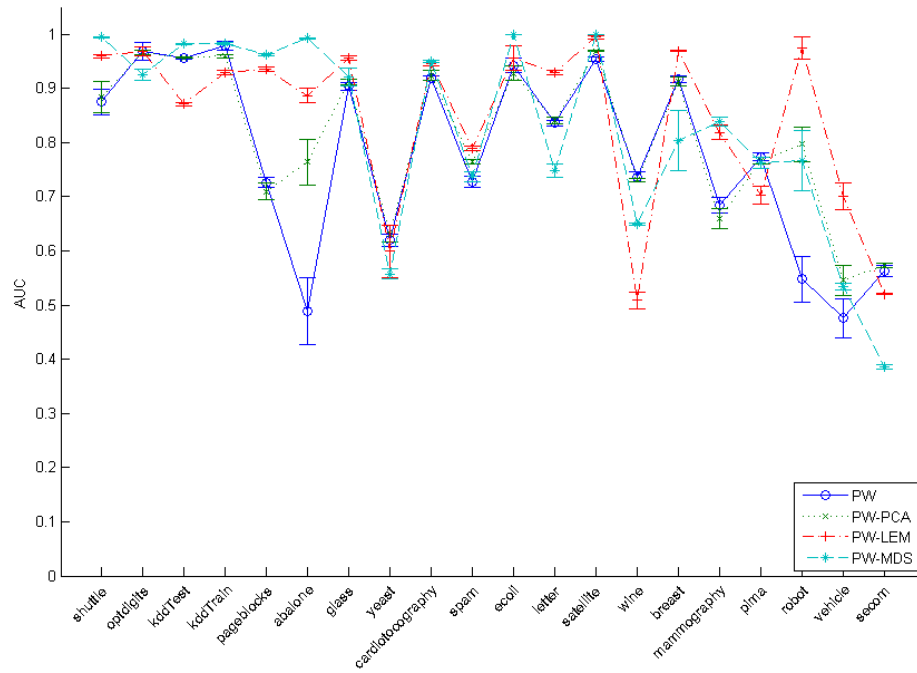


Figure 5.32. Plots of AUCs for PW with different spectral methods for the unsupervised case.

Table 5.18. Significant differences between spectral methods for each outlier detection method for the semi-supervised case (L: LEM, P: PCA, M: MDS O: no combination, only outlier detection method.).

AO	<u>L</u>	<u>P</u>	<u>O</u>	<u>M</u>
LOF	<u>L</u>	<u>M</u>	<u>O</u>	<u>P</u>
PW	<u>L</u>	<u>O</u>	<u>M</u>	<u>P</u>
SVM	<u>L</u>	<u>O</u>	<u>M</u>	<u>P</u>

Table 5.19. Significant differences between spectral methods for each outlier detection method for the unsupervised case (L: LEM, P: PCA, M: MDS O: no combination, only outlier detection method.).

AO	<u>L</u>	<u>P</u>	<u>O</u>	<u>M</u>
LOF	<u>L</u>	<u>M</u>	<u>O</u>	<u>P</u>
PW	<u>L</u>	<u>M</u>	<u>P</u>	<u>O</u>
SVM	<u>L</u>	<u>M</u>	<u>P</u>	<u>O</u>

Table 5.20. Wins/ties/losses of outlier detection methods combined with spectral methods for the semi-supervised case, a: AO, b: LOF, c: PW, d: SVM.

(a)

	AO	AO-PCA	AO-LEM	AO-MDS
AO				
AO-PCA	1/19/0			
AO-LEM	3/15/2	5/13/2		
AO-MDS	1/16/3	0/16/4	0/17/3	

(b)

	LOF	LOF-PCA	LOF-LEM	LOF-MDS
LOF				
LOF-PCA	0/16/4			
LOF-LEM	6/13/1	8/11/1		
LOF-MDS	6/9/5	6/9/5	2/12/6	

(c)

	PW	PW-PCA	PW-LEM	PW-MDS
PW				
PW-PCA	0/16/4			
PW-LEM	7/9/4	11/6/3		
PW-MDS	4/9/7	8/6/6	4/7/9	

(d)

	SVM	SVM-PCA	SVM-LEM	SVM-MDS
SVM				
SVM-PCA	1/12/7			
SVM-LEM	6/11/3	8/9/3		
SVM-MDS	2/9/9	7/5/8	4/9/7	

Table 5.21. Wins/ties/losses of outlier detection methods combined with spectral methods for the unsupervised case, a: AO, b: LOF, c: PW, d: SVM.

(a)

	AO	AO-PCA	AO-LEM	AO-MDS
AO				
AO-PCA	3/17/0			
AO-LEM	3/15/2	2/16/2		
AO-MDS	3/16/1	2/14/4	0/18/2	

(b)

	LOF	LOF-PCA	LOF-LEM	LOF-MDS
LOF				
LOF-PCA	0/19/1			
LOF-LEM	10/9/1*	12/8/0*		
LOF-MDS	10/8/2	10/9/1*	5/13/2	

(c)

	PW	PW-PCA	PW-LEM	PW-MDS
PW				
PW-PCA	4/15/1			
PW-LEM	12/3/5	9/6/5		
PW-MDS	9/7/4	9/5/6	6/7/7	

(d)

	SVM	SVM-PCA	SVM-LEM	SVM-MDS
SVM				
SVM-PCA	4/11/5			
SVM-LEM	11/6/3	9/8/3		
SVM-MDS	8/10/2	10/6/4	4/9/7	

5.4. Face Detection

We evaluate our spectral outlier detection method on a face detection problem. CBCL Face Detection data set [52] contains 19×19 images of face and non-faces. The training set contains 291 instances from the face class and the test set consists of 124 face and 1205 non-face instances. The typical class is considered to be the face class. We evaluate the accuracy of the Active-Outlier method individually and with PCA and LEM. With no transformation, AUC is 0.85 while PCA reports 0.76. The spectral outlier detection approach with LEM significantly increases accuracy and reaches 0.97. Furthermore, LEM reaches this reported accuracy using only two dimensions. We also plot the instances in two dimensions, seen in Figures 5.34 and 5.33, to show that the transformation achieved by LEM is superior to PCA.

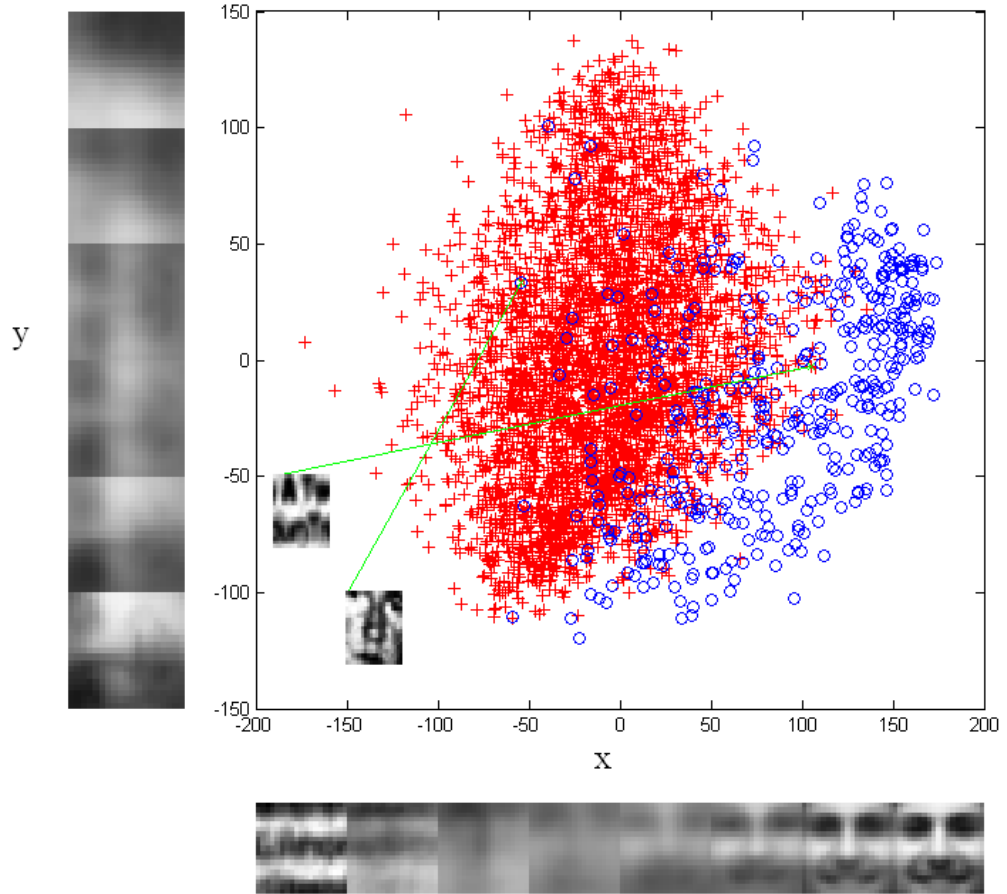


Figure 5.33. CBCL Face data set reduced to two dimensions with PCA.

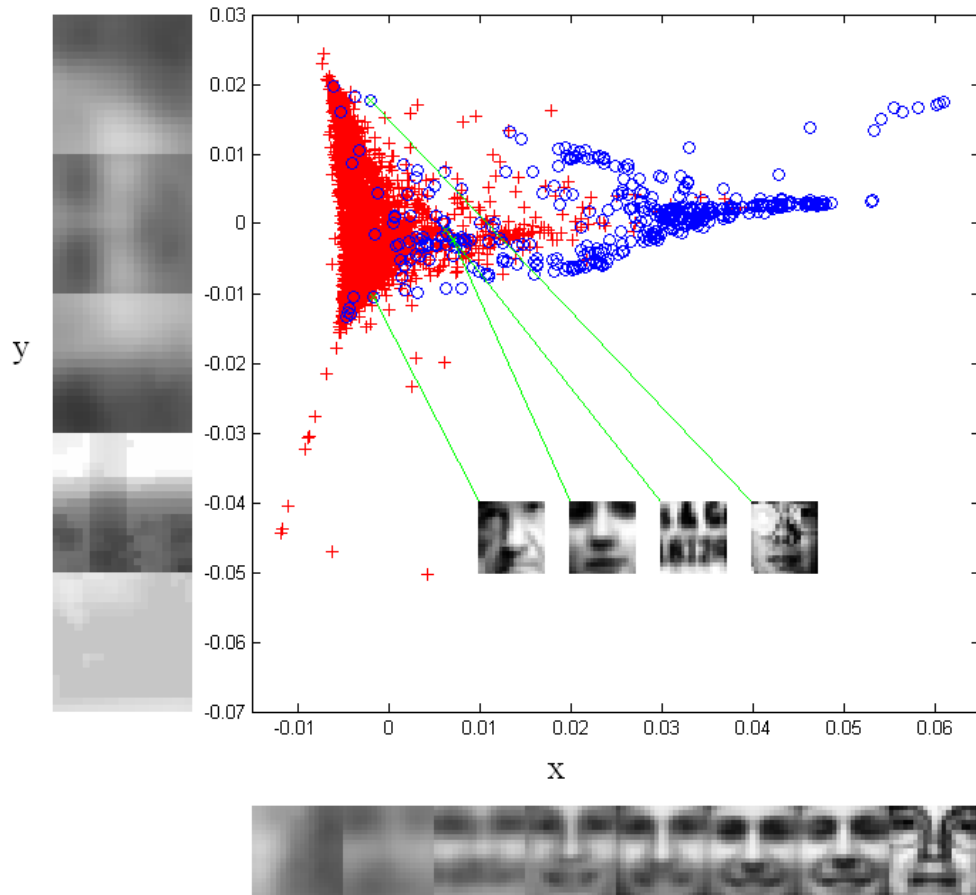


Figure 5.34. CBCL Face data set reduced to two dimensions with LEM (Gaussian kernel, $k = 3$ and $\sigma = 101.70$).

6. CONCLUSIONS AND FUTURE WORK

In this thesis, we propose a new method for outlier detection. Reducing the dimensionality of the data and transforming it to get a representation where the outliers are more easily identifiable has been shown to increase accuracy in previous works. We argue that the ability of spectral methods to reveal the non-linear structure in the data would be valuable for outlier detection. We review various spectral methods and discuss the similarities and the differences between them. Our spectral outlier detection algorithm involves having a spectral method before outlier detection. In order to evaluate the performance of our method, we carry out experiments on 20 data sets with four different outlier detection methods. The results of our experiments show us that although SVM seems to perform well overall, none of the outlier detection methods is significantly superior to the others and choosing the best one depends heavily on the specific setting of the problem in question.

All the methods discussed in this thesis, for outlier detection and spectral decomposition are implemented in MATLAB and this toolbox is made available; details are given in Appendix A.

When we compare the different combinations of outlier detection methods with spectral methods, we see that the performance differences between methods vanish in the semi-supervised case. This leads us to argue that all the methods are able to perform comparably well when only the typical data are given in the training set. The differences between methods appear in the unsupervised case, which is a more realistic scenario for outlier detection, since, most of the time we do not have labelled data. In the unsupervised case, using spectral transformation beforehand does not affect the accuracies of AO or PW much. This is expected for AO, because, it never deals with the distribution of input data and thus is not affected by it. The reason for similar performances in the case of PW with different spectral methods can be attributed to the fact that all of the spectral methods preserve local information in the data. So, it

is possible to find a parameter for PW method that gives good results in different input spaces. However, spectral transformations have an effect on the performances of LOF and SVM. The increase in LOF's performance when combined with LEM probably stems from the fact that LEM maps similar instances to closer points in the new space. This property increases the differences in the local densities, hence, making it easier to find outliers. Since the transformed instances are contained in a smaller volume compared to the original input space, SVM is also able to learn a smoother function. Therefore, by combining SVM or LOF with LEM, we are able to increase the outlier detection accuracy. If we compare SVM with LOF, we can say that SVM usually outperforms LOF and more importantly, being a discriminative method, SVM has a significantly lower time complexity.

Due to the ambiguity of the outlier concept and the lack of available data sets, we assumed the rare class classification approach for creating outlier detection problems. We have a very diverse set of data sets where some are artificial problems and most of them are actually not really outlier detection problems. There are even some data sets that have such high outlier percentages that it may not be rational to consider them outlier detection problems. More importantly, since we assume that the instances from the rare class to be outliers, outliers form clusters which is not quite realistic.

As future work, a more solid analysis from the perspective of spectral methods is possible that looks at the performances according to the properties of the data sets. Analyzing the data sets that LOF and SVM perform well will reveal when these methods are able to increase performance and in which scenarios they are more applicable.

Another future work would be to compare other spectral methods, such as Locally Linear Embedding [53] and ISOMAP [54], to see if they give better results than Laplacian Eigenmaps. Although we have carried out experiments for both the semi-supervised and the unsupervised case, our spectral methods were all unsupervised. One could modify Laplacian Eigenmaps to operate in a semi-supervised manner by

calculating the transformation using only the sample of typical examples. Then, for a test instance, we may find its neighbors in the input space and map to the new space by using the transformed neighbors. This approach may increase the accuracy of our method. A bolder future endeavor would be the design of a novel spectral method by defining a cost function that is specially crafted for outlier detection. It is important for the cost function to be convex and in particular, it would be better if the optimization problem could be written as a trace maximization/minimization problem.

APPENDIX A: OUTLIER DETECTION TOOLBOX IN MATLAB

For the evaluation of our spectral outlier detection algorithm, we have developed an outlier detection toolbox in MATLAB which can be downloaded from <http://gokererdogan.com/files/thesis/odtoolbox.zip>. It features:

- Implementations of the outlier detection methods; Active-Outlier [28], Local Outlier Factor [27], Parzen Windows [14], Feature Bagging [32] and decision tree (Decision tree is implemented by `classregtree` class which is available in MATLAB `statistics` toolbox)
- Implementations of the spectral methods; Principal Components Analysis [37], Laplacian Eigenmaps [41], Multidimensional Scaling [40] and Kernel Principal Components Analysis [38]
- A data set format, routines to read and pre-process data sets
- An experiment result format and functions for calculation of AUC for ROC and precision-recall (PR) curves
- Routines to visualize discriminants of methods, plot ROC (ROC curves are calculated with `croc` and `auroc` functions implemented by Dr Gavin C. Cawley taken from <http://theoval.cmp.uea.ac.uk/matlab/>) and PR curves

The source code is properly documented and information on any function can be seen by calling `help functionName`. We provide two GUIs for demonstration under `demo` folder. First demonstration, `demo.m`, lets the user to choose input points in 2D and kernel parameters and plots the spectral transformations. This demonstration can be started by typing `demo` in the MATLAB command line. A sample run of this demonstration can be seen in Figures A.1 and A.2.

In the second demonstration, `od.m`, the user is able to run the outlier detection methods, AO, LOF and PW with PCA, LEM, MDS and KPCA (without mean cen-

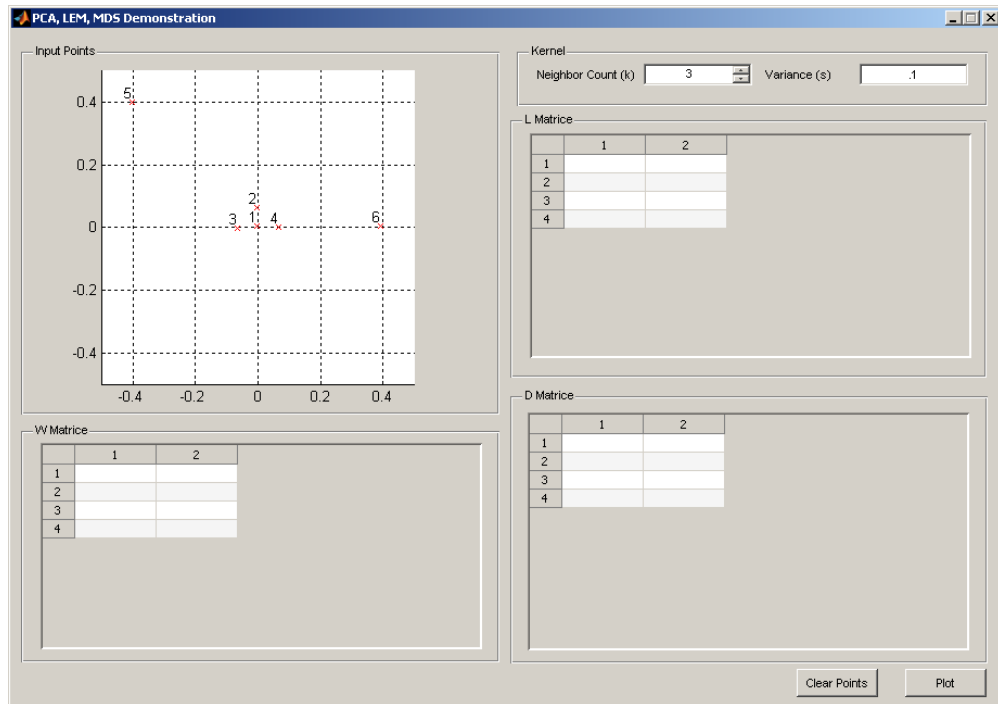


Figure A.1. Spectral methods demonstration `demo` script's first screen where points and kernel parameters are selected.

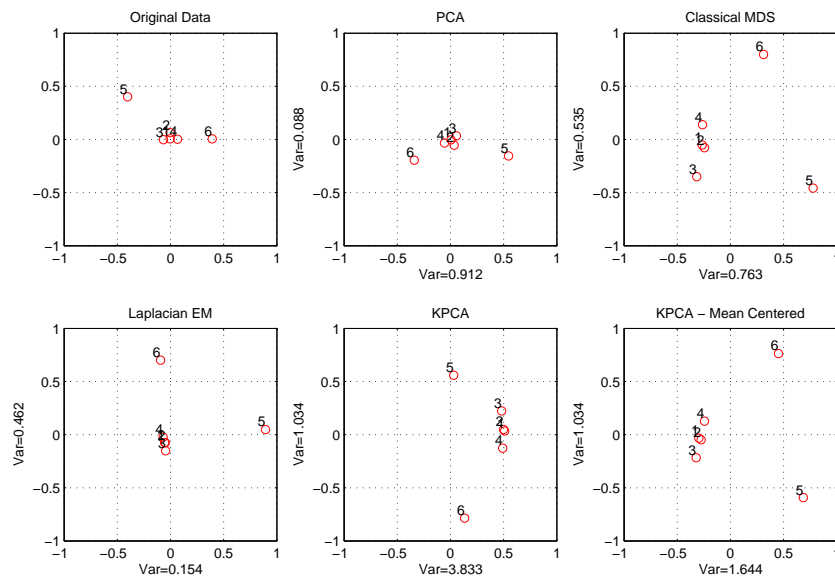


Figure A.2. Spectral methods demonstration `demo` script's second screen where spectral transformations are plotted.

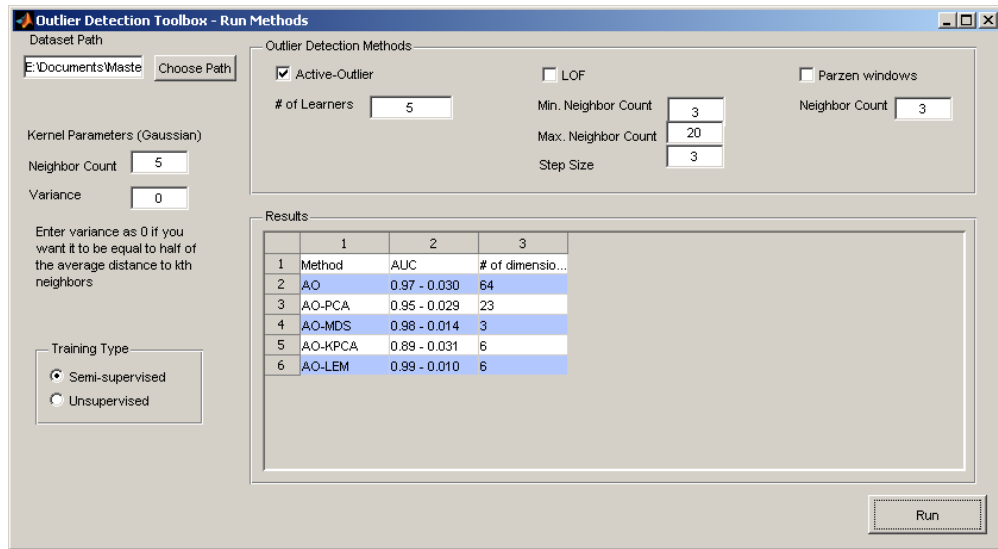


Figure A.3. Outlier detection toolbox demonstration od script's GUI.

tering) on a chosen data set. The user needs to select a folder containing the necessary data set files. Each data set requires five files; these are:

- `tvx.mat`: an $N \times d$ dimensional MATLAB matrix containing training and validation instances. Instances are on the rows and attributes are in the columns.
- `tv.y.mat`: an N dimensional vector of class labels for training/validation set
- `tsx.mat`: an $N_{test} \times d$ dimensional MATLAB matrix containing test instances
- `ts.y.mat`: an N_{test} dimensional vector of class labels for test set
- `def.txt`: data set definition file where the first line contains the data set name, the second line class labels separated by space for each typical class, the third line includes class labels for outlier class and the fourth line lists the indices of categorical attributes. A sample file can be seen under `datasets/optdigits1` folder.

The parameters for the Gaussian kernel, semi-supervised or unsupervised training selection and method specific parameters are also input by the user as seen in Figure A.3. The selected methods are evaluated on the chosen data set with no transformation, with PCA, LEM, MDS and KPCA. For spectral methods, the number of dimensions that give the best performance is found by cross validation and the AUC on the test

set is calculated with this dimensionality. The results are given in the GUI when the run completes. Additionally, the MATLAB structures containing the results for each run and ROC/PR curve plots are saved into the data set folder. An extra script to `od.m`, `od_script.m`, is also provided that shows how to run experiments with different methods and parameters. `odToolbox` is distributed under the GNU General Public License. It can be redistributed and modified freely for non-commercial use. We kindly request users of this toolbox to reference this thesis in their publications.

REFERENCES

1. Alpaydm, E., *Introduction to Machine Learning*, MIT Press, Cambridge, MA, USA, 2004.
2. Grubbs, F. E., “Procedures for Detecting Outlying Observations in Samples”, *Technometrics*, Vol. 11, No. 1, pp. 1–21, 1969.
3. Chandola, V., A. Banerjee and V. Kumar, “Anomaly Detection: A Survey”, *ACM Computing Surveys*, Vol. 41, pp. 15:1–15:58, 2009.
4. Minsky, M., *The Society of Mind*, Simon and Schuster, New York, NY, USA, 1986.
5. Augusteijn, M. F. and B. A. Folkert, “Neural Network Classification and Novelty Detection”, *International Journal of Remote Sensing*, Vol. 23, No. 14, pp. 2891–2902, 2002.
6. Cun, L., B. Boser, J. S. Denker, D. Henderson, R. E. Howard, W. Hubbard and L. D. Jackel, “Handwritten Digit Recognition with a Back-Propagation Network”, *Advances in Neural Information Processing Systems*, pp. 396–404, 1990.
7. Hwang, B. and S. Cho, “Characteristics of Auto-associative MLP as a Novelty Detector”, *International Joint Conference on Neural Networks*, Vol. 5, pp. 3086–3091, 1999.
8. Dasgupta, D. and F. Nino, “A Comparison of Negative and Positive Selection Algorithms in Novel Pattern Detection”, *IEEE International Conference on Systems, Man, and Cybernetics*, Vol. 1, pp. 125–130, 2000.
9. Albrecht, S., J. Busch, M. Kloppenburg, F. Metze and P. Tavan, “Generalized Radial Basis Function Networks for Classification and Novelty Detection: Self-organization of Optimal Bayesian Decision”, *Neural Networks*, Vol. 13, No. 10, pp.

1075 – 1093, 2000.

10. Fan, W., M. Miller, S. J. Stolfo and W. Lee, “Using Artificial Anomalies to Detect Unknown and Known Network Intrusions”, *Proceedings of the First IEEE International Conference on Data Mining*, pp. 123–130, 2001.
11. Rätsch, G., S. Mika, B. Schölkopf and K.-R. Müller, “Constructing Boosting Algorithms from SVMs: An Application to One-Class Classification”, *IEEE Transactions on Pattern Analysis and Machine Intelligence*, Vol. 24, No. 9, pp. 1184–1199, 2002.
12. Schölkopf, B., J. C. Platt, J. C. Shawe-Taylor, A. J. Smola and R. C. Williamson, “Estimating the Support of a High-Dimensional Distribution”, *Neural Computation*, Vol. 13, No. 7, pp. 1443–1471, 2001.
13. Roth, V., “Kernel Fisher Discriminants for Outlier Detection”, *Neural Computation*, Vol. 18, No. 4, pp. 942–960, 2006.
14. Parzen, E., “On Estimation of a Probability Density Function and Mode”, *The Annals of Mathematical Statistics*, Vol. 33, No. 3, pp. 1065–1076, 1962.
15. Laurikkala, J., M. Juhola and E. Kentala, “Informal Identification of Outliers in Medical Data”, *The Fifth International Workshop on Intelligent Data Analysis in Medicine and Pharmacology*, pp. 17–29, 2000.
16. Ye, N. and Q. Chen, “An Anomaly Detection Technique Based on a Chi-square Statistic for Detecting Intrusions into Information Systems”, *Quality and Reliability Engineering International*, Vol. 17, No. 2, pp. 105–112, 2001.
17. Rousseeuw, P. J. and A. M. Leroy, *Robust Regression and Outlier Detection*, John Wiley & Sons, Inc., New York, NY, USA, 1987.
18. Eskin, E., “Anomaly Detection over Noisy Data Using Learned Probability Distri-

- butions”, *Proceedings of the International Conference on Machine Learning*, pp. 255–262, 2000.
19. Abraham, B. and G. E. P. Box, “Bayesian Analysis of Some Outlier Problems in Time Series”, *Biometrika*, Vol. 66, No. 2, pp. 229–236, 1979.
 20. Eskin, E., “Modeling System Calls for Intrusion Detection with Dynamic Window Sizes”, *Proceedings of DARPA Information Survivability Conference and Exposition II (DISCEX)*, pp. 143–152, 2001.
 21. Desforges, M. J., P. J. Jacob and J. E. Cooper, “Applications of Probability Density Estimation to the Detection of Abnormal Conditions in Engineering”, *Proceedings of the Institution of Mechanical Engineers, Part C: Journal of Mechanical Engineering Science*, Vol. 212, No. 8, pp. 687–703, 1998.
 22. Yu, J. X., W. Qian, H. Lu and A. Zhou, “Finding Centric Local Outliers in Categorical/Numerical Spaces”, *Knowledge Information Systems*, Vol. 9, No. 3, pp. 309–338, 2006.
 23. He, Z., X. Xu and S. Deng, “Discovering Cluster-based Local Outliers”, *Pattern Recognition Letters*, Vol. 24, No. 9-10, pp. 1641–1650, 2003.
 24. Byers, S. and A. E. Raftery, “Nearest-Neighbor Clutter Removal for Estimating Features in Spatial Point Processes”, *Journal of the American Statistical Association*, Vol. 93, No. 442, pp. 577–584, 1998.
 25. Eskin, E., A. Arnold, M. Prerau, L. Portnoy and S. Stolfo, “A Geometric Framework for Unsupervised Anomaly Detection: Detecting Intrusions in Unlabeled Data”, *Applications of Data Mining in Computer Security*, pp. 319–330, 2002.
 26. Knorr, E. M., R. T. Ng and V. Tucakov, “Distance-based Outliers: Algorithms and Applications”, *The International Journal on Very Large Data Bases*, Vol. 8, No. 3-4, pp. 237–253, 2000.

27. Breunig, M. M., H. P. Kriegel, R. T. Ng and J. Sander, “LOF: Identifying Density-based Local Outliers”, *SIGMOD Record*, Vol. 29, pp. 93–104, 2000.
28. Abe, N., B. Zadrozny and J. Langford, “Outlier Detection by Active Learning”, *Proceedings of the 12th ACM SIGKDD International Conference on Knowledge Discovery and Data Mining*, pp. 504–509, 2006.
29. Freund, Y. and R. E. Schapire, “A Decision-theoretic Generalization of Online Learning and An Application to Boosting”, *Proceedings of the Second European Conference on Computational Learning Theory*, pp. 23–37, 1995.
30. Breiman, L., “Bagging Predictors”, *Machine Learning*, Vol. 24, pp. 123–140, 1996.
31. Breiman, L., “Random Forests”, *Machine Learning*, Vol. 45, No. 1, pp. 5–32, 2001.
32. Lazarevic, A. and V. Kumar, “Feature Bagging for Outlier Detection”, *Proceedings of the Eleventh ACM SIGKDD International Conference on Knowledge Discovery in Data Mining*, pp. 157–166, 2005.
33. Vapnik, V., *The Nature of Statistical Learning Theory*, Springer, New York, NY, USA, 2000.
34. L.K. Saul, J. H. H. F. S., K.Q. Weinberger and D. D. Lee, “Spectral methods for dimensionality reduction”, *Semi-Supervised Learning*, pp. 293–300, 2006.
35. Eckart, C. and G. Young, “The Approximation of One Matrix by Another of Lower Rank”, *Psychometrika*, Vol. 1, pp. 211–218, 1936.
36. Saad, Y., *Numerical Methods for Large Eigenvalue Problems*, Halstead Press, New York, NY, USA, 1992.
37. Jolliffe, I., *Principal Component Analysis*, Springer-Verlag, New York, NY, USA, 2002.

38. Schölkopf, B., A. J. Smola and K.-R. Müller, “Kernel Principal Component Analysis”, *International Conference on Artificial Neural Networks*, pp. 583–588, 1997.
39. Schölkopf, B., A. J. Smola and K.-R. Müller, “Nonlinear Component Analysis as a Kernel Eigenvalue Problem”, *Neural Computation*, Vol. 10, No. 5, pp. 1299–1319, 1998.
40. Cox, T. and M. Cox, *Multidimensional Scaling*, Chapman & Hall, London, UK, 1994.
41. Belkin, M. and P. Niyogi, “Laplacian Eigenmaps for Dimensionality Reduction and Data Representation”, *Neural Computation*, Vol. 15, No. 6, pp. 1373–1396, 2003.
42. Shyu, M.-L., S.-C. Chen, K. Sarinnapakorn and L. Chang, “A Novel Anomaly Detection Scheme Based on Principal Component Classifier”, *Proceedings of the IEEE Foundations and New Directions of Data Mining Workshop, in Conjunction with the Third IEEE International Conference on Data Mining (ICDM’03)*, pp. 172–179, 2003.
43. Wang, W., X. Guan and X. Zhang, “A Novel Intrusion Detection Method Based on Principal Component Analysis”, *Advances in Neural Networks, International IEEE Symposium on Neural Networks*, pp. 657–662, 2004.
44. Parra, L., G. Deco and S. Miesbach, “Statistical Independence and Novelty Detection with Information Preserving Nonlinear Maps”, *Neural Computation*, Vol. 8, pp. 260–269, 1995.
45. Dutta, H., C. Giannella, K. D. Borne and H. Kargupta, “Distributed Top-K Outlier Detection from Astronomy Catalogs Using the DEMAC System.”, *SIAM International Conference on Data Mining*, pp. 110–121, 2007.
46. Salzberg, S. L., “C4.5: Programs for Machine Learning”, *Machine Learning*, Vol. 16, pp. 235–240, 1994.

47. Chang, C.-C. and C.-J. Lin, “LIBSVM: A Library For Support Vector Machines”, *ACM Transactions on Intelligent Systems and Technology*, Vol. 2, No. 3, pp. 27:1–27:27, 2011.
48. Frank, A. and A. Asuncion, *UCI Machine Learning Repository*, 2010, <http://archive.ics.uci.edu/ml>, 10.09.2011.
49. Friedman, M., “The Use of Ranks to Avoid the Assumption of Normality Implicit in the Analysis of Variance”, *Journal of the American Statistical Association*, Vol. 32, No. 200, pp. 675–701, 1937.
50. Alpaydm, E., “Combined 5×2 Cv F Test for Comparing Supervised Classification Learning Algorithms.”, *Neural Computation*, Vol. 11, No. 8, pp. 1885–1892, 1999.
51. Nemenyi, P. B., *Distribution-free Multiple Comparisons*, Ph.D. Thesis, Princeton University, 1963.
52. MIT Center For Biological and Computation Learning, *CBCL Face Database*, 2000, <http://cbcl.mit.edu/software-datasets/FaceData2.html>, 15.01.2012.
53. Roweis, S. T. and L. K. Saul, “Nonlinear Dimensionality Reduction by Locally Linear Embedding”, *Science*, Vol. 290, No. 5500, pp. 2323–2326, 2000.
54. Tenenbaum, J. B., V. d. Silva and J. C. Langford, “A Global Geometric Framework for Nonlinear Dimensionality Reduction”, *Science*, Vol. 290, No. 5500, pp. 2319–2323, 2000.